University Politehnica Timişoara

Mechanical Engineering Faculty

Mechatronics Department

Corina-Mihaela Gruescu

Contributions to development of optical design in mechatronic applications

Habilitation thesis

2019

Table of contents

Table of contents 2

Abstract 5

Rezumat 9

I. Introduction 13

II. Scientific achievements regarding optical design in mechatronic applications 19

1. Basic optical design. Glass choice 19
    - 1.1 Statement of problem 19
    - 1.2 Theoretical basis 20
    - 1.3 Numerical results 21
    - 1.4 Application 22
    - 1.5 Possibility to increase the aperture of triplets by introducing aspheric surfaces 27
    - 1.6 Conclusions and contributions 30
2. Optical engineering applied in laser machining 32
    - 2.1 Optics optimization in laser spot radius minimization 32
        - 2.1.1 Statement of problem 32
        - 2.1.2 Optics design for a 10.6 µM laser technology 34
        - 2.1.3 Conclusions and contributions 40
    - 2.2 Experimental optimization of process parameters in laser cutting of polycarbonate gears 41
        - 2.2.1 Statement of problem 41
        - 2.2.2 Experimental equipment 42
        - 2.2.3 General design of the experimental optimization program 43

2.2.4 Choice of influence parameters and working combinations in order to apply Taguchi method in processes optimization ... 43
2.2.5 CAD of gears and generation of NC code ... 48
2.2.6 Experimental results ... 49
2.2.7 Optimization of process parameters by means of Taguchi method ... 51
2.2.8 Conclusions and contributions ... 55
3. Document digitization ... 57
3.1 Digitization equipment and techniques in retrieval of mechanism and machine science resources ... 57
3.1.1 Statement of problem ... 57
3.1.2 Workflow ... 58
3.1.3 Scanning equipment ... 60
3.1.3.1 General requirements ... 60
3.1.3.2 Optical and mechanical design ... 61
3.1.3.3 Design of software tools ... 66
3.1.4 Conclusions and contributions ... 67
3.2 Interactive animation production by means of advanced image processing ... 69
3.2.1 Statement of problem ... 69
3.2.2 The TU-Ilmenau digitizer ... 69
3.2.3 The UPT digitizer ... 71
3.2.4 The AIS-generator software ... 73
3.2.5 Conclusions and contributions ... 74
4. Optical engineering in medical investigation ... 76
4.1 Modeling of human spinal column and evaluation of spinal deformities ... 76
4.1.1 Statement of problem ... 76
4.1.2 Equipment and software to provide data for modeling ... 77
4.1.3 Software development ... 83
4.1.3 Modeling of vertebrae and simulation of column deformations ... 87
4.1.4 Conclusions and contributions ... 90
4.2 Experimental method for evaluation of spinal column deformation ... 91
4.2.1 Statement of problem ... 91
4.2.2 Mathematical approach and equipment ... 93
4.2.3 Equipment for the experimental measurement of coordinates along the spinal column ... 96
4.2.4 Example of data acquisition and processing results ... 97
4.2.5 Performing measurements and interpreting data ... 99

4.2.6 Conclusions and contributions 103

III. Academic and professional achievements 105

IV. Career evolution and development plans 109

V. References 112

Anexa. 10 lucrări relevante 119

Abstract

The present habilitation thesis is structured in five sections: (I) Introduction, (II) Scientific achievements, (III) Academic and professional achievements, (IV) Career evolution and development plans and (V) References.

The scientific, academic and professional achievements cover the period 2008 - 2018.

Section (I) provides an overview on the thesis content and highlights the papers published by the author in ISI indexed Journals (3), ISI indexed Conferences (2), and Scopus indexed Conferences (5).

Section (II) describes several scientific achievements within the author´s research directions and is organized in four chapters. Each chapter has a unitary structure including *Statement of the problem*, *Theoretical and/or experimental contributions* to the stated problem and *Conclusions and contributions* of the author.

The first chapter, *Basic optical design. Glass choice*, offers a solution to the problem of choosing the suitable sorts of glass by means of stating mathematical criteria implemented in software application. The practical solutions provided by the application lead to high image quality for apertures twice larger than the traditional ones. Aspheric surfaces can also bring substantial improvement in image quality for systems, which are mainly affected by spherical residual aberration. The proper generating noncircular curve is hard to find without specialized soft and needs appropriate skills of he human operator.

The second chapter refers to *Optical engineering applied in laser machining*. The first paragraph develops *Optics optimization in laser spot radius minimization*. The research starts from the observation that progress in precision and efficiency in laser machining is strongly connected to the quality of the optical system, which ensures the travel of the beam emitted by the source and then the focusing of radiant energy to the machining point. Furthermore, infrared optics needs specific algorithms, which take into account the small number of available materials, the monochromatic radiation and its high power density. The present work provided original solutions for the expander and focusing objective in two variants (spherical and aspheric objective). Both solutions are diffraction limited and may be regarded as very good from optical point of view. In addition, they take minimal costs of manufacturing as only singlet lenses are used.

The second paragraph is dedicated to *Experimental optimization of process parameters in laser cutting of polycarbonate gears*. Fractional factorial experiments plans stated by Taguchi method and a specialized software – Qualitek – proved to be quick, economic (only 40 samples needed effective machining for optimizing six parameters in two levels and one interaction organized in 8 combinations) and very efficient. For the pieces machined in optimal conditions S/N ratio is better than the predicted one and the mean value is very close to the nominal target, which significantly improves the quality of the lot of pieces. The machining became very precise, considering the optimization criterion (nominal value). As well, the process itself became desirable instead of traditional technology. Auxiliary devices such as molds were totally eliminated and the machining duration decreased considerably (3…4 minutes/piece in function of number of teeth).

The third chapter develops some aspects regarding the *Document digitization*. Two paragraphs are dedicated to *Digitization Equipment and Techniques in Retrieval of Mechanism and Machine Science Resources* and *Interactive animation production by means of advanced image processing*.

Digitization techniques are used on the purpose of retrieving the history of mechanism science and of creating a coherent description of its development since early ages until present days. Digitization of analogue documents requires special resources regarding equipment and software. The team from the University Politehnica Timisoara, as partner in the thinkMOTION project, developed a workstation specialized in digitization of all-type documents. Design and assembling of the scanning equipment as well as the capturing, stocking and managing raw image files software were developed as original contributions of the team. The scanning equipment is a complex mechatronic system, involving optoelectronics, mechanics and software integration. The resulting working station is different from the all-purpose products on the market and gathers selected characteristics, imposed by the specific application. Thousands of high quality pages are now available online for a large range of users (academic staff, students, Ph.D. students, engineers, historians etc.) at www.dmg-lib.org. Beside documents, the library also displays physical demonstration models and mechanism descriptions.

The physical working models of the mechanisms are digitally recorded as a sequence of images, usually covering a full rotation of the input (driving) element. With further handling steps, these image sequences are composed to interactive animations, which can be started inside the DMG-Lib internet portal with a special player or can be downloaded as video files for local use.

The fourth chapter develops several applications, which implement *Optical engineering in medical investigation*. The first paragraph describes the *Modeling of human spinal column and evaluation of spinal deformities.* A large number of numerical parameters were suggested for the description of the column’s shape. A special software – INBIRE – was developed to work with the all purpose imaging system InSpeck. The program provides an interactive database and the facility to export data to the modeling program 3Dmax. Using anthropometrical data, the individual vertebrae and finally the entire column was modeled as a standard. The coordinates provided by INBIRE allow modeling of personalized spinal columns, which can be stored and used by physicians to monitor the evolution of the deformities.

The achievements of the research project contribute to development of local or national healthcare programs, bringing in numerical precision and efficiency in screening and monitoring spinal deformities, which are wide-spread, hard and costly to treat in advanced stages.

The second paragraph covers the subject *Experimental method for evaluation of spinal column deformation*, based on data acquired with a system of accelerometers and advanced image processing. The paper proposes a new investigation method, based on data provided by a set of eight accelerometers, which are stuck on the body of the vertebrae during the whole therapy exercises. The goal of the study is to develop a method to record the Cobb angles variation, which should provide in the future an evaluation of the therapy exercises. The acquired angular data is used to compute an eighth degree polynomial as a model of the spine. Appropriate mathematical algorithm is developed in order to compute the co-ordinates, the coefficients of the polynomial and the Cobb angles. The polynomial approximation was validated by comparing its results with reference data provided by a sure method. The reference is considered the image taken during acquiring data with the accelerometers.

Section III of the habilitation thesis presents the main achievements of the candidate within the past 20 years, since defending the PhD thesis, on May 15th 1998, at the University Politehnica Timişoara.

The teaching activities at University Politehnica Timişoara comprised courses, seminars, laboratory activities or project activities on *Descriptive geometry and engineering design, Technical optics, Optical apparatuses, Photometers and spectrophotometers, Medical optics, Reliability in mechatronics, Optical sensors* and *Illumination ergonomics*. A number of 12 books were published in printed or electronic format to support these topics.

The research activities were developed in areas similar to the teaching activities, within 8 projects funded at national and European level.

The results of the research work were published in 7 papers indexed in ISI Journals, 12 papers indexed in ISI Proceedings, 19 papers indexed in SCOPUS and over 100 papers indexed in other databases.

The publishing activities were completed with reviewing activities on main Journals and Conferences (ASME - Measurement Journal, Optical Engineering, ASME - Journal of Mechanisms and Robotics, 14th IFToMM World Congress - Taipei 2015, MTM&Robotics 2016 - Aachen, Germany, Scientific Bulletin of the Politehnica University of Timisoara, SYROM 2017 - Brasov, RO, MESROB 2018 – Cassino, It, MEDER 2018 – Udine, It and others).

The candidate is member of an international professional association, IFToMM (International Federation of Mechanism and Machine Science) since 2014 as observer member of the Technical Committee Linkages and Mechanical Controls. The candidate contributed as member of the organizing committee to preparing and developing of 2 international conferences and one summer school supported by IFToMM and was co-editor to one volume of proceedings published by Springer.

Section V renders the references used in the previous sections.

Rezumat

Teza de abilitare este structurată în cinci secțiuni: (I) Introducere, (II) Realizări științifice, (III) Realizări academice și profesionale, (IV) Evoluția carierei și planuri de dezvoltare și (V) Referințe. Realizările științifice, academice și profesionale acoperă perioada 1998-2018.

Secțiunea I oferă o imagine de ansamblu asupra conținutului tezei și prezintă lucrările publicate de autor în reviste indexate ISI (3), conferinţe indexate ISI (2) şi conferinţe indexate Scopus (5).

Secțiunea II descrie câteva realizări științifice în cadrul direcțiilor de cercetare ale autorului și este organizată în patru capitole. Fiecare capitol are o structură unitară, care include Punerea problemei, Contribuții teoretice și/sau experimentale la problema specificată și Concluzii și contribuții ale autorului.

Primul capitol, *Proiectarea optica de bază. Alegerea materialelor*, oferă o soluție la problema alegerii unor tipuri adecvate de sticlă, prin stabilirea unor criterii matematice implementate într-o aplicație software. Soluțiile practice oferite de aplicație conduc la o calitate ridicată a imaginii pentru aperturi de două ori mai mari decât cele tradiționale. Suprafețele asferice pot aduce, de asemenea, o îmbunătățire substanțială a calității imaginii pentru sistemele care sunt, în principal, afectate de aberațiile reziduale sferice. Generarea curbei necirculare corespunzătoare este greu de găsit fără un soft specializat și necesită abilități adecvate ale operatorului uman.

Al doilea capitol se referă la *Ingineria optică aplicată în prelucrarea cu laser*. Primul paragraf dezvoltă *Optimizarea sistemului optic prin minimizarea razei petei laser*. Cercetarea pornește de la observația că progresul în precizie și eficiență în prelucrarea cu laser este puternic legat de calitatea sistemului optic, care asigură ghidarea fasciculului emis de sursă și apoi focalizarea energiei radiante către punctul de prelucrare. În plus, optica în infraroșu necesită algoritmi specifici, care iau în considerare numărul redus de materiale disponibile, radiația monocromatică și densitatea de putere mare a acesteia. Lucrarea a oferit soluții originale pentru obiectivul de expandare și focalizare în două variante (obiectiv sferic și asferic). Ambele soluții sunt limitate la difracție și pot fi considerate foarte bune din punct de vedere optic. În plus, ele necesită costuri minime de fabricație, deoarece se utilizează numai lentile singulare.

Al doilea paragraf este dedicat *Optimizării experimentale a parametrilor procesului de tăiere cu laser a roţilor dinţate din policarbonat*. Planurile de experineţe factoriale fracționate determinate de metoda Taguchi și un software specializat - Qualitek - s-au dovedit a fi rapide și economice (doar 40 de probe au necesitat o prelucrare eficientă pentru optimizarea a șase parametri pe două nivele și o interacțiune organizate în 8 combinații) și foarte eficiente. Pentru piesele prelucrate în condiții optime, raportul S/N este mai bun decât cel prognozat, iar valoarea medie este foarte apropiată de ținta nominală, ceea ce îmbunătățește semnificativ calitatea lotului de piese. Prelucrarea a devenit foarte precisă, având în vedere criteriul de optimizare (valoarea nominală). De asemenea, procesul în sine a devenit de dorit în locul tehnologiei tradiționale. Dispozitivele auxiliare, cum ar fi matrițele, au fost eliminate în totalitate, iar durata de prelucrare a scăzut considerabil (3 ... 4 minute/ bucată în funcție de numărul de dinți).

Capitolul al treilea dezvoltă câteva aspecte privind *Digitizarea documentelor*. Cele două paragrafe sunt intitulate *Echipamente și tehnici de digitizare în recuperarea resurselor de cunoaştere în domeniul mecanismelor și științei mașinilor* și *Producția de animații interactive prin intermediul procesării avansate a imaginilor*.

Tehnicile de digitizare sunt utilizate în scopul recuperării istoriei științei mecanismelor și al creării unei descrieri coerente a dezvoltării sale de la începuturi până în zilele actuale. Digitizarea documentelor analogice necesită resurse speciale în ceea ce privește echipamentele și software-ul. Echipa de la Universitatea Politehnica Timisoara, ca partener în proiectul thinkMOTION, a dezvoltat o staţie de lucru specializată în digitizarea documentelor de toate categoriile. Proiectarea şi asamblarea echipamentului de scanare, precum şi software-ul de captare, stocare şi gestionare a fişierelor brute au fost dezvoltate ca şi contribuții originale ale echipei. Echipamentul de scanare este un sistem mecatronic complex, care implică integrarea domeniilor optoelectronic, mecanic şi software. Staţia de lucru rezultată este diferită de produsele de uz general de pe piaţă şi oferă caracteristicile impuse de aplicația specifică. Mii de pagini de înaltă calitate sunt acum disponibile online pentru o gamă largă de utilizatori (personal academic, studenţi, doctoranzi, ingineri, istorici etc.) la www.dmg-lib.org. Pe lângă documente, biblioteca afișează, de asemenea, modele demonstrative fizice şi descrieri ale mecanismelor.

Modelele fizice de lucru ale mecanismelor sunt înregistrate digital ca o secvență de imagini, de obicei acoperind o rotație completă a elementului de intrare (de conducere). Cu pași suplimentari de manipulare, aceste secvențe de imagini sunt compuse în animații interactive, care pot fi pornite din portalul DMG-Lib cu un player special sau pot fi descărcate ca fișiere video pentru uz local.

Cel de-al patrulea capitol dezvoltă aplicații care implementează *Ingineria optică în investigaţiile medicale*. Primul paragraf descrie *Modelarea coloanei vertebrale umane și evaluarea deformaţiilor coloanei vertebrale,* pe baza implementării unei metode de investigare complet neinvazivă pentru coloana vertebrală, care este frecvent afectată de deformări. Un număr mare de parametri numerici au fost sugerați pentru descrierea formei coloanei. Un software special - INBIRE - a fost dezvoltat pentru a lucra cu sistemul InSpeck, creat pentru imagistică în general. Programul oferă o bază de date interactivă și facilitatea de a exporta date în programul de modelare 3Dmax. Folosind date antropometrice, vertebrele individuale și, în final, întreaga coloană a fost modelată ca standard. Coordonatele furnizate de INBIRE permit modelarea coloanei vertebrale personalizate, care poate fi stocată și utilizată de către medici pentru a monitoriza evoluția deformaţiilor.

Realizările proiectului de cercetare poate contribui la dezvoltarea programelor locale sau naționale de asistență medicală, aducând precizie numerică și eficiență în depistarea și monitorizarea deformaţiilor coloanei vertebrale, care sunt larg răspândite, greu și costisitor de tratat în stadii avansate.

Al doilea paragraf acoperă subiectul *Metoda experimentală pentru evaluarea deformaţiilor coloanei vertebrale*, pe baza datelor obținute cu un sistem de accelerometre și procesarea avansată a imaginii. Se propune o metodă nouă de investigare, pe baza datelor furnizate de un set de opt accelerometre, care sunt ataşate de corpul vertebrelor în timpul întregului exercițiu de terapie. Scopul studiului este de a dezvolta o metodă de înregistrare a variației unghiurilor Cobb, care ar trebui să furnizeze un criteriu de evaluare a exercițiilor de terapie. Datele unghiulare obținute sunt utilizate pentru a calcula un polinom de grad opt ca model al coloanei vertebrale. Algoritmul matematic adecvat este dezvoltat pentru a calcula coordonatele, coeficienții polinomului și unghiurile Cobb. Aproximarea polinomială a fost validată prin compararea rezultatelor sale cu datele de referință furnizate printr-o metodă sigură. Referința este considerată imaginea realizată în timpul preluării datelor cu accelerometrele.

Secțiunea III a tezei de abilitare prezintă principalele realizări ale candidatului în ultimii 20 de ani, de la susţinerea tezei de doctorat, în 15 mai 1998, la Universitatea Politehnica Timișoara.

Activitățile didactice de la Universitatea Politehnica Timișoara au cuprins cursuri, seminarii, activități de laborator sau activități de proiect la disciplinele *Geometria descriptivă și desen tehnic, Optica tehnică, Aparate optice, Fotometre și spectrofotometre, Optica medicală, Fiabilitatea sistemelor mecatronice, Senzori optici și Ergonomia iluminării*. Un număr de 12 cărți au fost publicate în format tipărit sau electronic pentru a susține aceste discipline.

Activitățile de cercetare au fost dezvoltate în domenii similare activităților didactice, în cadrul a 7 proiecte finanțate la nivel național și european.

Rezultatele lucrărilor de cercetare au fost publicate în 7 lucrări indexate în reviste ISI, 12 lucrări indexate în ISI Proceedings, 19 lucrări indexate în SCOPUS și peste 100 de lucrări indexate în alte baze de date.

Activitățile de publicare au fost completate cu activități de recenzare la reviste și conferințe (Journal of Mechanisms and Robotics, Measurement Journal, Optical Engineering, 14th IFToMM World Congress, MTM & Robotics 2016 - Aachen, Germania, Buletinul științific al Universității Politehnica din Timișoara, SYROM 2017 - Brașov, RO, MESROB 2018 – Cassino, It, MEDER 2018 – Udine, It și altele).

Candidatul este membru al unei asociații profesionale internaționale, IFToMM (International Federation of Mechanism and Machine Science) din 2014, în calitate de membru observator al Technical Committee Linkages and Mechanical Controls. Candidatul a contribuit în calitate de membru al comitetului organizator la pregătirea și desfăşurarea a două conferințe internaționale și o școală de vară sprijinite de IFToMM și a fost co-editor la un volum publicat de Springer.

Secțiunea V conţine referințele apelate în capitolele anterioare.

I. Introduction

Nowadays, optical engineering is frequently used in technical applications of all kinds. Mechatronic assemblies include optical modules, which ensure sensing, measuring or imaging.

The traditional optical instruments, such as the camera, the microscope, the telescope and the simple magnifier have evolved to a large range of devices and apparatuses, which exploit not only refraction and reflection of light, but also phenomena described by wave and quantum optics, such as interference, diffraction, and polarization of the electromagnetic radiation. There are plenty of new classes of apparatuses such as spectrophotometers, colorimeters, measuring apparatuses and machining assemblies and a class of devices, called generically optical sensors. They use electromagnetic radiation and optical phenomena in order to measure a physical size, to detect the presence or absence of a target, to detect a certain state etc.

The optical systems are used in two large types of applications:

- Imaging applications (fig. 1)
- Non-imaging applications (fig. 2).

Imaging applications contain an optical system, which projects the image of an object on a screen, a sensing surface or directly to the human eye. These applications are developed mostly in the visible range.

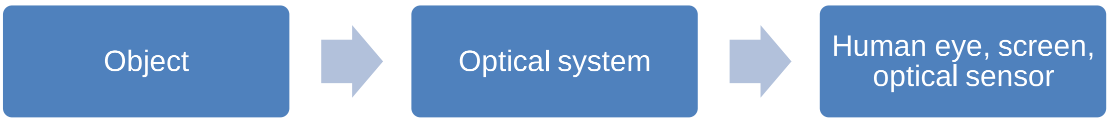

Figure 1 Scheme of an imaging application

Non-imaging applications do not need the image of an object. They use different properties of the object interacting with an optical beam. The emerging beam is intercepted by a physical sensor, which provides a signal, processed in order to get information of various natures on the object.

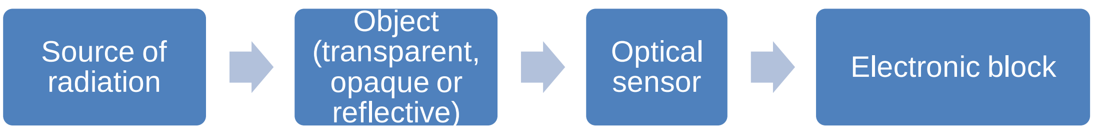

Figure 2 Scheme of a non-imaging application

No matter what the principle and the purpose of the assembly is, there is always needed an optical system, which interacts with an incident radiant beam and guides it toward a human observer or a physical detector. The optical system consists of different components, such as lenses, mirrors, diffraction gratings, prisms, fibers and others, depending on the optical phenomenon on which the application is based on.

The quality of the image or the characteristics of the emerging radiant beam depend on the geometry of the components, the apertures in the system and the properties of the material of which the elements are made of.

The image quality can be evaluated through an extended number of parameters, which, basically, are classified in:

- Geometric parameters
- Wave front parameters
- Fourier parameters.

These classes of parameters result from different mathematical approaches. Table 1 presents a synthesis of the parameters and the mathematic nature of the algorithms to compute them.

Table 1 Evaluation of image quality. Parameters

Parameter	**Notation**	**Mathematical basis**	**Short description**
Geometric parameters			
Longitudinal and lateral spherical aberration [mm]	dy’, ds’	Paraxial and extra-axial tracing of the objective rays	Variation of focus with aperture
Tangential and sagittal coma [mm]	k_T, k_S	Paraxial and extra-axial tracing of the objective rays and principal ray	Variation of magnification with aperture in oblique bundles of rays
Tangential and sagittal field curvatures [mm]	z_T, z_S	Paraxial and extra-axial tracing of the objective rays and principal ray	Variation of focus with aperture with skew rays
Distortion [%]	dy’	Paraxial and extra-axial tracing of the objective rays and principal ray	Variation of magnification with aperture
Spot Diagram	-	Vectorial ray tracing	Figure made of the points in the image plane
Spherocromatism [mm]	ds'_{cr}, dy'_{cr}	Paraxial and extra-axial tracing of the objective rays, with different refractive indexes	Variation of focus with aperture and refractive index
Wave front parameters			
Optical path difference (peak-to-valley and root mean square) [number of primary wavelengths]	P-V OPD, RMS OPD	Geometrical calculus	Distance between the real emerging wave front and the reference sphere
Rayleigh criterion	RL	States the maximum value of OPD=λ/4 for diffraction limited systems	Criterion to classify optical systems

Fourier parameters			
Point spread function (PSF [mm-2])	PSF	Fourier analysis	Normalized illumination distribution in the image point
Modulation transfer function [-]	MTF	Fourier analysis (geometric or diffraction calculus)	Ratio between image modulation and object modulation
Phase transfer function [deg]	PTF	Fourier analysis	Displacement of image (distortion)
Strehl ratio [-]	Strehl	Ratio of MTF of the real system and the ideal one	Global energy distribution

Optical systems are classified in diffraction limited, precise and commercial systems, based on Rayleigh criterion. Table 2 presents the equivalent values of geometrical, wave front and Fourier parameters for these classes of systems.

Table 2 Classes of optical systems

OPD	RMS OPD	Strehl ratio	ds' (axial spherical aberration)	k_T (tangential coma)	z_T, z_S (astigmatic curvatures)	System quality
0.0	0.0	1.00				ideal
0.25 RL=λ/16	0.018λ	0.99				
0.5 RL=λ/8	0.036λ	0.95				
1.0 RL=λ/4	0.07λ	0.80	$ds'_{Mmax} = \pm 16\lambda\left(\frac{f'}{D}\right)^2$	$k_T = \pm\frac{1.5\lambda}{n'\sin\tilde{\sigma}'}$	$\delta = \pm 2\lambda\left(\frac{f'}{D}\right)^2$	diffraction limited
2.0 RL=λ/2	0.14λ	0.40				precise
3.0 RL=0.75λ	0.21λ	0.10				commercial
4.0 RL=λ	0.29λ	0.00				

Generally, an optical application is based on the fundamental sizes, illustrated in figure 3:

- field of view (area on the surface of the sensor, on which the image/beam is projected)
- working distance (distance from the lens to the object)
- depth of field (distance along which the object can be displaced without changing the image quality)
- resolution (distance between the nearest two points that can be grasped as separated)
- size of the sensor (conventionally the horizontal size for design calculus)
- primary magnification (ratio of the sensor size and field of view)
- system magnification (ratio between the size of the final image on the monitor and the object size)

- ❒ aperture (f-Number or f/#, defined as the ratio between the focal length and the aperture stop diameter).

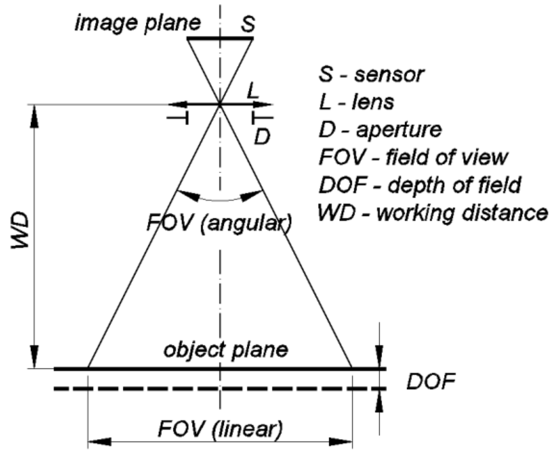

Figure 3 Fundamental sizes of an optical application

There is no direct analytical correlation between WD, FOV, PMAG and the focal length f'. For each application, the designer must create a model of the optical system and then optimize sizes such as optical power, f-number and WD.

The most important components that influence the fundamental sizes are the lenses. The optical systems consist of different combinations of three basic entities:

- ❒ single lens
- ❒ doublet
- ❒ triplet.

Doublets and triplets can be cemented or air-spaced.

Each application needs to follow the steps illustrated in figure 4.

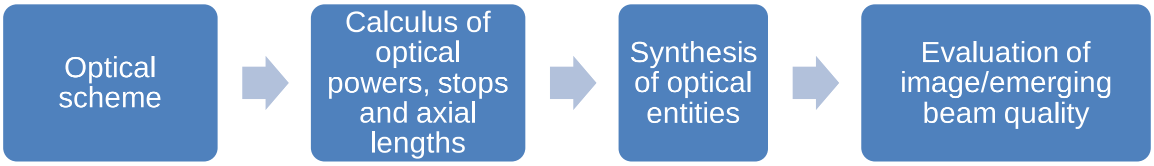

Figure 4 Stages in optical systems' design

Shortly, these stages can be defined as follows:

- ❒ The optical scheme is imposed by the function of the system. Within this stage, the designer establishes the functional assemblies or components. For instance, imaging systems include an objective as the main element and auxiliary components such as field lens, stops, eyepiece, screen or a projection surface.

- ❒ Given the input data depending on the application (working distance, magnification, position of the image or others), a calculus is performed in order to get the focal length of the assemblies and auxiliary components, their aperture and relative position along the optical axis.
- ❒ The optical basic entities must be synthetized through specific algorithms, considering the focal length and aperture obtained above and selecting compatible materials.
- ❒ After designing the full geometry of the components must be analyzed in order to evaluate the quality of the image or the characteristics of the emerging beam. The quality of the optical systems is a delicate issue, as the quality parameters are measured in number of wavelengths.

All these stages are subject to improvement or innovation and, thus to research.

The following chapters of the thesis describe results of research in all stages of design for optical systems integrated into mechatronic and medical applications.

The habilitation thesis shows the main scientific achievements after defending the PhD thesis at the University Politehnica Timişoara, on May 15th 1998.

The research results were systematized in four main thematic areas and illustrated through 10 selected papers, as follows:

1. Glass choice for basic optical entities

1.1 Gruescu C., Nicoara I., Popov D., Bodea R., Hora H. 2008 Optical Glass Compatibility For the Design of Apochromatic Systems *Science of Sintering* **40** 131-140.

2. Optical engineering applied in laser machining

2.1 Gruescu C., Lovasz E.-C., Ciupe V. 2014 Optics Optimization in Laser Spot Radius Minimization, *International Conference on Production Research – Regional Conference Africa, Europe and the Middle East, 3rd International Conference on Quality and Innovation in Engineering and Management* 231-234.

2.2 Gruescu C., Ionescu C., Nicoara I., Lovasz A. 2012 Experimental Optimization of Process Parameters in Laser Cutting of Polycarbonate Gears *Mechanika Journal* **18**(2) 233-238.

3. Document digitization

3.1 Lovasz E-Ch., Gruescu C.M., Ciupe V., Carabas I., Margineanu D., Maniu I. and Dehelean N. 2012 Advanced Digitization Techniques in Retrieval of Mechanism and Machine Science *Proc. of the XIth TMM Liberec 2012 Mechanisms and Machine Science* **8** 35-42.

3.2 Ciupe V., Lovasz E-C., Gruescu C.M. 2012 High Quality Document Digitization Equipment *Mechanisms, Mechanical Transmissions and Robotics, Applied Mechanics and Materials* 162 589-596.

3.3 Ciupe V., Lovasz E.C., Reessing M., Henkel V., Gruescu C.M., Zabava E.S. 2014 Interactive animation production by means of advanced image processing *SYROM 2013, Mechanisms and Machine Science* **17** 329-337.

4. Optical engineering in medical investigation

4.1 Gruescu C.M., Garaiman A., Lovasz E.-C. 2015 Modeling of human spinal column and simulation of spinal deformities *Mechanika Journal* **3** 214-219.

4.2 Lovasz E-C., Gruescu C. M., Garaiman A., Carabas I., Bodea R. 2013 Scanning System Integrated within Biometric Measurements*New Trends in Medical and Service Robots. Theory and Integrated Applications. MeSRob 2013 Mechanisms and Machine Science* **16** 131-144.

4.3 Vutan A.M., Ciupe V., Gruescu C.M., Lovasz E.-C. 2018 Experimental Method for Dynamic Evaluation of Spinal Column Deformation Exercises *Proc. of The 12th IFToMM International Symposium on Science of Mechanisms and Machines (SYROM 2017) MMS* **47** 137-146.

4.4 Vutan A.-M., Gruescu C.M., Ciupe V., Margineanu D.and Lovasz E.-C.2018 Effectiveness of Physical Exercises in the Treatment of Scoliosis - Mathematical Approach *MESROB 2018 MMS* **65** 25-34.

II. Scientific achievements regarding optical design in mechatronic applications

1. Basic optical design. Glass choice

1.1 Statement of problem

The design of optical basic entities (singlet, doublet and triplet) is based on algorithms, which assume that the properties of the optical materials are known. The most important properties of optical glasses for lens design are the refractive and dispersive ones. The quality parameters of the resulting system depend on these properties and on the compatibility of the materials used for doublets and triplets. The literature is poor in glass choice recommendations [2, 32, 36, 53, 56, 70], and the offer of optical glass is actually very rich [86, 102]. The designer must find some criteria based on reason in choosing the suitable sorts. The random choice is very inefficient and, in most cases, unsuccessful. The results of this research offer a solution to this problem. The practical solutions described below provide very high image quality for apertures twice larger than the traditional ones.

The most complex optical entity is the triplet. It is an apochromatic optical system, which needs a specific combination of optical glass sorts, whose dispersive properties insure the correction of longitudinal chromatic aberrations and secondary spectrum. An apochromatic system accomplishes the superposition of image abscissas for three wavelengths, so that the secondary spectrum is much lower than for any other optical entity. The traditional optical system, which satisfies these conditions, is the cemented apochromatic triplet (fig.1.1). The assembly contains two positive lenses and one negative lens.

The design algorithm supposes that the operator has already chosen the glass sorts. The literature offers only general recommendations or a minimum number of compatible glasses [36, 70]. An efficient use of the large number of glass sorts needs a mathematical approach.

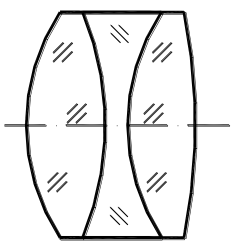

Figure 1.1 The apochromatic cemented triplet

The database to investigate contains the glass sorts offered by the Schott Catalogue [86]. The parameters taken into account are the refractive indexes of the spectral lines g, F', e, C', s, the Abbe number ν_e and the relative partial dispersion P_{ge}.

The Schott Catalogue contains over120 glass sorts available for the visible range. The choice of three compatible glasses from a 120 elements string is difficult or impossible to achieve by permutations or randomization, not to mention the time needed. The designer should find some mathematical criteria, which can lead to exact solutions.

1.2 Theoretical basis

The design of the cemented triplet intends to correct the longitudinal chromatic aberration and secondary spectrum using the following system of equations [36]:

$$\begin{cases} c_a = \dfrac{1}{f' \cdot E(\nu_a - \nu_c)}\left(\dfrac{P_b - P_c}{\Delta n_a}\right) \\ c_b = \dfrac{1}{f' \cdot E(\nu_a - \nu_c)}\left(\dfrac{P_c - P_a}{\Delta n_b}\right) \\ c_c = \dfrac{1}{f' \cdot E(\nu_a - \nu_c)}\left(\dfrac{P_a - P_b}{\Delta n_c}\right) \end{cases}, \tag{1.1}$$

where c is the curvature of the elements

f' – the effective focal length of the triplet

ν - the Abbe number

Δn – the main dispersion

P – the relative partial dispersion

a, b, c – the indexes of the three component lenses.

In the expression of the curvatures (1.1), the denominator contains the size E:

$$E = \frac{\nu_a(P_b - P_c) + \nu_b(P_c - P_a) + \nu_c(P_a - P_b)}{\nu_a - \nu_c}, \tag{1.2}$$

which depends on the dispersive parameters of the glasses. The previous design experience shows that proper glasses to form a triplet must cover characteristics satisfying the relations:

$$\nu_a > \nu_b > \nu_c \wedge P_a < P_b < P_c, \tag{1.3}$$

which indicates the sorts choice in the families FK (Flour - Crown) – KzFS (special short Flint) – SF (dense Flint) [36].

The size E has no physical significance and it is not a dispersive parameter, however, it is very important. From algebraic point of view, E must be a negative number and on absolute value, E should be as large as possible. Keeping these conditions, positive curvatures for the lenses a and c, respectively negative curvature for the lens b are obtained. Also, small curvatures (respectively, large radii and small powers) are insured. Usually, large amount of geometrical aberrations, especially spherical, which are hard or impossible to correct, affect the resulted systems because the design of the triplet only considers the correction of the chromatic aberrations and secondary spectrum. In addition, the triplets are always low speed systems, limited to f-numbers in the range from f/8 to f/10, due to uncorrected geometrical aberrations.

Since the glass sort offer became larger and larger, original selection software was developed. The appropriate combinations for the apochromatic triplet were found using the Schott database [86], the selection conditions (1.3), completed with the condition ABS(E)>0.0145.

1.3 Numerical results

Suited combinations for the cemented apochromatic triplet, obtained by using the original software, are presented in Table 1.1. The first column indicates the value of the size E, computed with relative dispersions $P_{e\text{-}g}$ and Abbe numbers ν_e. The columns 2…4 indicate the suitable sorts for apochromatic triplets with the structure: positive-negative-positive elements

Table 1.1 Twenty-two solutions of compatible glasses for apochromatic triplets

E	Sort a	Sort b	Sort c
-0.01455	FK51	KZFS1	TIF6
-0.01517	FK51	KZFSN2	TIF6
-0.01501	FK52	KZFSN2	TIF6
-0.01494	FK54	BK3	TIF6
-0.01517	FK54	KZFS1	TIF6
-0.01485	FK54	KZFS6	TIF6
-0.01547	FK54	KZFSN2	SF57
-0.01486	FK54	KZFSN2	SF58
-0.01546	FK54	KZFSN2	SF59
-0.01623	FK54	KZFSN2	TIF6
-0.01470	FK54	KZFSN9	TIF6
-0.01470	FK54	LAK16A	TIF6
-0.01461	FK54	LAK28	TIF6
-0.01501	FK54	LAK31	TIF6
-0.01466	FK54	LAK33	TIF6
-0.01492	FK54	LAK8	TIF6
-0.01463	FK54	LAK9	TIF6
-0.01503	FK54	LAKL21	TIF6
-0.01498	FK54	LAKN14	TIF6
-0.01492	KZFS7A	SFL57	TIF6
-0.01495	KZFSN5	SF58	TIF6
-0.01541	KZFSN5	SF59	TIF6

1.4 Application

Based on the results in table 1.1, it has been developed a study, which included the synthesis and the analysis of 88 triplets. The design input data was f'=100, s= $-\infty$ (object abscissa), $\omega=5^o$ (half – field). For each glasses combination, four options were taken into account: $0.5c_a$, $0.6c_a$, $0.7c_a$ and $0.8c_a$, representing values of the first curvature. Regarding this aspect, the literature indicates a c_1/c_a ratio of about 0.6 [36, 70]. The design algorithm was enriched by widening the ratio range and, practically, all possible solutions were found.

The triplets designed using original software were analyzed with the program OSLO LT, from Lambda Research Ltd. The study allows, synthetically, to the following remarks:

- ❐ The glass choice and the c_1/c_a ratio influence the shape of the lenses
- ❐ There are seven possible combinations of lens shapes, presented in figure 1.2
- ❐ The most significant influence parameter on the image quality is the materials combination, meaning the relationship between the refractive and dispersive characteristics
- ❐ The best solutions follow the C(convergent)- D(divergent) – C(convergent) scheme and also, global biconvex or convergent meniscus shape
- ❐ From diffraction point of view, the best quality is obtained for the c_1/c_a ratio within the range (0.5…0.6).

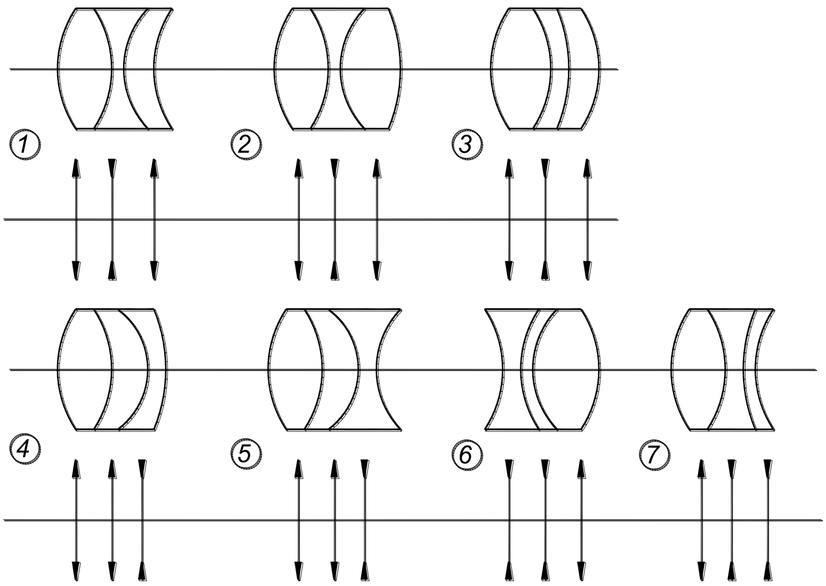

Figure 1.2 Seven possible shapes of lenses forming an apochromatic triplet

- ❐ The most favorable glass combinations contain for the first lens a sort from the flour-crown family (FK), for the middle lens a sort from the short flint (KZFS) or crown-lanthanum (LAK) and for the last lens a sort from flint-lanthanum family (TIF)

- ❒ Diffraction limited systems result only for f-numbers higher than f/5. The primary solutions, obtained by applying the design algorithm, are obviously not high quality systems, therefore they can be improved by defocusing
- ❒ Bending is not at all efficient in increasing quality, thus the geometry found by applying the algorithm is unchangeable
- ❒ The triplets, which were studied, are very good from chromatic point of view, meaning that the longitudinal chromatic aberration and the secondary spectrum are corrected, but the spherical residual aberration, which establishes the aperture, cannot be decreased.

The diffraction-limited solutions are briefly presented in table 1.2. The short flint sorts (SF) combinations are not present in the table because even for f/10 they are not diffraction limited. The diffraction-limited solutions are indicated with grey filling, while the solutions, which preserve high image quality, are marked with yellow filling.

Table 1.2 Diffraction limited apochromats designed using the compatible glass triplets mathematically chosen

f'=100, s= -∞, ω=5°							
ID	**sorts**	**shape**	**c_1/c_a**	**f'/D**	**h [mm]**	**RMS OPD**	**Strehl**
1	**FK51-KZFS1-TIF6 (488.841; 616.483; 621.307)** 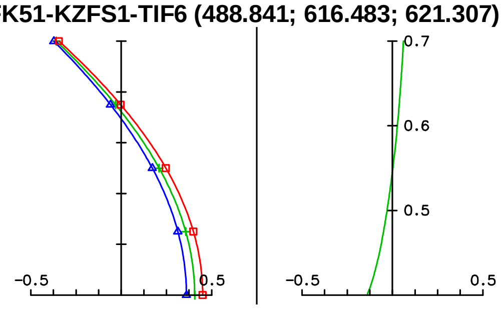	2	0.5	**1/10**	**5**	**0.016**	**0.963**
				1/8	**6.25**	**0.025**	**0.948**
				1/7	**7**	**0.033**	**0.929**
				1/6.25	**8**	**0.049**	**0.874**
				1/5	**10**	**0.124**	**0.567**
				1/4	**12**	**0.318**	**0.124**
		1	0.6	**1/10**	**5**	**0.036**	**0.948**
				1/8	**6.25**	**0.077**	**0.785**
				1/7	**7**	**0.116**	**0.527**
				1/6.25	**8**	**0.193**	**0.222**
		1	0.7	**1/10**	**5**	**0.086**	**0.745**
				1/8	**6.25**	**0.195**	**0.239**
2	**FK51-KZFSN2-TIF6 (488.841; 561.540; 621.307)** 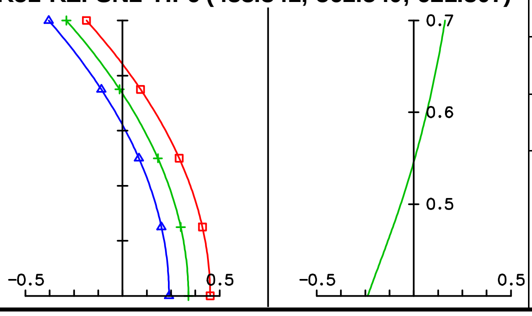	1	0.5	**1/10**	**5**	**0.151**	**0.351**
		1	0.6	**1/10**	**5**	**0.079**	**0.781**
				1/8	**6.25**	**0.164**	**0.371**
		1	0.7	**1/10**	**5**	**0.189**	**0.288**
		1	0.8	**1/10**	**5**	**0.309**	**0.150**

3	FK52-KZFSN2-TIF6 (487.814; 561.540; 621.307) 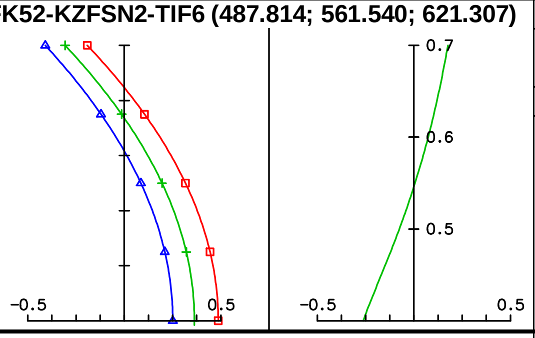	1	0.5	1/10	5	0.190	0.178
		1	0.6	1/10	5	0.086	0.755
				1/8	6.25	0.177	0.332
		1	0.7	1/10	5	0.216	0.226
		1	0.8	1/10	5	0.341	0.131
4	FK54-KZFS1-TIF6 (438.903; 616.483; 621.307) 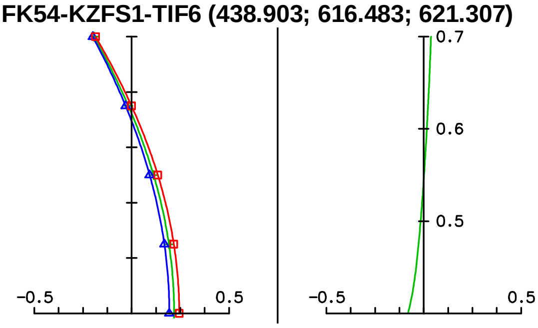	3	0.5	1/10	5	0.015	0.964
				1/8	6.25	0.033	0.929
				1/7	7	0.051	0.869
				1/6.25	8	0.089	0.695
				1/5	10	0.249	0.180
		2	0.6	1/10	5	0.027	0.970
				1/8	6.25	0.061	0.854
				1/7	7	0.095	0.683
				1/6.25	8	0.159	0.337
5	FK54-KZFS6-TIF6 (438.903; 595.483; 621.307) 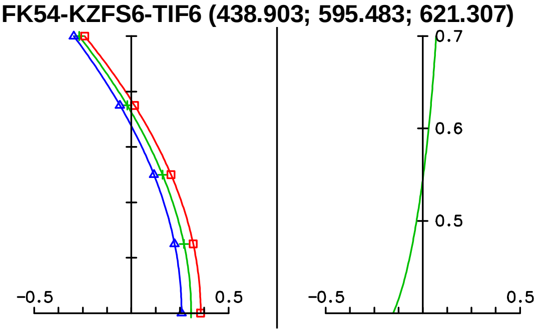	4	0.5	1/10	5	0.030	0.963
				1/8	6.25	0.064	0.848
				1/7	7	0.096	0.685
				1/6.25	8	0.159	0.352
		7	0.6	1/10	5	0.043	0.926
				1/8	6.25	0.093	0.700
				1/7	7	0.141	0.440
		4	0.7	1/10	5	0.040	0.932
				1/8	6.25	0.086	0.739
				1/7	7	0.130	0.503
		5	0.8	1/10	5	0.055	0.887
				1/8	6.25	0.120	0.560
				1/7	7	0.184	0.268
6	FK54-KZFSN2-SF57 (438.903; 561.540; 855.236) 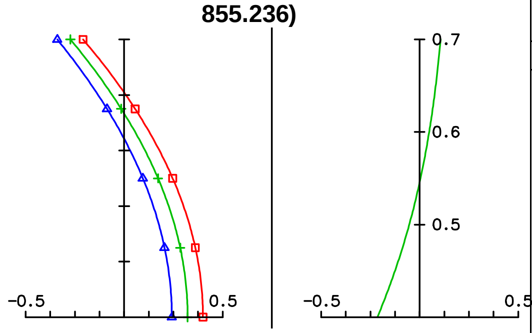	2	0.5	1/10	5	0.139	0.398
		1	0.6	1/10	5	0.073	0.805
				1/8	6.25	0.159	0.370
		1	0.7	1/10	5	0.174	0.332
		1	0.8	1/10	5	0.312	0.142
7	FK54-KZFSN2-SF58 (438.903; 561.540; 928.213) 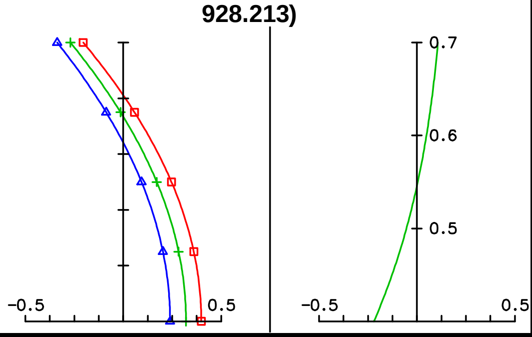	2	0.5	1/10	5	0.153	0.323
		1	0.6	1/10	5	0.073	0.803
				1/8	6.25	0.158	0.375
		1	0.7	1/10	5	0.178	0.325
		1	0.8	1/10	5	0.322	0.147

8	**FK54-KZFSN2-SF59 (438.903; 561.540; 963.202)** 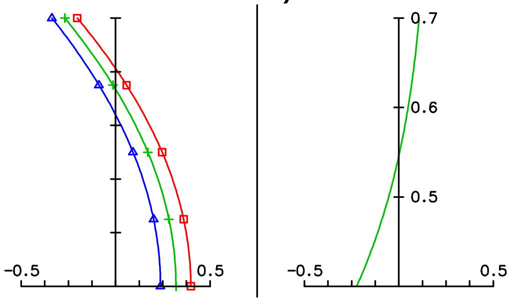	2	0.5	**1/10**	**5**	**0.167**	**0.254**
		7	0.6	**1/10**	**5**	**0.073**	**0.803**
				1/8	**6.25**	**0.158**	**0.377**
		1	0.7	**1/10**	**5**	**0.173**	**0.333**
		1	0.8	**1/10**	**5**	**0.326**	**0.149**
9	**FK54-KZFSN2-TIF6 (438.903; 561.540; 621.307)** 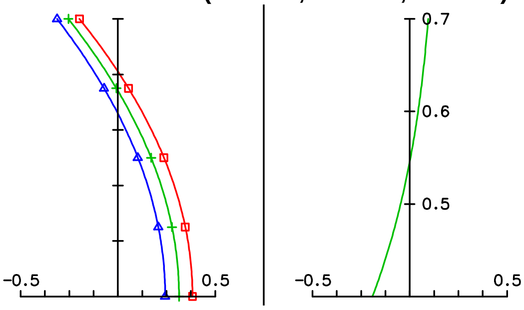	2	0.5	**1/10**	**5**	**0.084**	**0.707**
				1/8	**6.25**	**0.134**	**0.441**
				1/7	**7**	**0.173**	**0.266**
		1	0.6	**1/10**	**5**	**0.067**	**0.832**
				1/8	**6.25**	**0.148**	**0.408**
		1	0.7	**1/10**	**5**	**0.158**	**0.379**
		1	0.8	**1/10**	**5**	**0.278**	**0.138**
10	**FK54-LAK16A-TIF6 (438.903; 737.516; 621.307)** 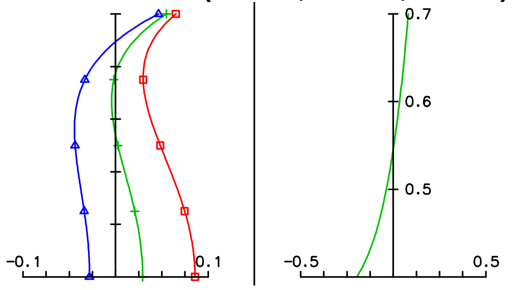	3	0.5	**1/10**	**5**	**0.207**	**0.228**
		2	0.6	**1/10**	**5**	**0.028**	**0.970**
				1/8	**6.25**	**0.039**	**0.942**
				1/7	**7**	**0.045**	**0.923**
				1/6.25	**8**	**0.052**	**0.896**
		1	0.7	**1/10**	**5**	**0.113**	**0.594**
		1	0.8	**1/10**	**5**	**0.579**	**0.070**
11	**FK54-LAK28-TIF6 (438.903; 748.505; 621.307)** 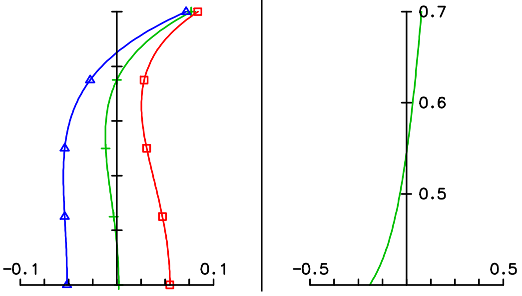	3	0.5	**1/10**	**5**	**0.081**	**0.729**
				1/8	**6.25**	**0.729**	**0.240**
		2	0.6	**1/10**	**5**	**0.028**	**0.975**
				1/8	**6.25**	**0.035**	**0.951**
				1/7	**7**	**0.041**	**0.935**
				1/6.25	**8**	**0.052**	**0.899**
				1/5	**10**	**0.119**	**0.550**
		1	0.7	**1/10**	**5**	**0.106**	**0.632**
				1/8	**6.25**	**0.245**	**0.135**
		1	0.8	**1/10**	**5**	**0.228**	**0.166**
12	**FK54-LAK31-TIF6 (438.903; 700.562; 621.307)** 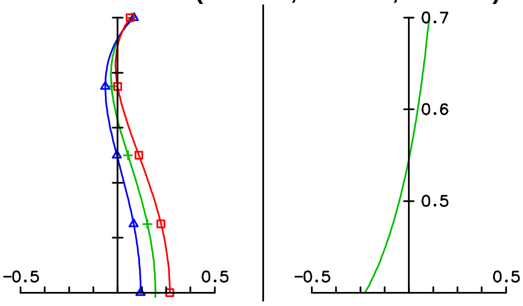	3	0.5	**1/10**	**5**	**0.134**	**0.472**
		1	0.6	**1/10**	**5**	**0.042**	**0.935**
				1/8	**6.25**	**0.064**	**0.855**
				1/7	**7**	**0.079**	**0.791**
				1/6.25	**8**	**0.098**	**0.700**
				1/5	**10**	**0.111**	**0.658**
		1	0.7	**1/10**	**5**	**0.155**	**0.393**
		1	0.8	**1/10**	**5**	**0.315**	**0.113**

13	**FK54-LAK33-TIF6 (438.903; 757.522; 621.307)** 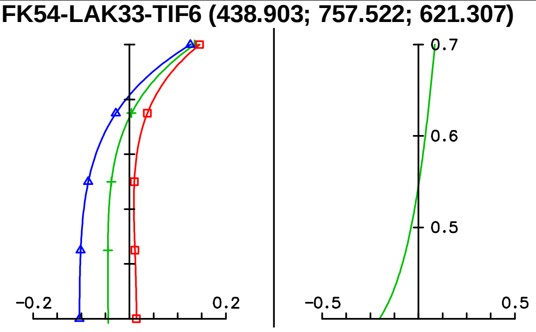	3	0.5	**1/10**	**5**	**0.101**	**0.627**
		2	0.6	**1/10**	**5**	**0.029**	**0.967**
				1/8	**6.25**	**0.042**	**0.933**
				1/7	**7**	**0.051**	**0.899**
				1/6.25	**8**	**0.073**	**0.803**
		1	0.7	**1/10**	**5**	**0.115**	**0.264**
		1	0.8	**1/10**	**5**	**0.249**	**0.138**
14	**FK54-LAK8-TIF6 (438.903; 716.536; 621.307)** 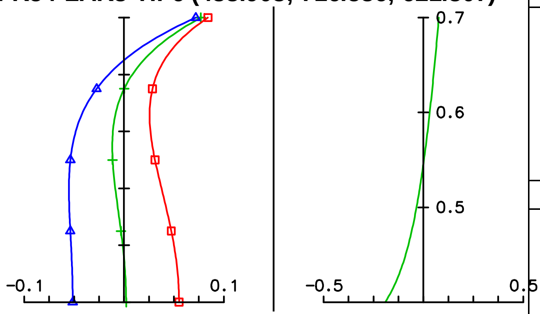	3	0.5	**1/10**	**5**	**0.097**	**0.649**
		2	0.6	**1/10**	**5**	**0.033**	**0.957**
				1/8	**6.25**	**0.049**	**0.911**
				1/7	**7**	**0.058**	**0.879**
				1/6.25	**8**	**0.067**	**0.843**
				1/5	**10**	**0.085**	**0.741**
		1	0.7	**1/10**	**5**	**0.180**	**0.507**
		1	0.8	**1/10**	**5**	**0.271**	**0.130**
15	**FK54-LAK9-TIF6 (438.903; 694.545; 621.307)** 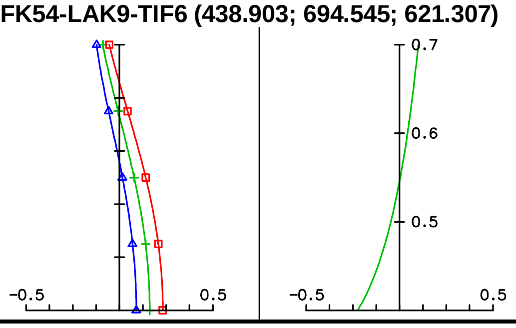	3	0.5	**1/10**	**5**	**0.099**	**0.640**
		1	0.6	**1/10**	**5**	**0.039**	**0.940**
				1/8	**6.25**	**0.062**	**0.862**
				1/7	**7**	**0.080**	**0.792**
				1/6.25	**8**	**0.103**	**0.685**
				1/5	**10**	**0.123**	**0.584**
		1	0.7	**1/10**	**5**	**0.148**	**0.424**
		1	0.8	**1/10**	**5**	**0.301**	**0.126**
16	**FK54-LAKL21-TIF6 (438.903; 643.596; 621.307)** 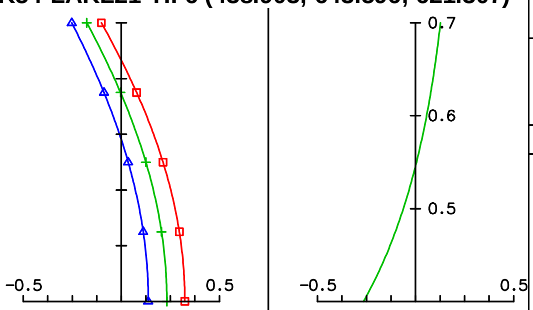	3	0.5	**1/10**	**5**	**0.075**	**0.783**
				1/8	**6.25**	**0.186**	**0.237**
		1	0.6	**1/10**	**5**	**0.066**	**0.841**
				1/8	**6.25**	**0.136**	**0.555**
				1/7	**7**	**0.191**	**0.313**
		1	0.7	**1/10**	**5**	**0.207**	**0.234**
		1	0.8	**1/10**	**5**	**0.395**	**0.107**
17	**FK54-LAKN14-TIF6 (438.903; 700.552; 621.307)** 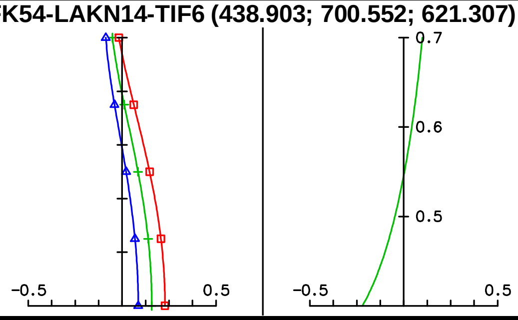	3	0.5	**1/10**	**5**	**0.081**	**0.750**
				1/8	**6.25**	**0.204**	**0.186**
		1	0.6	**1/10**	**5**	**0.039**	**0.942**
				1/8	**6.25**	**0.063**	**0.870**
				1/7	**7**	**0.074**	**0.812**
				1/6.25	**8**	**0.096**	**0.720**
				1/5	**10**	**0.113**	**0.687**
				1/4	**12**	**0.275**	**0.315**
		1	0.7	**1/10**	**5**	**0.147**	**0.437**
		1	0.8	**1/10**	**5**	**0.300**	**0.125**

The meaning of the numbers and images in the table above is as follows:

- The glasses combination with the codes attached and a brief graphical description of aberrations (spherochromatism and chromatic focal shift) are presented in column 1.
- According to the numbers in figure 1.2, the shape of the triplets is indicated in column 2 for each glass combination.
- The c_1/c_a ratio is presented in column 3.
- The f-number, respectively the incidence height are shown in columns 4 and 5.
- The last two columns, 6 and 7, provide the quality parameters (wavefront statistical analysis and energetic characteristics) – RMS OPD and Strehl ratio.

The diffraction-limited solutions and their acceptable apertures are synthesized in table 1.3.

Table 1.3 Synthetic table containing diffraction limited apochromats and their maximum permissible apertures

Glass combination	c_1/c_a	f'/10	f'/8	f'/7	f'/6.25
FK51-KZFS1-TIF6	0.5	x	x	x	x
	0.6	x	x		
FK51-KZFSN2-TIF6	0.6	x			
FK52-KZFSN2-TIF6	0.6	x			
FK54-KZFS1-TIF6	0.5	x	x	x	
	0.6	x	x	x	
FK54-KZFS6-TIF6	0.5	x	x		
	0.6	x			
	0.7	x			
	0.8	x			
FK54-KZFSN2-SF57	0.6	x			
FK54-KZFSN2-SF58	0.6	x			
FK54-KZFSN2-SF59	0.6	x			
FK54-KZFSN2-TIF6	0.6	x			
FK54-KZFSN9-TIF6	0.5	x	x		
FK54-LAK16A-TIF6	0.6	x	x	x	x
FK54-LAK28-TIF6	0.6	x	x	x	x
FK54-LAK31-TIF6	0.6	x	x	x	
FK54-LAK33-TIF6	0.6	x	x	x	x
FK54-LAK8-TIF6	0.6	x	x	x	x
FK54-LAK9-TIF6	0.6	x	x	x	
FK54-LAKL21-TIF6	0.5	x			
	0.6	x			
FK54-LAKN14-TIF6	0.6	x	x	x	

1.5 Possibility to increase the aperture of triplets by introducing aspheric surfaces

As the previous paragraph shows, only 53 solutions of 88 are diffraction limited (for f-numbers within f/10…f/5). It is possible to improve the solutions with high f-number or bring the low quality ones into the category of diffraction limited as follows. For instance, figure 1.3 presents the solution FK54-LAK33-TIF6 (table 1.2, ID 13, c_1/c_a=0.6) which is diffraction limited (RMS OPD <0.07λ and Strehl ratio>0.80) up to the aperture f/6.25.

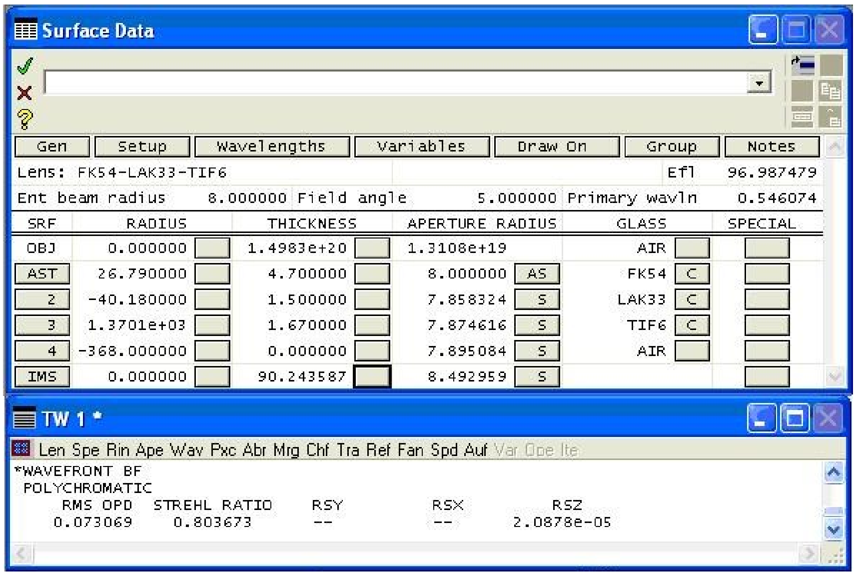
Surface Data

Gen | Setup | Wavelengths | Variables | Draw On | Group | Notes

Lens: FK54-LAK33-TIF6 Efl 96.987479

Ent beam radius 8.000000 Field angle 5.000000 Primary wavln 0.546074

SRF	RADIUS	THICKNESS	APERTURE RADIUS		GLASS		SPECIAL
OBJ	0.000000	1.4983e+20	1.3108e+19		AIR		
AST	26.790000	4.700000	8.000000	AS	FK54	C	
2	-40.180000	1.500000	7.858324	S	LAK33	C	
3	1.3701e+03	1.670000	7.874616	S	TIF6	C	
4	-368.000000	0.000000	7.895084	S	AIR		
IMS	0.000000	90.243587	8.492959	S			

TW 1 *

Len Spe Rin Ape Wav Pxc Abr Mrg Chf Tra Ref Fan Spd Auf Var Ope Ite

*WAVEFRONT BF
POLYCHROMATIC

RMS OPD	STREHL RATIO	RSY	RSX	RSZ
0.073069	0.803673	--	--	2.0878e-05

Figure 1.3 Surface data and wavefront parameters at aperture f/6.25

A small increase of the aperture produces a fast loss of quality. At h=8 mm (f/6.25) the Strehl ratio is 0.803, as shown in figure 1.3. At h=10 mm (f/5) the Strehl ratio becomes 0.209, as shown in figure 1.4, which is unacceptable. This large decrease is due to a fast increase of longitudinal spherical aberration, which is in a strongly nonlinear relationship to the height (the aberration is approximately proportional to the square of the height).

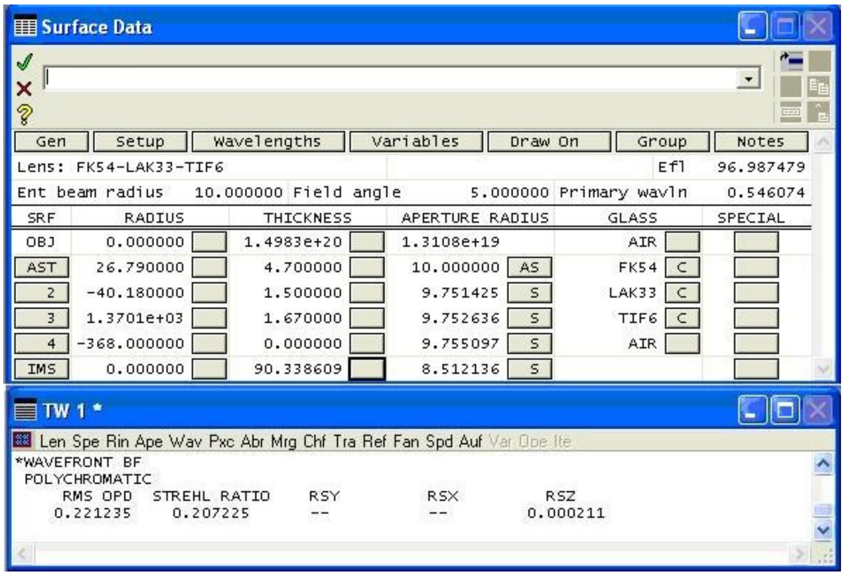
Surface Data

Gen | Setup | Wavelengths | Variables | Draw On | Group | Notes

Lens: FK54-LAK33-TIF6 Efl 96.987479

Ent beam radius 10.000000 Field angle 5.000000 Primary wavln 0.546074

SRF	RADIUS	THICKNESS	APERTURE RADIUS		GLASS		SPECIAL
OBJ	0.000000	1.4983e+20	1.3108e+19		AIR		
AST	26.790000	4.700000	10.000000	AS	FK54	C	
2	-40.180000	1.500000	9.751425	S	LAK33	C	
3	1.3701e+03	1.670000	9.752636	S	TIF6	C	
4	-368.000000	0.000000	9.755097	S	AIR		
IMS	0.000000	90.338609	8.512136	S			

TW 1 *

Len Spe Rin Ape Wav Pxc Abr Mrg Chf Tra Ref Fan Spd Auf Var Ope Ite

*WAVEFRONT BF
POLYCHROMATIC

RMS OPD	STREHL RATIO	RSY	RSX	RSZ
0.221235	0.207225	--	--	0.000211

Figure 1.4 Surface data and wavefront parameters at aperture f/5

Indeed, as figure 1.5 shows, the longitudinal spherical aberration has a very high gradient in respect with the height. The spherochromatism indicates that the apochromatism is preserved as well as the focal chromatic shift. That means the chromatic characteristics are independent to incidence height and the vulnerable element is the spherical residual aberration. In figure 1.6 are shown the spherochromatism and the chromatic focal shift.

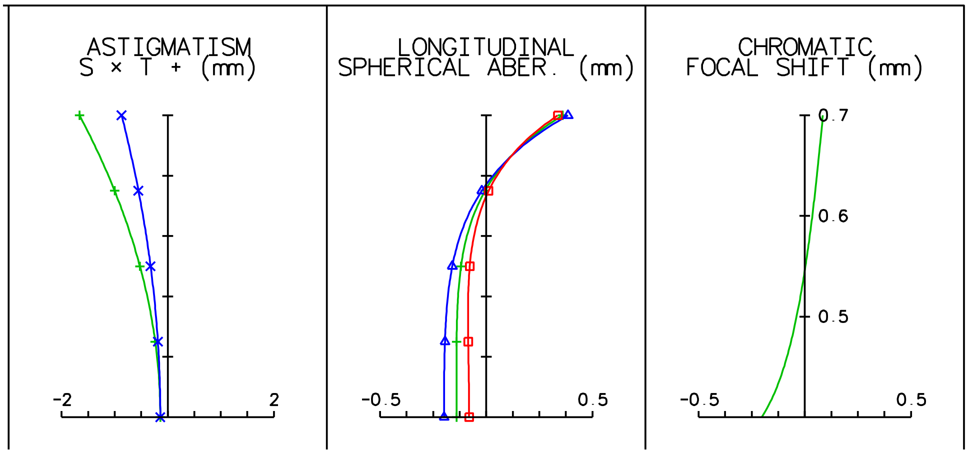

Figure 1.5 Spherochromatism and chromatic focal shift at a double aperture (f/5)

Small changes of radii or thicknesses actually introduce only smaller or larger amounts of defocusing but have no effect on curves' shape; therefore bending is not efficient in changing the shape of spherochromatism curves.

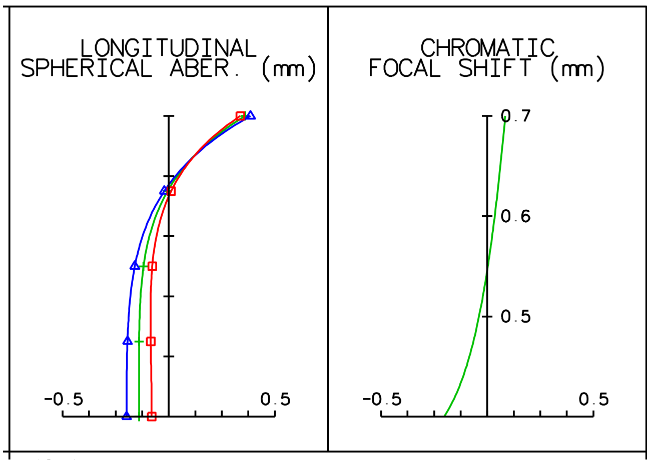

Figure 1.6 Spherochromatism and chromatic shift are not affected by increasing aperture

The only possibility to change the spherochromatic curves' shape is to turn one of the spherical surfaces into an aspheric one. The suggestion is to transform for the last surface (the fourth one).As the thickness of the middle lens (TH2) controls the position of the spherochromatic curves along the optical axis and the conic constant of the forth surface (CC4) can modify the spherical residual aberration, the slider-wheel setup defined TH2 and CC4 as variable parameters. The aspheric system, scaled to exactly f'=100mm is presented in figure 1.7.

The conic constant, equal to 89, shows that the generating curve is an ellipse. The conic constant and the radius of the osculate circle at the surface vertex are needed for the generating ellipse.

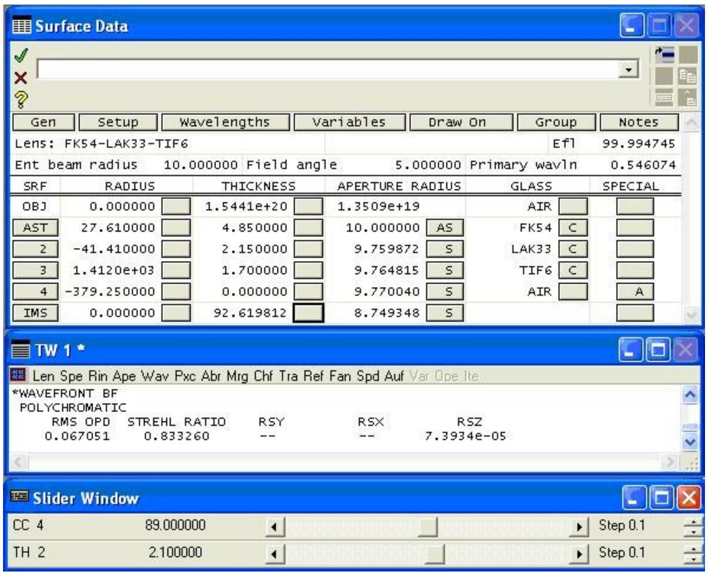

Figure 1.7 Full data of the scaled aspheric system

These values are k=89 and r= 378.25 (which is the radius of the initial sphere). Considering a and b the half-axis of the ellipse along the optical axis and, respectively, along the y-axis, the following relations are useful:

$$k = \frac{b^2}{a^2} - 1 \qquad r = \frac{b^2}{a} \tag{1.4}$$

Solving the system (1.4) the solutions are a=4.31 mm; b=40.43 mm.

The equation of the generating ellipse becomes:

$$z = \frac{r\left(1 - \sqrt{1 - (k+1)\frac{y^2}{r^2}}\right)}{k+1} = 28.586\left(1 - \sqrt{1 - 5.56.10^{-4} y^2}\right) \tag{1.5}$$

1.6 Conclusions and contributions

The research work developed within the present chapter can be summarized as follows:

- The literature is poor in glass choice recommendations and the offer of optical glass is actually very large.
- The results of this work offer a solution to the problem of choosing the suitable sorts by means of stating mathematical criteria, implemented in software application.
- The practical solutions provided by the application lead to high image quality for apertures twice larger than the traditional ones.

- Aspheric surfaces can also bring substantial improvement in image quality for systems, which are mainly affected by spherical residual aberration. The proper generating noncircular curve is hard to find without specialized soft and needs appropriate skills of the human operator.

The original contributions in this chapter are:

- Mathematical formulation of criteria to choose compatible optical materials suited for the design of cemented triplets.
- Development of software application to apply the above formulation on an optical glass database (Schott catalogue containing over 120 sorts).
- Synthesis and analysis of 88 apochromatic triplets built with combinations of glasses resulted from the application.
- Demonstration that appropriate glass choice provides high quality entities. Residual spherical aberration, chromatic aberration and secondary spectrum are very small, so that the systems qualify as diffraction limited at large apertures. The literature recommends the use of apochromatic triplets with f-numbers up to 1/8…1/10. The results of this work provided systems which are diffraction limited up to 1/5…1/6.25.
- Application of choice of one aspheric surface, which turns a low quality system into a diffraction limited one.

2. Optical engineering applied in laser machining

2.1 Optics optimization in laser spot radius minimization

2.1.1 Statement of problem

Laser technology develops in fast progress, aiming to increase precision and efficiency, to reduce material and time waste. Non-conventional technologies replace conventional ones and, in addition, perform operations impossible to apply with older technologies.

Rapid spread and improvement of laser technologies implies better or new optical systems.

Laser optics comprise of two basic components, namely the expender and the focusing objective. The expander is a reversed Galileo telescope and the objective is a positive lens. Usually, the expanders ensure a magnification within the range of [1.5…10] X, depending on the aperture of the laser beam source and the power density admitted by the lens material.

The objectives are designed for effective focal lengths within the range of [40…200] mm, depending on the working distance needed in the application. Objectives may consist of a singlet, a doublet or a system of more lenses, especially in the schemes of scanning laser systems.

Optical design is often referred to as general scheme in books [2, 17, 56, 70] or papers [14]. Optical parameters such as working distance and defocusing are called in relation with the spot size [4, 66]. The spot size and shape establish the actual energy distribution and finally, the precision and efficiency of the process.

The spot size depends on the quality of the optical system. Nowadays, the quality is expressed in wavefront parameters, sometimes related directly to Airy disk.

Most industrial power lasers work within the infrared range. The optical design is more difficult than for the visible range because of the small number of materials available for lens manufacturing.

The basic principles in laser optics design, recommended by manufacturers [108, 111] can be summarized as follows:

- The optical assemblies of the expander are singlets. This major simplifying is possible because of monochromatic radiation and theoretically zero slope of the beam. The residual spherical aberration remains the most important problem. As it influences directly the size of the spot, the design of lenses must apply algorithms based on spherical aberration minimization.

- ❐ The objective, large-sized in aperture, is also exposed mainly to spherical aberration.
- ❐ The most important parameters refer to focus abscissa, shape and size of the spot and depth of focus.
- ❐ Ideally, the spot should be circular for a uniform energy distribution. Its size can be optically controlled.

Practically, the spot size assumes two additive components, one due to diffraction and second due to residual spherical aberration:

$$d_{spot\ total} = d_{spot\ difractional} + d_{spot\ aberational}, \tag{2.1.1}$$

where:

$$d_{spot\ difractional} = \frac{4\lambda M^2 f}{\pi D}, \tag{2.1.2}$$

$$d_{spot\ aberational} = \frac{kD^3}{f^2}. \tag{2.1.3}$$

In relationships (2.1.2) and (2.1.3) λ represents the wavelength [µm], M – modal parameter of the beam [-], f – effective focal length of the objective [mm], D – aperture of the objective [mm], k – non-dimensional coefficient depending on the refractive index [-].

The spot size is strongly dependent on the f-number of the objective (denoted f/#):

$$f/\# = \frac{f}{D}. \tag{2.1.4}$$

Practically, the design input data asks for the focal length as well as for the aperture. The literature recommends estimation relations for one of them in case the other one is given. If the focal length is fixed, the optimum aperture is:

$$D = \sqrt[4]{\frac{4\lambda M^2 f^3}{3\pi k}}. \tag{2.1.5}$$

If the aperture is imposed, the recommendation for the focal length is:

$$f = \sqrt[3]{\frac{\pi k D^4}{2\lambda M^2}}. \tag{2.1.6}$$

Usually, the aperture is fixed because it is imposed by the expanded beam diameter of the radiation emitted from the laser source. The magnification of the expander results according to material admitted power density.

The spot abscissa and the depth of focus are correlated and influence directly the spot size. The spot abscissa is adjustable by defocusing. Approximately, the depth of focus can be estimated as:

$$DOF = \frac{8\lambda M^2}{\pi}\sqrt{\rho^2 - 1}\left(\frac{f}{D}\right)^2, \tag{2.1.7}$$

where ρ is a tolerance factor (for instance ρ=1.10 signifies a growth of 10% of the spot diameter).

The relations above may be used for dimensioning the optical power and clear apertures in the system. The actual quality parameters depend on the synthesis of the components.

2.1.2 Optics design for a 10.6 μM laser technology

The present application describes the design of an optical system included in the scheme of a laser cutting machine. The radiation source is a CO2 laser (10.6μm), emitting a 17 mm diameter beam, at the power of 500 W, needed to tailor polycarbonate parts.
Performing the calculus with imposed aperture and considering a tolerance factor of 10%, the following data results:

- Expander magnification: ~1.7 X (f1 = 86mm, f2 = 144 mm)
- Length of the expander: ~ 56 mm
- Effective focal length of the objective: ~155 mm
- Clear aperture of the objective: 17 mm.

Specific infrared materials were chosen and verified in regard with power density limit.

The calculus of the expander is based on the traditional algorithm of telescopes.

The quality of the system will depend on lens shape. Both lenses of the expander and objective can be designed using the algorithm for best shape lens, which aims to minimize the spherical aberration. Considering the power of a thin lens:

$$\Phi = \frac{1}{f} = (n-1)\left(\frac{1}{r_1} - \frac{1}{r_2}\right) = (n-1)(c_1 - c_2) = (n-1)c\ , \tag{2.1.8}$$

where Φ is the optical power, f – effective focal length, n – refractive index, r_1, r_2 – radii, c_1, c_2 – curvatures (inverse of radii), c – total curvature, and the condition of minim spherical aberration (2.1.9):

$$-G_2c^2 + 2G_4 \cdot c \cdot c_1 - G_5c\frac{1}{s} = 0\ , \tag{2.1.9}$$

where $G_{2,4,5}$ are coefficients depending on the refractive index, s – object abscissa, the relationships for the curvatures are:

$$\begin{cases} c_1 = \dfrac{n(2n+1)c}{2(n+2)} \\ c_2 = \dfrac{2n^2 - n - 4}{n(2n+1)} c_1 \end{cases} \wedge s = -\infty . \tag{2.1.10}$$

The entire calculus is accomplished with original software, written as VB application. The following figures show captures of graphical interface presenting its main frames: the interface of the program (fig. 2.1.1), input data and estimated values (fig. 2.1.2), materials choice and power density checking (fig. 2.1.3), solution for the expander (fig. 2.1.4) and solutions for the focusing objective (fig. 2.1.5).

The numerical solutions provided by the software application were analyzed with the software OSLO 4.6.

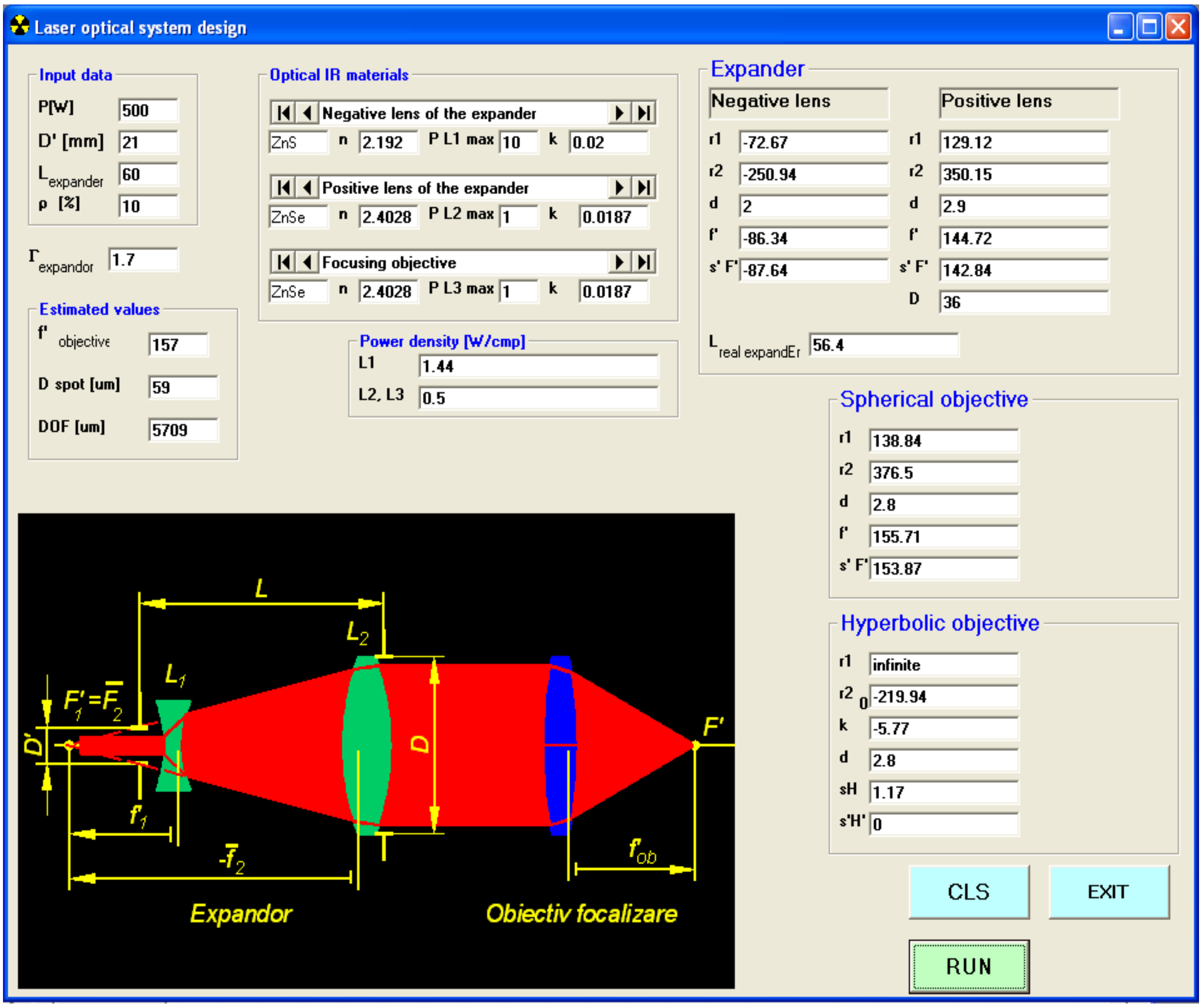

Figure 2.1.1 Graphical interface of the software application

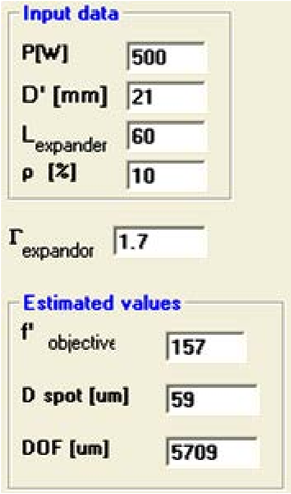

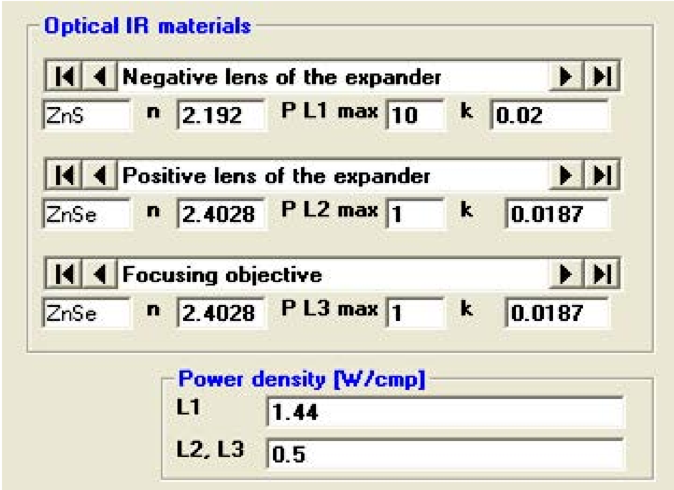

Figure 2.1.2 Input data and estimated values Figure 2.1.3 Materials choice and power density checking

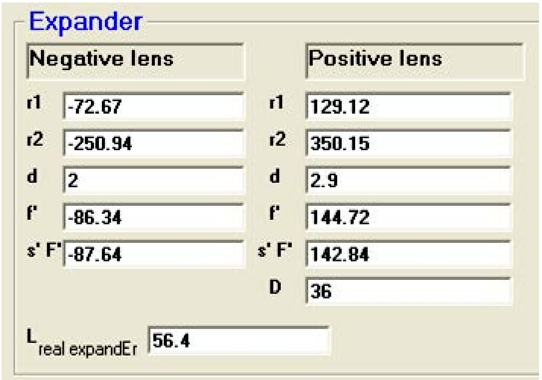

Figure 2.1.4 Solution for the expander

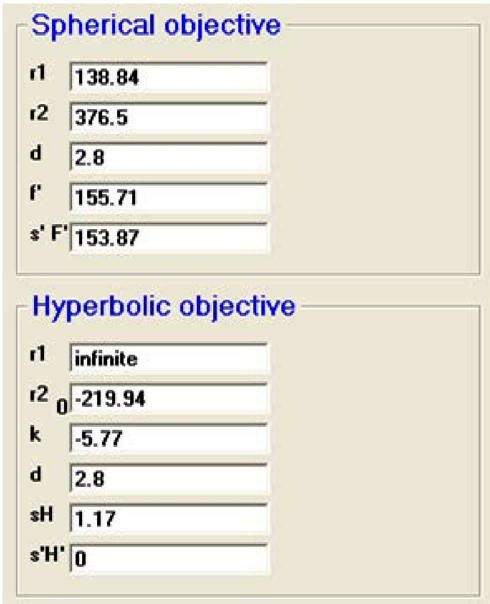

Figure 2.1.5 Solutions for the focusing objective

Figure 2.1.6 presents a drawing of the expander and objective showing the path of a tangential beam of rays.

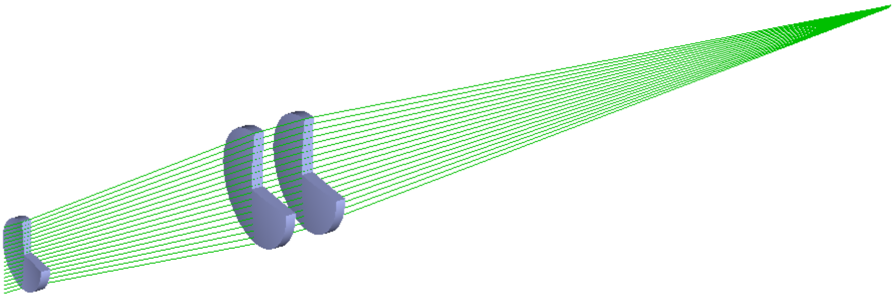

Figure 2.1.6 Drawing of the optical system (expander and objective)

A print screen of the Surface Data window is shown in figure 2.1.7. Below data is given the wavefront analysis window, which indicates a diffraction limited system.

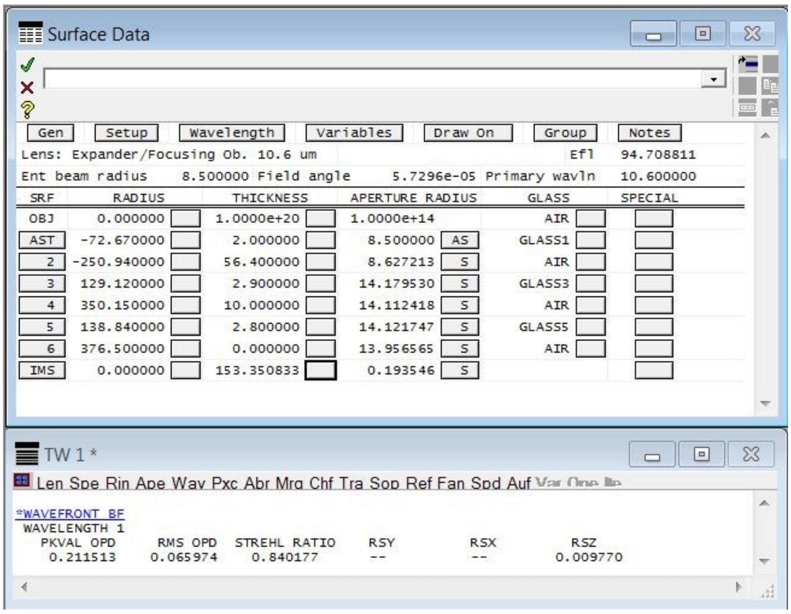

Figure 2.1.7 Surface Data and Wavefront analysis window

The wavefront analysis result is a good premise for the spot size, which requires a deeper research. The tool proposed for this analysis is the spot diagram. A general spot diagram built for a focus shift of ±5 mm is given in figure 2.1.8.

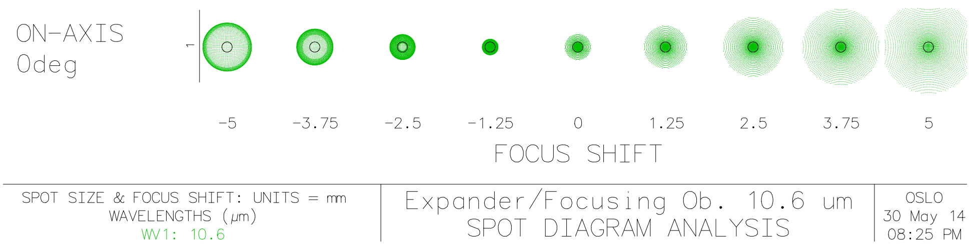

Figure 2.1.8 Spot diagram for focus shift within the range of ±5 mm

Within the range of [-3.5 ... +2] mm in focus shift, step 0.5 mm, single spot diagrams were generated and specific data was collected. The Airy disk radius and the actual radius of the spot due to both diffraction and geometric causes are given in table 2.1.1.

Table 2.1.1 Spot size and focus shift

Focus shift [mm]	R spot [mm]	R Airy [mm]
-3.5	0.1977	0.0697
-3.0	0.1670	
-2.5	0.1372	
-2.0	0.1094	
-1.5	0.0852	
-1.0	0.0687	
-0.5	0.0661	
0	0.0785	
0.5	0.1008	
1.0	0.1277	
1.5	0.1569	
2.0	0.1874	

Values in table 2.1.1 show the radius of Airy disk of ~70μm and actual radii 10% bigger for a shift focus of (0...-1.5) mm, which may be regarded as the actual depth of focus (cells with grey filling in table 2.1.1).

Comparing the estimation in eq. (2.1.1) (R= 0.065μm), which considers only the focal length of the objective, it results that the real system including the geometric and diffraction effects of the expander lenses is very good.

Figure 2.1.9 illustrates the shape of the beam and emphasizes the Airy radius.

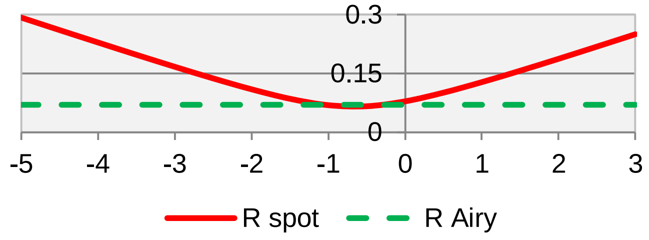

Figure 2.1.9 Shape of the beam on different focus shift

However, the system may be still improved by means of using an aspheric objective.

A hyperbolic plan-convex lens is proposed (conic constant -18.16) as focusing objective. The Surface Data and the quality parameters are shown in figure 2.1.10.

Their values qualify the system almost ideal. The spot size and depth of focus can be evaluated by studying the spot diagrams at different focus shift (fig. 2.1.11). Single spot diagram analysis provides data in table 2.1.2 and figure 2.1.12.

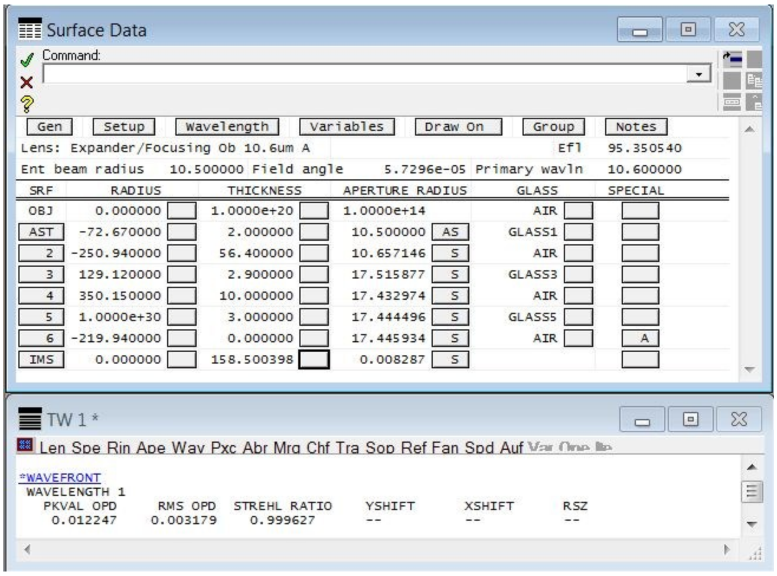

Figure 2.1.10 Surface data and quality parameters of the system with aspheric objective

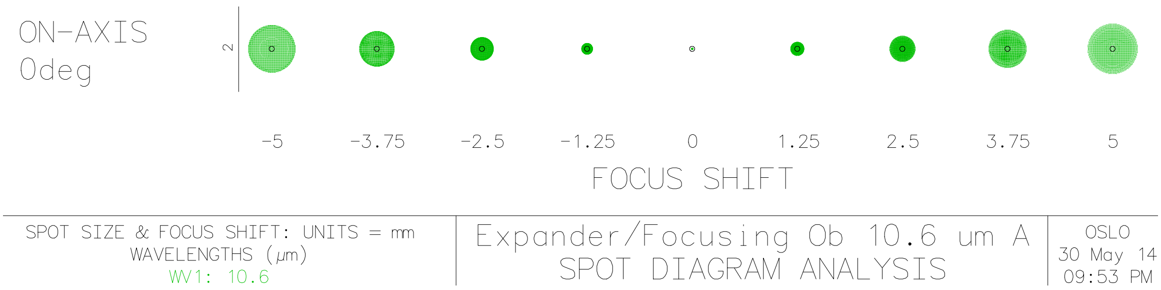

Figure 2.1.11 Spot diagram for the system with aspheric objective

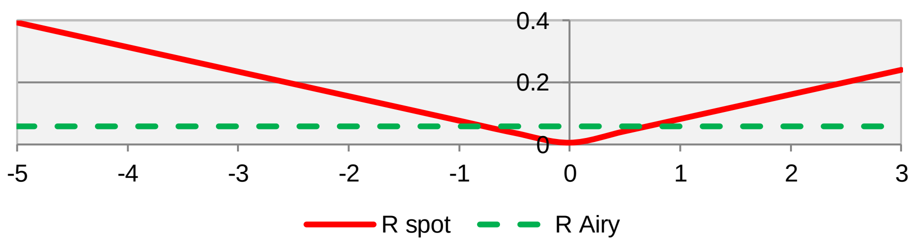

Figure 2.1.12 Shape of the beam on different focus shift (aspheric objective)

Table 2.1.2 Spot size and focus shift (aspheric objective)

Focus shift [mm]	R spot [mm]	R Airy [mm]
-3.0	0.2349	0.0584
-2.5	0.1953	
-2.0	0.1557	
-1.5	0.1162	
-1.0	0.0766	
-0.5	0.0371	
0	0.0056	
0.5	0.0426	
1.0	0.0821	
2.0	0.1613	

The spot size is less than 80 μm for (-1 ... +0.5) mm focal shift, which expresses, in fact, the real depth of field (cells with grey filling in Table 2.2). Both characteristics are fully convenient, so the original system designed can be qualified as very good. The aspheric solution provides a smaller spot size (Airy disk radius ~0.06 mm) and a larger depth of focus (~ 2 mm).

2.1.3 Conclusions and contributions

The research work developed within the present chapter can be summarized as follows:

- Progress in precision and efficiency in laser machining is strongly connected to the quality of the optical system, which ensures the travel of the beam emitted by the source and then the focusing of radiant energy to the machining point.
- Infrared optics needs specific algorithms, which take into account the small number of available materials, the monochromatic radiation and its high power density. Nevertheless, appropriate mathematical approach and software tools may provide very good quality lenses for the expander and focusing assembly.

The original contributions in this chapter are:

- Writing of algorithms to design the optical system associated with a laser machining application. The systems consist of two assemblies: the expander and the focusing objective. The expander is an inverse Galileo telescope made of singlets and the focusing objective is a positive singlet. All lenses are designed as “best shape lenses”.
- Development of a VB application, which considers the laser source known (in regard with power and diameter of the beam), takes into account a materials database and provides the geometry of all components. The focusing objective may be chosen among two solutions (spherical and aspheric).
- Modeling of beam travel through the system and evaluation of non-imaging characteristics, such as spot radius and depth of focus. The spot radius is compared to Airy disk radius and the depth of focus is analyzed by defocusing within a range of several millimeters.
- Both numerical solutions are diffraction limited. The spherical objective ensures a best focus spot size of ~80 μm at a depth of focus of ~1.5 mm. At the same size of the spot, the aspheric objective provides a larger depth of focus, of ~2mm. Both solutions may be regarded as very good from optical point of view. In addition, they take minimal costs of manufacturing as only singlet lenses are used.

2.2 Experimental optimization of process parameters in laser cutting of polycarbonate gears

2.2.1 Statement of problem

Polycarbonate is widely used due to its mechanical, optical, thermal and chemical properties. Tensile strength (55…75 MPa), Young's modulus (2…2.4 MPa) and hardness (~70HRC) recommend the material also for manufacturing of gears, which work with low power or special conditions transmissions. Molding and extrusion, commonly used to machine polycarbonate pieces, are not appropriate to obtain complex shape and preciseness as gears require. A non – conventional technology for instance laser cutting suites much better.

Still, laser cutting is not very simple to apply. Targets regarding piece's characteristics (precision in shape and dimension, roughness, thermal side-effects etc.), time of machining and energetic supply needed, are hard to attain without a process optimization. The large number of parameters involved, exclude the choice by random of their values. There are optical, electrical and mechanical factors, which influence the laser cutting process. Different combinations of their possible values might satisfy requirements to attain different target criteria (diverse in nature and value). From optical standpoint, laser cutting is a non – imaging application. The quality of the optical system included in the structure of a laser cutting machine, influences directly the general traits of the process. Flexibility and preciseness are required in order to ensure easy transforming of radiant beam's properties (spot size, defocus facilities, and variable energetic density).

Control of electrical parameters, such as power supply, ensures appropriate energetic properties of the cutting beam (for pulse lasers, also pulse duration and pause duration are very important).

Mechanical design of the nozzle, precision and speed of cutting head's displacement are involved in accuracy and efficiency of machining. Establishing the most suited combination of values for all these parameters needs a mathematical approach. There are several optimization process methods, among which, the Taguchi method proved to be one of the best.

The subject of machining is a set of four gears making part of a two – step transmission. Geometrical complexity, precision of tooth pitch, roughness of flanks, variety of modulus and number of teeth recommend a flexible technology such as laser cutting.

2.2.2 Experimental equipment

Effective machining of sample pieces was achieved using an existing laser cutting machine, whose optical system was improved [108, 30, 70, 53]. The computer aided equipment uses a CO2 pulse laser source, 2kW power. The machine belongs to C.A.L.F.A. laboratories at I.U.T. Bethune, Universite d'Artois, France. A general image and the scheme of the machine are presented in figure 2.2.1.

The general features of a laser cutting machine are wavelength [µm], beam divergence [deg], emitted power [W], cutting speed [mm/s], vertical position of the spot, duration of pulse and pause [ms], chemical nature, pressure and flow of the gas, distance between nozzle and piece [mm], nozzle's internal geometry and exit diameter. Some of these parameters are fixed so their values can not be changed. Others are variable within certain ranges and can be used to optimize the machining process.

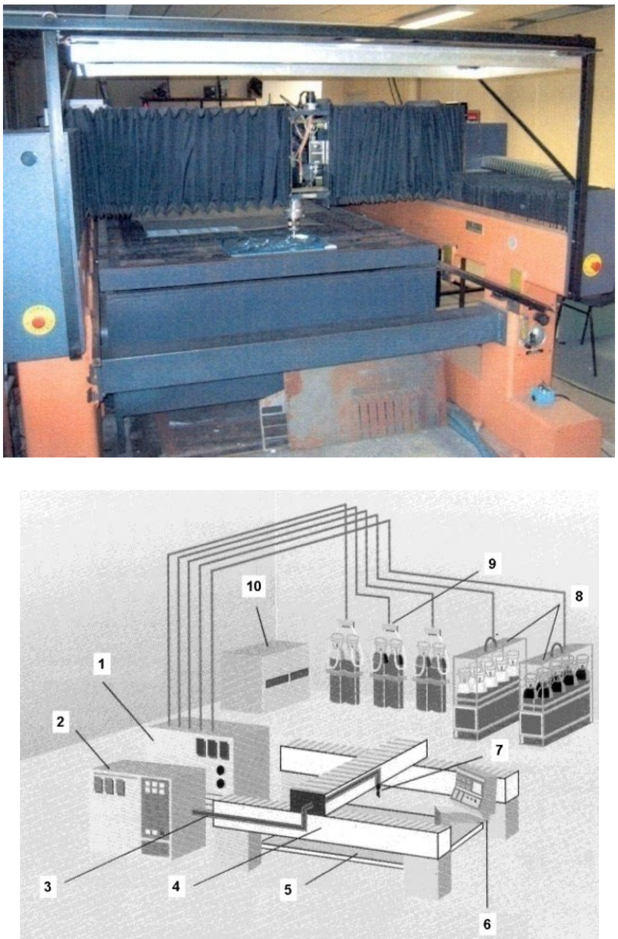

Figure 2.2.1 Image and scheme of the laser cutting machine

1 – power supply block, 2 – CO_2 laser source, 3 – optical beam path, 4 – mechanical structure, 5 – material to machine, 6 – numerical command block, 7 – cutting head, 8 – assemblies to provide and control auxiliary gas (He, Ar, N_2, O_2), 9 – assembly for CO_2 supply, 10 – cooling block

2.2.3 General design of the experimental optimization program

The plan on which the optimization program developed is briefly presented in figure 2.2.2.

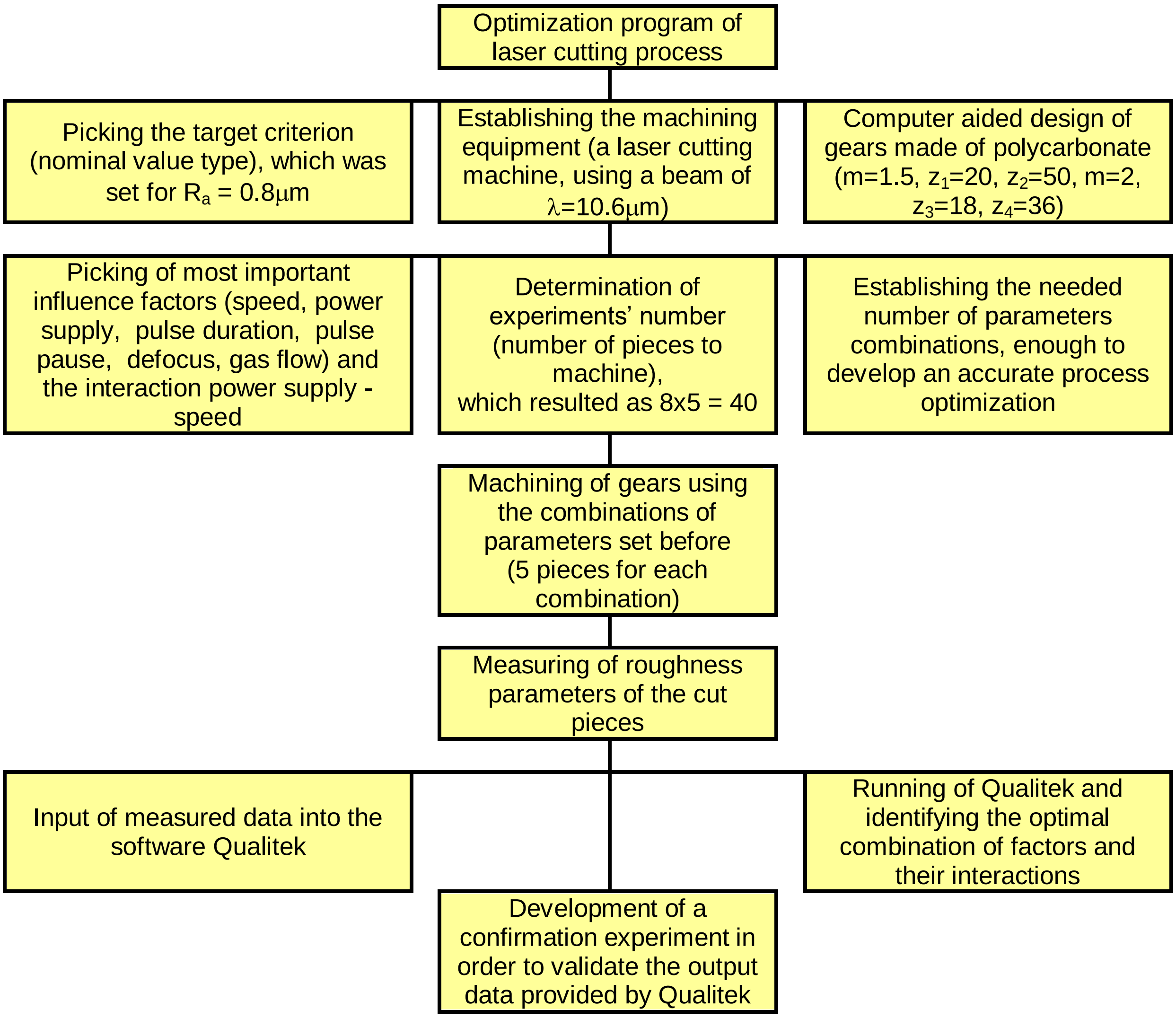

Figure 2.2.2 Logical and chronological scheme for the experimental program development

2.2.4 Choice of influence parameters and working combinations in order to apply Taguchi method in processes optimization

Traditional quality optimization methods search for dispersion or unsteadiness of a product's feature and aim to reduce or eliminate causes. Taguchi strategy introduces the concept of noise for the sources which spoil quality and states that minimization of noise – factors' impact brings in better efficiency in processes optimization [72, 73, 63].

According to Taguchi's concept (fig. 2.10), loss of quality occurs not only if the product is outside the tolerance limits, but even if it is inside these limits. The quadric function of quality loss, defined by Taguchi for target criteria is mathematically expressed as:

$$L(y) = k(y - y_N)^2 \qquad (2.2.1)$$

where: L(y) – value of loss expressed in currency/product; y – value of the quality feature involved; y_N – nominal value (target); k – constant to quantify global financial loss.

For a sample containing n pieces, measuring allows computation of mean value, $\bar{y}$ and standard deviation s. The function of quality loss becomes:

$$L(y) = k \cdot s'^2 = k \cdot \left[s\left(\frac{y_N}{\bar{y}} \right) \right]^2 = k \cdot y_N^2 \cdot \frac{s^2}{\bar{y}^2} \qquad (2.2.2)$$

In relation (2.2.2) k and y_N are constant, so that loss minimization requires maximization of the ratio $\bar{y}^2 / s^2$, which mathematically corresponds to tendency $n \to \infty$. The expression of the signal/noise ratio for target criteria is given in relation (2.2.3):

$$\frac{S}{N} = 10\log\left[\frac{\bar{y}^2}{s^2} - \frac{1}{n} \right] \quad [dB] \qquad (2.2.3)$$

The complete factorial experiments plan studies all possible combinations of selected factors' levels. Theoretically, they are complete. However, the time needed for experiments is very long and costs are very high (for instance, an experiment involving 15 factors at 2 levels requires 2^{15}=32768 pieces).

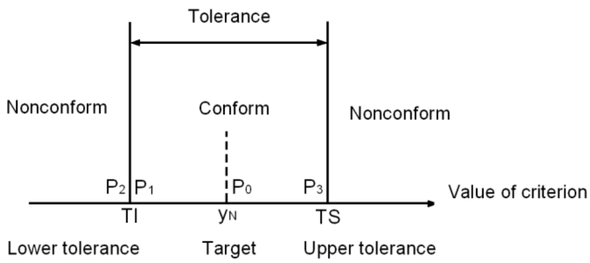

Figure 2.2.3 Taguchi concept base. Difference of quality between product P_1 (still good) and P_2 (unacceptable) is very small. Difference between P_1 and P_3 (still good) is very large. The best product is P_0 (value of criterion equal to the target)

The fractional factorial experiments plan is based on the idea that certain possible combinations of factors provide enough efficient information, so that the number of effective experiments may be considerably reduced. Table 2.2.1 presents a complete factorial experiment in a classic version for 3 factors at 2 levels. Table 2.2.2 shows a complete factorial Taguchi plan. Tables 2.2.3 and 2.2.4 illustrate two alternatives of fractional factorial Taguchi plan.

Table 2.2.1 Complete classic experimental plan

		C1	C2
A1	B1	R1	R2
	B2	R3	R4
B1	B1	R5	R6
	B2	R7	R8

Table 2.2.2 Complete Taguchi experimental plan

Nr. exp.	Factors under study A B C			Result of experiment
1	1	1	1	R1
2	1	1	2	R2
3	1	2	1	R3
4	1	2	2	R4
5	2	1	1	R5
6	2	1	2	R6
7	2	2	1	R7
8	2	2	2	R8

In order to compute the effects of an independent factor, the experimental plan must be orthogonal.

Table 2.2.3 Fractional experimental Taguchi plan (alternative I)

Nr. exp.	Factors under study A B C			Result of experiment
1	1	1	1	R1
4	1	2	2	R4
6	2	1	2	R6
7	2	2	1	R7

Table 2.2.4 Fractional experimental Taguchi plan (alternative II)

Nr. exp.	Factors under study A B C			Result of experiment
2	1	1	2	R2
3	1	2	1	R3
5	2	1	1	R5
8	2	2	2	R8

Triangle shaped tables and linear graphs are associated to most of standard Taguchi matrices and are used to define columns which study interactions. Taguchi method, generally, uses a standard L8 matrix (tab. 2.2.5).

Practical procedure to fulfill a Taguchi experimental plan assumes the creation of a table, containing influence parameters, measured values and responses (tab. 2.2.6).

It is necessary to compute the mean effect S/N of each level's factor and the value of interactions related to the mean value of response S/N. Responses related to factors and interactions are written in matrices (theoretically illustrated in tables 2.2.7 and 2.2.8).

Table 2.2.5 Standard L8 matrix

Nr. experiment	Factors under study							Result of experiment
	A	B	C	D	E	F	G	
1	1	1	1	1	1	1	1	R1
2	1	1	1	2	2	2	2	R2
3	1	2	2	1	1	2	2	R3
4	1	2	2	2	2	1	1	R4
5	2	1	2	1	2	1	2	R5
6	2	1	2	2	1	2	1	R6
7	2	2	1	1	2	2	1	R7
8	2	2	1	2	1	1	2	R8

Table 2.2.6 Complete table of parameters, measured values and responses

Nr exp	Factors under study						Int	Measured values							
	A	B	C	D	E	F	AD	nr.1	nr.2	nr.3	nr.4	nr.5	mean	s	S/N[dB]
1	1	1	1	1	1	1	1	x11	x12	x13	x14	x15	$\bar{x}_1$	s1	(S/N)1
2	1	1	1	2	2	2	2	x21	x22	x23	x24	x25	$\bar{x}_2$	s2	(S/N)2
3	1	2	2	1	2	2	1	x31	x32	x33	x34	x35	$\bar{x}_3$	s3	(S/N)3
4	1	2	2	2	1	1	2	x41	x42	x43	x44	x45	$\bar{x}_4$	s4	(S/N)4
5	2	1	2	1	1	2	3	x51	x52	x53	x54	x55	$\bar{x}_5$	s5	(S/N)5
6	2	1	2	2	2	1	4	x61	x62	x63	x64	x65	$\bar{x}_6$	s6	(S/N)6
7	2	2	1	1	2	1	3	x71	x72	x73	x74	x75	$\bar{x}_7$	s7	(S/N)7
8	2	2	1	2	1	2	4	x81	x82	x83	x84	x85	$\bar{x}_8$	s8	(S/N)8

Table 2.2.7 Effects of parameters A…F at two levels upon the S/N ratio

Factor	Effect upon the ratio S/N	
	Level 1	Level 2
A	EA1,S/N	EA2,S/N
B	EB1,S/N	EB2,S/N
C	EC1,S/N	EC2,S/N
D	ED1,S/N	ED2,S/N
E	EE1,S/N	EE2,S/N
F	EF1,S/N	EF2,S/N

Table 2.2.8 Effects of interactions between factors A and D upon the ratio S/N

Interaction	A1D1	A1D2	A2D1	A2D2
Effect upon the ratio S/N	IA1D1,S/N	IA1D2,S/N	IA2D1,S/N	IA2D2,S/N

For the given application, a set of parameters, considered to be most influent on the process of machining, were selected. They are speed, power supply, duration of pulse, duration of pause, defocus and gas flow.

For each of the six parameters above, two levels and one interaction was set. That means 2^7 experiments are needed. The optimization criterion was established to be the value of flank roughness parameter R_a. The target is "nominal value" type (R_a = 0.8 μm). Further mathematical approach is based on fractional factorial experiments plans provided by Taguchi method. These plans considerably reduce the number of required experiments (to only 8). Tables 2.2.9…2.2.16 indicate the values of the process factors for 8 combinations (A…H).

Each table indexes and designates the parameter or interaction (first column), indicates the numerical values and the measuring units (second column) and assigns a level number (third column).

Table 2.2.9 Factors combination A

Nr. column / factor	Description of level	Nr. of level
1. speed	3000 mm/min	1
2. power	170 W	1
3. interaction 1x2	int 1x2	1
4. duration of pulse	5 ms	1
5. duration of pause	3 ms	1
6. nozzle distance	4 mm / 5 mm	1
7. gas flow	20 l/min	1

Table 2.2.10 Factors combination B

Nr. column / factor	Description of level	Nr. of level
1. speed	3000 mm/min	1
2. power	170 W	1
3. interaction 1x2	int 1x2	1
4. duration of pulse	3 ms	2
5. duration of pause	5 ms	2
6. nozzle distance	4 mm / 2,5 mm	2
7. gas flow	10 l/min	2

Table 2.2.11 Factors combination C

Nr. column / factor	Description of level	Nr. of level
1. speed	3000 mm/min	1
2. power	180 W	2
3. interaction 1x2	int. 1 x 2	2
4. duration of pulse	5 ms	1
5. duration of pause	3 ms	1
6. nozzle distance	4 mm / 2,5 mm	2
7. gas flow	10 l/min	2

Table 2.2.12 Factors combination D

Nr. column / factor	Description of level	Nr. of level
1. speed	3000 mm/min	1
2. power	180 W	2
3. interaction 1x2	int. 1 x 2	2
4. duration of pulse	3 ms	2
5. duration of pause	5 ms	2
6. nozzle distance	4 mm / 5 mm	1
7. gas flow	20 l/min	1

Table 2.2.13 Factors combination E

Nr. column / factor	Description of level	Nr. of level
1. speed	4500 mm/min	2
2. power	170 W	1
3. interaction 1x2	int 1x2	2
4. duration of pulse	5 ms	1
5. duration of pause	5 ms	2
6. nozzle distance	4 mm / 5 mm	1
7. gas flow	10 l/min	2

Table 2.2.14 Factors combination F

Nr. column / factor	Description of level	Nr. of level
1. speed	4500 mm/min	2
2. power	170 W	1
3. interaction 1x2	int 1x2	2
4. duration of pulse	3 ms	2
5. duration of pause	3 ms	1
6. nozzle distance	4 mm / 2,5 mm	2
7. gas flow	20 l/min	1

Table 2.2.15Factors combination G

Nr. column / factor	Description of level	Nr. of level
1. speed	4500 mm/min	2
2. power	180 W	2
3. interaction 1x2	int 1x2	1
4. duration of pulse	5 ms	1
5. duration of pause	5 ms	2
6. nozzle distance	4 mm / 2,5 mm	2
7. gas flow	20 l/min	1

Table 2.2.16 Factors combination H

Nr. column / factor	Description of level	Nr. of level
1. speed	4500 mm/min	2
2. power	180 W	2
3. interaction 1x2	int 1x2	1
4. duration of pulse	3 ms	2
5. duration of pause	3 ms	1
6. nozzle distance	4 mm / 5 mm	1
7. gas flow	10 l/min	2

2.2.5 CAD of gears and generation of NC code

The laser cutting equipment used to machine the gear samples is supplied together with the software Laser DX3, which is an extension of AutoCAD so it is able to import *.dxf files. Dimensioning and geometrical calculus of the transmission with total transmission ratio i = 4, was accomplished and for each type of gear an AutoCAD drawing was saved in *.dxf format. Flank shape is normal convolute. First step of the transmission needed a modulus $m_{1,2}$ = 1.5. The second one was dimensioned at $m_{3,4}$ = 2. The four types of gears machined for the experiment are shown in figure 2.2.4.

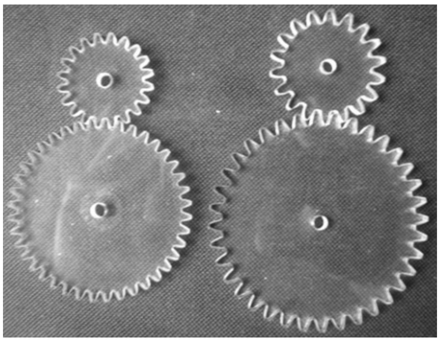

Figure 2.2.4 Four types of gears machined for the experiment with the laser cutting machine

($m_{1,2}$ = 1.5, z_1 = 20, z_2 = 40, $m_{3,4}$ = 2, z_3 = 18, z_4 = 36)

The constructive design module of Laser DX3 (fig. 2.2.5) imports *.dxf files and prepares them for the next module. Technological design module processes the *.dxf file and converts it into a *.txt one, representing the NC machining code. The numerical command file, adapted to the management file format, specific to the machine's software allows the transfer of the numerical code from Laser DX3 to equipment's computer. The numerical code translates the drawing of the piece into complete commands regarding entrance and exit points of the nozzle, displacement of the cutting head along a path, which reproduces the contour of the piece, displacement segments without cutting and so on.

Figure 2.2.5 Constructive design module

2.2.6 Experimental results

Five gears were machined for each of parameters combinations A…H. Each gear sample was measured with a electronic measuring device Mahr. Tables 2.2.17…2.2.24 present the results of measurement. First column of the tables indicates the combination (A….H) and denotes the sample (A1…A5….H1…H5). The last line indicates the mean value of the parameters R_a, R_q, R_z, R_{zi}, R_{max}, R_p (DIN designation), for a given combination.

Table 2.2.17 Texture parameters - Combination A

A	Ra	Rq	Rz	Rzj	Rmax	Rp
A1	1.027	1.243	3.958	5.275	1.579	2.380
A2	0.895	1.147	3.945	6.150	2.091	1.853
A3	0.977	1.274	3.922	4.97	1.714	2.208
A4	0.944	1.125	3.101	3.814	1.683	1.418
A5	0.867	1.037	3.750	4.653	1.946	1.804
	0.942	1.165	3.735	4.972	1.802	1.932

Table 2.2.18 Texture parameters - Combination B

B	Ra	Rq	Rz	Rzj	Rmax	Rp
B1	1.498	2.059	6.687	11.02	2.841	3.846
B2	1.327	1.591	5.397	6,.77	2.466	2.93
B3	1.242	1.542	5.682	8.174	2.726	2.956
B4	1.520	2.021	7.528	11.84	3.979	3.549
B5	1.591	2.015	7.017	10.51	3.284	3.733
	1.435	1.845	6.462	9.664	3.059	3.402

Table 2.2.19 Texture parameters - Combination C

C	Ra	Rq	Rz	Rzj	Rmax	Rp
C1	0.496	0.610	2.358	3.387	1.237	1.120
C2	0.712	0.874	2.742	3.242	1.536	1.206
C3	0.525	0.651	2.222	3.194	1.141	1.081
C4	0.725	1.562	3.074	5.442	1.562	1.512
C5	0.714	0.873	2.823	4.174	1.535	1.287
	0.634	0.914	2.644	3.888	1.402	1.241

Table 2.2.20 Texture parameters - Combination D

D	Ra	Rq	Rz	Rzj	Rmax	Rp
D1	1.415	1.835	6.642	8.628	3.074	3.569
D2	1.189	1.507	4.618	7.120	2.214	2.404
D3	1.145	1.416	5.207	6.757	2.542	2.665
D4	1.337	1.688	5.804	8.797	2.865	2.939
D5	1.379	1.683	6.116	7.402	3.077	3.039
	1.293	1.626	5.677	7.741	2.754	2.923

Table 2.2.21 Texture parameters - Combination E

E	Ra	Rq	Rz	Rzj	Rmax	Rp
E1	1.275	1.572	5.664	7.740	2.120	3.543
E2	1.282	1.579	5.720	7.067	2.585	3.135
E3	1.354	1.630	5.275	7.235	2.739	2.537
E4	1.175	1.447	4.697	7.318	2.318	2.379
E5	1.305	1.613	5.578	7.449	2.906	2.672
	1.278	1.568	5.387	7.362	2.534	2.853

Table 2.2.22 Texture parameters - Combination F

F	Ra	Rq	Rz	Rzj	Rmax	Rp
F1	1.092	1.426	4.857	7.920	2.356	2.501
F2	0.982	1.216	4.191	5.062	2.176	2.015
F3	0.969	1.296	4.596	6.950	2.026	2.570
F4	1.092	1.364	4.568	6.085	2.335	2.233
F5	0.928	1.129	3.911	4.731	2.088	1.823
	1.013	1.286	4.425	6.150	2.196	2.228

Table 2.2.23 Texture parameters - Combination G

G	Ra	Rq	Rz	Rzj	Rmax	Rp
G1	1.104	1.409	5.261	6.877	2.684	2.577
G2	0.987	1.213	4.859	6.644	2.197	2.662
G3	0.978	1.243	4.791	6.668	2.153	2.638
G4	1.054	1.412	5.060	6.714	3.103	1.957
G5	1.058	1.303	3.770	4.995	1.888	1.881
	1.036	1.316	4.748	6.380	2.405	2.343

Table 2.2.24 Texture parameters - Combination H

H	Ra	Rq	Rz	Rzj	Rmax	Rp
H1	1.175	1.437	5.118	6.310	2.573	2.545
H2	1.179	1.530	5.121	7.726	2.954	2.167
H3	1.165	1.409	4.634	6.210	2.194	2.440
H4	1.164	1.526	4.820	6.652	1.917	2.904
H5	1.151	1.420	4.821	5.499	2.707	2.114
	1.167	1.464	4.903	6.479	2.469	2.434

Any of these roughness parameters could be used to characterize the active surface of pieces. R_a – average roughness – (fig. 2.2.6) was chosen for further computation as it is generally used in standard design specifications regarding surface texture.

Figure 2.2.6 Mahr device for texture parameters measurement

2.2.7 Optimization of process parameters by means of Taguchi method

The complex array statistical calculus required by Taguchi method implementation needs automated computation. The appropriate software Qualitek was run in order to process the numerical data. The following figures contain print – screens of different stages in developing the application.

Figure 2.2.7 shows the window where the influence factors at two levels and the interaction of the first two parameters are introduced as general input data. The program builds the inner array accordingly to fractional factorial experiments plan and using for the terms in array the measured values of roughness (R_a parameter) from tables 2.2.17…2.2.24 (fig. 2.2.8).

	Factors	Level 1	Level 2
1	viteza	3000 mm/m	4500 mm/min
2	puterea	170 W	180 W
3	INTER COLS 1 x 2	*INTER*	------------
4	timpul de impuls	5 ms	3 ms
5	timpul de repaus	3 ms	5 ms
6	duza / distanta d	d4mm / 5m	d4mm / 2.5 mm
7	debitul de gaz	20 l/min	10 l/min

Figure 2.2.7 Preliminary input data in Qualitek

	1	2	3	4	5	6	7
1	1	1	1	1	1	1	1
2	1	1	1	2	2	2	2
3	1	2	2	1	1	2	2
4	1	2	2	2	2	1	1
5	2	1	2	1	2	1	2
6	2	1	2	2	1	2	1
7	2	2	1	1	2	2	1
8	2	2	1	2	1	1	2

Inner Array

1	2	3	4
1.027	.895	.977	.944
1.498	1.32	1.242	1.52
.496	.712	.525	.725
1.415	1.189	1.145	1.337
1.275	1.282	1.354	1.175
1.092	.982	.969	1.092
1.104	.987	.978	1.054
1.175	1.179	1.165	1.164

Results

Figure 2.2.8 Configuration of inner array and input of numerical roughness data

The next window (fig. 2.2.9) displays data type, which is “signal/noise ratio”, optimization criterion type, which is “nominal is the best”. Nearby the criterion type is written the target value of the criterion, R_a = 0.8 μm. Bellow these settings, all 40 values are put into a matrix, where each line corresponds to a certain combination of parameters. The last column shows the S/N ratio of each line. At the lower side of the window, inside round brackets are written the average value of all 40 measurements (1.099) and the standard deviation (0.25).

Average effects of each factor and interaction tested are presented in figure 2.2.10. As a matter of fact, the first three factors (pause duration, duration of pulse and gas flow) are mainly influent upon the thermal effects over the irradiated area. The next influence factor is defocus, which determines the energy distribution at the interaction zone.

Expt. File: LASER2.Q4W Data Type: S/N Ratio

QC Type: Nominal is the Best Nominal = .8

Conditions	Sample# 1	Sample# 2	Sample# 3	Sample# 4	Sample# 5	Sample# 6	S/N Ratio
Trial# 1	1.027	0.895	0.977	0.944	0.867		16.303
Trial# 2	1.498	1.32	1.242	1.52	1.591		3.773
Trial# 3	0.496	0.712	0.525	0.725	0.714		14.229
Trial# 4	1.415	1.189	1.145	1.337	1.379		5.944
Trial# 5	1.275	1.282	1.354	1.175	1.305		6.343
Trial# 6	1.092	0.982	0.969	1.092	0.928		13.034
Trial# 7	1.104	0.987	0.978	1.054	1.058		12.363
Trial# 8	1.175	1.179	1.165	1.164	1.151		8.708
							10.087

(All results: Avg.= 1.099, StDev.= .25)

Figure 2.2.9 S/N ratio, mean values, optimization criterion and target value

Column # / Factors	Level 1	Level 2	L2 - L1
1 viteza	10.062	10.112	.05
2 puterea	9.863	10.311	.448
3 INTER COLS 1 x 2	10.287	9.887	-.401
4 timpul de impuls	12.31	7.865	-4.446
5 timpul de repaus	13.069	7.106	-5.964
6 duza / distanta d	9.324	10.85	1.525
7 debitul de gaz	11.911	8.263	-3.648

Figure 2.2.10 Mean effects of factors and interaction

Beside the interaction included in the experience plan, all possible interactions between the six factors were tested. Qualitek accomplishes an automatic test for presence of interactions. Studying the severity of interactions, results that power supply and displacement speed of the cutting head strongly interact with defocus. Therefore, correct correlation of these parameters is essential in getting the desired texture of surface. The other interactions are moderate (for instance, the interaction speed – power supply) or insignificant (duration of pulse – defocus or pause duration – defocus).

Column # / Factor	Level Description	Level	Contribution
1 viteza	4500 mm/min	2	.024
2 puterea	180 W	2	.223
3 INTER COLS 1 x 2	*INTER*	1	.199
4 timpul de impuls	5 ms	1	2.222
5 timpul de repaus	3 ms	1	2.981
6 duza / distanta d	d4mm / 2.5 mm	2	.762
7 debitul de gaz	20 l/min	1	1.823
Total Contribution From All Factors.........			8.233
Current Grand Average Of Performance...			10.087
Expected Result At Optimum Condition...			18.321

Figure 2.2.11 Optimal combinations of factors and interaction levels and expected value of S/N ratio

Current Status	Average Performance	1.098	StDev. = .25
	Nominal / Target	0.8	
	S/N Ratio (SN1)	10.087	
Improved Status	S/N Ratio (SN2)	18.321	
	Quality Characteristic	Nominal is the Best	

Figure 2.2.12 Current status and expected status properties of the process

Finally, an optimal combination of factors resulted. It is presented in figure 2.2.11. The last row predicts an S/N ratio of ~18 (initially it was ~10), which means that using the optimum parameters the roughness of the lot of pieces will get values much more gathered around the target.

Next window summarizes the current status and expected status properties of the process (fig. 2.2.12). Figure 2.2.13 shows graphically the scattering of results corresponding to current state and predicted one. One can notice that for the current state the distribution curve is displaced with respect to the target.

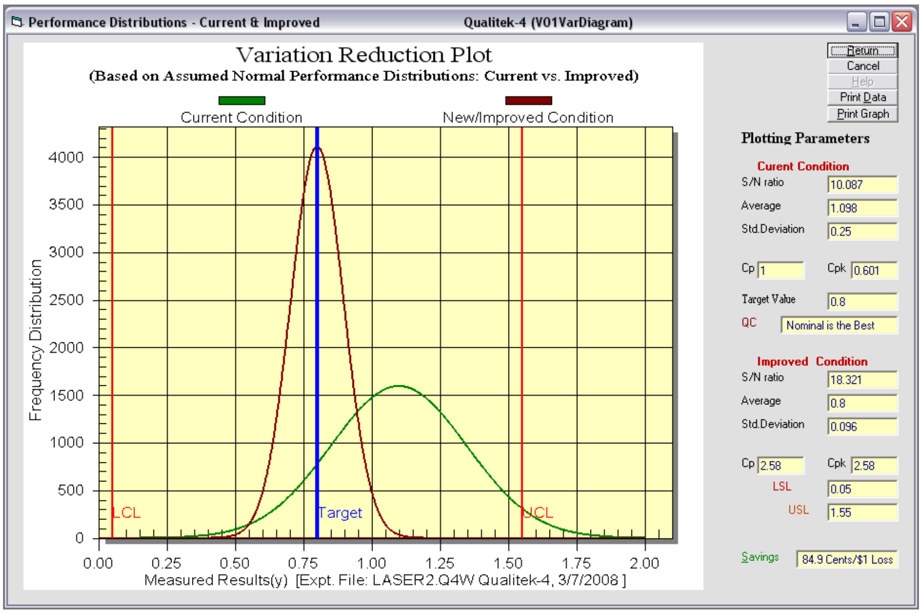

Figure 2.2.13 Graph of reduced variation for optimal factors compared to initial ones (hypothesis of normal distribution)

In optimal conditions, the dispersion is much less than $\pm 3\sigma$ (limited by vertical lines). The frequency curve (drawn in brown) presents a peak ~2.5 higher and a narrow aperture centered about the target vertical line.

In order to validate the theoretical optimization, a confirmation experiment was achieved. A set of five sample gears were machined using the optimal combination of factors indicated by Qualitek (tab. 2.2.25). The pieces were measured and the results are presented in table 2.2.26.

Table 2.2.25 Optimal values indicated by Qualitek

Nr. column / factor	Description of level	Nr. of level
1. speed	4500 mm/min	2
2. power	180 W	2
3. interaction 1x2	int 1x2	1
4. duration of pulse	5 ms	1
5. duration of pause	3 ms	1
6. nozzle distance	4 mm / 2,5 mm	2
7. gas flow	20 l/min	1

Table 2.2.26 Roughness parameters (confirmation experiment)

	Ra	Rq	Rz	Rzj	Rmax	Rp	Rv
1	0.80	0.96	3.43	4.10	1.58	1.85	0.80
2	0.78	0.95	4.04	5.14	2.06	1.98	0.78
3	0.83	1.06	3.97	4.81	1.94	2.02	0.83
4	0.89	1.11	4.30	5.49	2.07	2.22	0.89
5	0.71	0.86	3.36	3.95	1.71	1.64	0.71
	0.806	0.99	3.82	4.70	1.87	1.94	0.80

The analysis of data got with the confirmation experiment indicates a better value of S/N ratio (24.459) than the predicted one (18.321). Quality statistical data of the pieces machined at experimentally chosen parameters improved substantially after optimal values were used in a confirmation experiment (tab. 2.2.27).

Table 2.2.27 Comparative data regarding initial, predicted and practically achieved conditions

Feature	initial conditions	estimated conditions	validation experiment
S/N ratio	10.087	18.321	24.459
mean value	1.098	0.800	0.805
standard deviation	0.250	0.096	0.047

2.2.8 Conclusions and contributions

The research work developed within the present chapter can be summarized as follows:

- Fractional factorial experiments plans stated by Taguchi method and a specialized software – Qualitek – proved to be quick, economic (only 40 samples needed effective machining for optimizing six parameters in two levels and one interaction organized in 8 combinations) and very efficient.
- For the pieces machined in optimal conditions S/N ratio is even better than the predicted one. The mean value is very close to the nominal target, which significantly improves the quality of the lot of pieces. The machining became very precise, considering the optimization criterion. As well, the process itself became desirable instead of traditional technology. Auxiliary devices such as molds were totally eliminated and the machining duration decreased considerably (3…4 minutes/piece in function of number of teeth).

The original contributions in this chapter are:

- General design of an experimental optimization program, created for laser machining of polycarbonate gears
- Choice of influence parameters and working combinations in order to apply Taguchi method in processes optimization. The influence parameters are speed, power

supply, duration of pulse, duration of pause, defocus and gas flow. For each of the six parameters above, two levels and one interaction (speed/power) was set.

- Establishment of optimization criterion to be the value of flank roughness parameter Ra. The target is “nominal value” type (Ra = 0.8 µm).
- Establishment of 8 combinations (A…H) of the six parameters on two levels and one interaction.
- CAD design, CN code generation and machining of 40 gears (five pieces in each combination).
- Measurement and recording of texture parameters for the machined gears.
- Use of numerical data (combinations of influence parameters and measured values of roughness) in the software application Qualitek, which provides the optimal combination of parameters.
- Development of a confirmation experiment. In optimal conditions, the dispersion is much less than $\pm 3\sigma$. The frequency curve presents a peak ~2.5 higher and a narrow aperture centered about the target vertical line assigned to the nominal value. The mean value of R_a within the confirmation experiment was 0.806.

3. Document digitization

3.1 Digitization equipment and techniques in retrieval of mechanism and machine science resources

3.1.1 Statement of problem

The European project thinkMOTION [112] is intended to offer knowledge in the field of mechanisms and machine science through the portal Europeana [101] on a specialized site called DMG-Lib [98] – fig. 3.1.1. DMG-Lib is a digital library, which provides content originating from a large range of sources (universities, technical libraries, museums, patent offices, individual owners etc.).

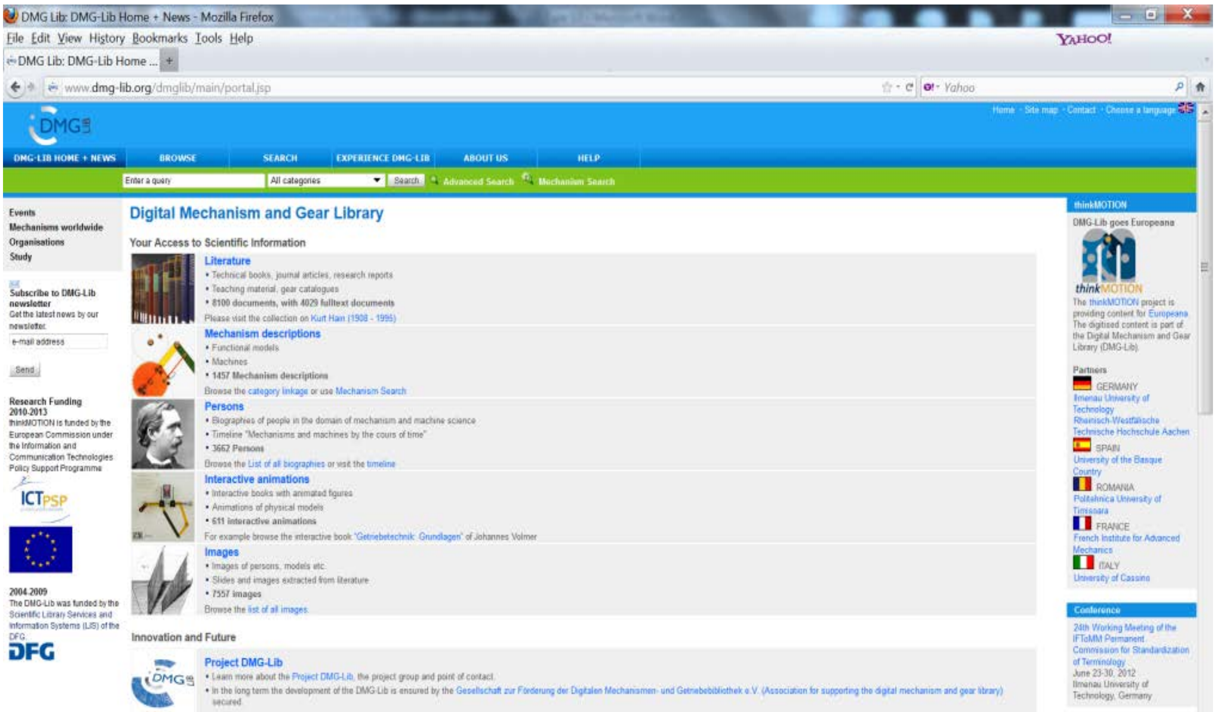

Figure 3.1.1 The web-site of DMG-Lib

The content posted on DMG-Lib presents information in more categories: books, articles, proceedings, PhD theses, contributions, journals, reports, biographies, images, interactive animations, software and so on. One of the main goals of the project is the retrieval of mechanism science in its history [16, 35, 6, 8]. Almost all content before 1990 exists in analogue form, written, printed or drawn on paper support. Getting back and gathering national historical treasures in a well-organized collection requires digitization of a large amount of documents. The digital library offers a novel way of describing the history of development in mechanism science field, from antiquity up to now-days.

The partners in the project are Ilmenau University of Technology (Germany), University of Basque Country (Spain), University Politehnica Timisoara (Romania), RWTH Aachen University (Germany), French Institute of Advanced Mechanics (France) and University of Cassino (Italy). The partners put together content from national sources and from providers in the neighborhood areas, willing to collaborate. No matter what the original source is, it requires digitization and preparation of high-quality web-compliant files to be posted online.

3.1.2 Workflow

Digitization of heterogeneous support-type documents at high quality of online items is resource consuming from both technical and duration point of view.

The processing of an item starting with an analogue document and ending up to having a high-quality online information was planned to follow the workflow presented in figure 3.1.2.

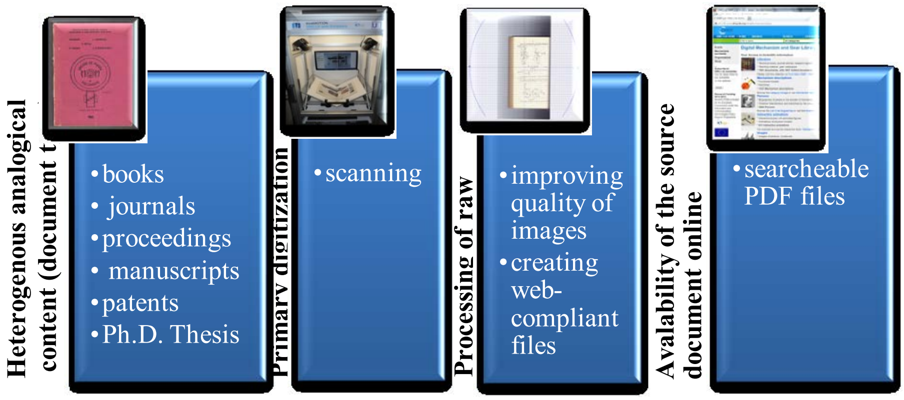

Figure 3.1.2 Workflow of the digitization process

The workflow consists of the following steps:

- ❒ locating of potential content providers, having the rights of use granted by the owner of intellectual property and getting the physical support carrying content
- ❒ performing the primary digitization by means of specially designed equipment, in order to obtain raw scanned images of the original document
- ❒ processing the raw images with appropriate software so that the quality of images matches an imposed standard and the final files are web-compliant
- ❒ posting the items online.

Figure 3.1.3 illustrates the input and the output of digitization, quality improvement and web-compliant conversion.

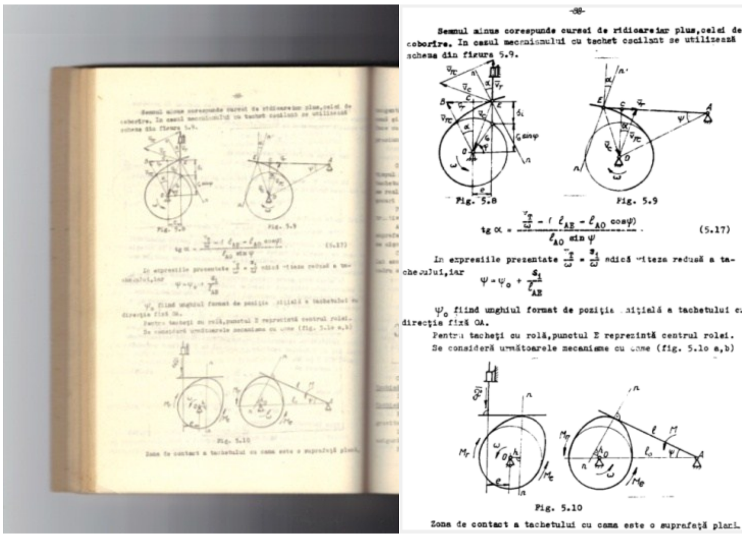

Figure 3.1.3 Raw scanned image of a page book (left) and its final digitized look online (right)

Raw images got by scanning require professional processing, which take a lot of operations:

- splitting of pages (fig. 3.1.4)
- deskewing of pages (fig. 3.1.5)

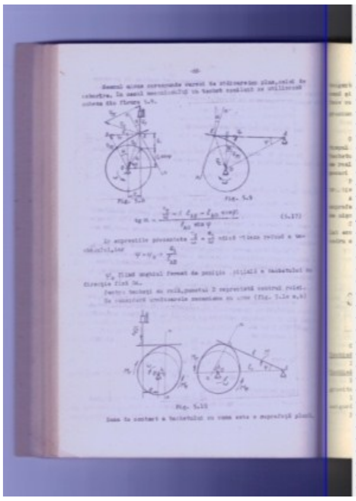

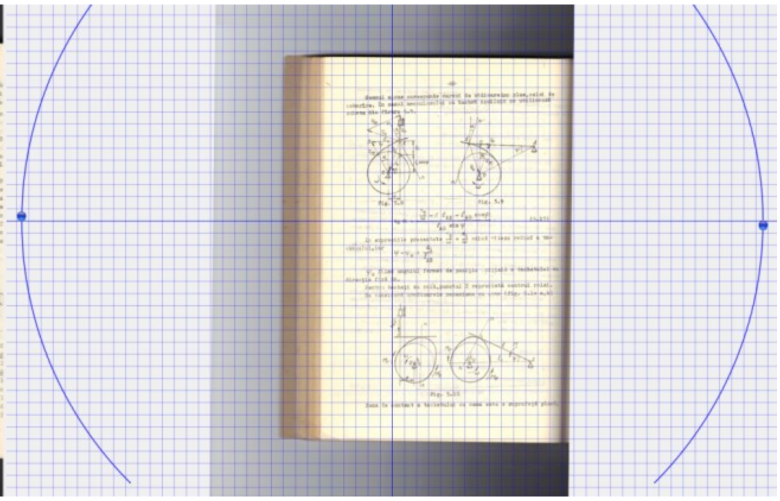

Figure 3.1.4 Splitting of pages **Figure 3.1.5 Deskewing of the page**

- selection of content (fig. 3.1.6)
- setting margins of page (fig. 3.1.7)
- despeckling and setting color mode (color/gray scale/black and white) and setting final resolution.

All processing operations, briefly defined above were performed using the software Scan Tailor [92].

The images in graphic format require processing for conversion to searchable PDF files. Multi-page searchable PDF files were got by means of software Abby Fine Reader [95].

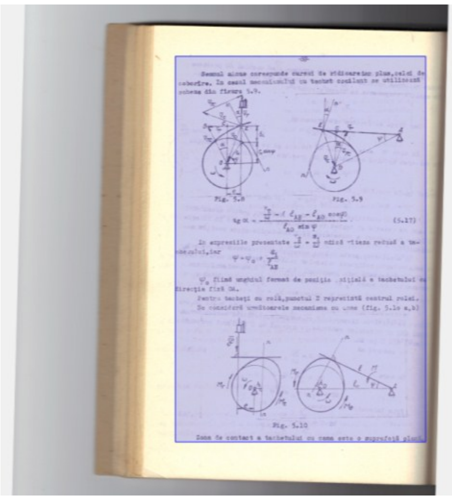 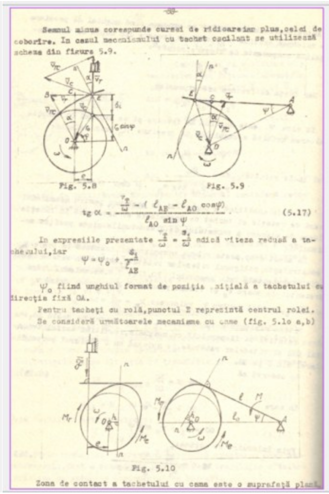

Figure 3.1.6 Selection of content **Figure 3.1.7 Setting margins of page**

The image of a page posted online was presented in figure 3.1.1 (right). Software used for the management of image taking process, the stocking of digital copies and the assurance of compatibility with further advanced processing programs were developed by members of the thinkMOTION team of Timisoara.

3.1.3 Scanning equipment

3.1.3.1 General requirements

Digital copies of analogue documents are very common in nowadays. Digitization is performed on purpose of creating multiple copies or original digital documents. The market offers a wide range of standard scanners, featuring very different technical parameters and designated to single document or thin printed matter processing [93, 94, 100, 105]. A particular class of scanners is specially designed for book scanning [109, 107, 106, 114,97].

The requirements imposed by the activities of thinkMOTION project led to conceiving and building of original scanning equipment.

These requirements refer to:

- possibility of scanning any type of document (single sheet, journal and book) without damaging in any way the original paper (bending, folding, scratching, tearing, heating etc.). This totally non-destructive feature is very important especially for old documents, with fragile pages, which exist in a small number of copies or even may be one of a kind
- maximum document size ~ 400 x 260 mm. Maximum page size taken into account was A4 (297x210 mm). A safety range of 50 mm was considered reasonable along three edges (top, bottom, left/right) for large non-standard old documents and also for

efficiency of work on any size of page. The operator should not waste time because of a restricted positioning area

- high degree of resemblance of the copy in respect with the original. The problem of distortion toward outer sides and corners is present for most all-purpose scanners on the market, in case the original document is a thick book. Furthermore, the thicker the book is, the bending and folding are stronger
- high quality of the digitized copy. The optical resolution was imposed at 300 dpi, at least
- flexible color mode (color and gray scale)
- high speed scanning. The large amount of analogue documents intended to be digitized imposed a high-speed work. The equipment was designed to deliver up to 600 copies per hour
- software facilities regarding management of image taking process, stocking of digital copies and assurance of compatibility with advanced processing programs.

The object of scanning is printed matter, which exists exclusively in paper form and originates from different periods of scientific evolution. The mechanical design was based on criteria such as:

- flatness of active surfaces
- quick placement and removal of the original document
- mechanical raw focusing facilities
- adjustment regarding the thickness of the original document
- finding constructive solutions so that no damage is inflicted upon the original document.

3.1.3.2 Optical and mechanical design

From optical point of view, the equipment is conceived to achieve simultaneous scanning of two pages, which doubles the efficiency of the assembly.

Two similar optical systems were designed to capture images of left and right page of a book. The basic scheme in figure 3.1.8 illustrates the general concept of taking images. Two digital cameras endowed with CMOS sensors are mounted on a fixed frame in a position that provides an angle of 90^o between their crossed optical axes. For a given working distance WD, outcomes a certain field of view FOV, both for left and right side of the cradle, where the book lies.

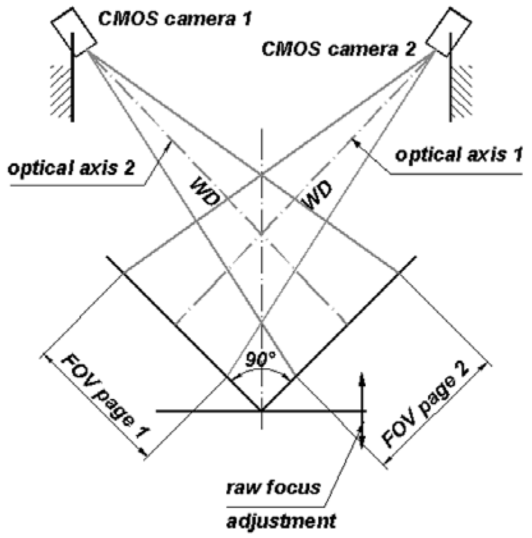

Figure 3.1.8 Optical scheme of the scanning equipment

Most scanning assemblies available on the market feature a flat bed or a V-shaped cradle, 110^{o} in opening. Photometric optimization, based on minimization of reflected light and uniformity of illumination, proved the angle of 90^{o} to be the most convenient.

For each optical system, the following preliminary calculus was performed [70, 50]:

- ❒ numerical option for WD and FOV. Considering the maximum dimensions of the assembly, the following choices were accepted: WD ~ 500 mm and linear FOV ~ 400. Figure 3.1.9 emphasizes the main optical parameters involved in further calculus

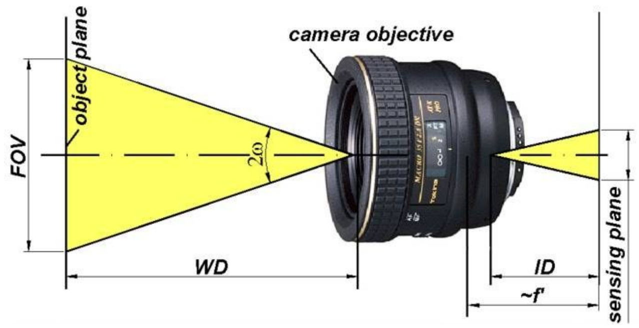

Figure 3.1.9 Main parameters involved in optical design

- ❒ computation of angular FOV, necessary in lens's selection. According to notations in figure 3.1.9, the half-angle of view, ω, is:

$$\omega[\deg] = \arctan\left(\frac{FOV}{2 \cdot WD}\right) \cong 22^{o} . \tag{3.1.1}$$

- considering the image distance ID (between the lens and the sensor area) of approximately 60 mm, the focal length of the objective should be:

$$f' = \frac{WD \cdot ID}{WD - ID} \cong 54mm. \tag{3.1.2}$$

Preliminary data allows the selection of a digital camera and a high quality objective. The choices went to a CMOS camera type Canon EOS 550D [96] equipped with an objective Tokina AF 35mm [113]. Main specifications of the camera and objective are presented in tables 3.1.1 and 3.1.2.

Table 3.1.1 Camera specifications

IMAGE SENSOR	
Type	22.3 x 14.9 mm CMOS
Effective Pixels	Approx. 18.0 megapixels
Aspect Ratio	3:2
LENS	
Focal Length	Equivalent to 1.6x the focal length of the lens
FOCUSING	
AF System/ Points	9 AF points (f/5.6 to f/2.8)
AF Point Selection	Automatic selection, Manual selection
Selected AF Point Display	Superimposed in viewfinder and indicated on LCD monitor
Predictive AF	Yes, up to 10m
SHUTTER	
Type	Electronically-controlled focal-plane shutter
Speed	30-1/4000 sec
FILE TYPE	
Image Size	JPEG: (L) 5184x3456 (M) 3456x2304, (S) 2592x1728 RAW: (RAW) 5184x3456
File Numbering	(1) Consecutive numbering; (2) Auto reset; (3) Manual reset
INTERFACE	
Computer	Hi-Speed USB
Other	Video output (PAL/NTSC) (integrated with USB terminal)

Table 3.1.2 Objective specifications

Parameter	Value
Focal length	35mm
Maximum/ Minimum aperture	f/2.8 - f/22
Optical construction	9 elements in 8 groups
Angle of view	43°
Minimum focus distance	14mm
Lens length	60.4mm

Taking into account the characteristics of both camera and objective, the following remarks are relevant:

- the camera and objective form a very flexible system from optical point of view. Clear and sharp images are taken from distances comprised within the range of 14 mm (where PMAG = 1) up to infinity (theoretically, where PMAG = 0)

- the autofocus feature works on manual/automatic mode in 9 steps. The cameras on the equipment were set on automatic mode. The raw focus is achieved by the operator at the beginning of a new task
- the points of autofocus are correlated with suited f-numbers (f/#) in order to preserve image quality
- the aspect ratio provided by the camera (3:2) matches the dimensions of the active area on each side of the cradle (400x260 mm), so that space is efficiently used
- the output image file features *.jpeg format, which can be used in any common software dedicated to image processing
- the video output signal is compatible to any modern display device
- the integration of the capturing image assembly into the entire system is very easy as it requires a simple USB connection.

The specifications above allow calculus of all characteristics for the imaging system, as follows:

- primary magnification, PMAG:

$$\mathrm{PMAG} = \frac{\mathrm{sensor\ size}(\mathrm{H})}{\mathrm{FOV}} = 0.05575, \tag{3.1.3}$$

- pixel size (H):

$$\mathrm{pixel\,size}\,(\mathrm{H}) = \frac{\mathrm{sensor\ size}\,(\mathrm{H})}{\mathrm{max\ image\,size\ RAW}(\mathrm{H})} = 4.3\,\mu\mathrm{m}, \tag{3.1.4}$$

- pixel size (V):

$$\mathrm{pixel\,size}\,(\mathrm{V}) = \frac{\mathrm{sensor\ size}\,(\mathrm{V})}{\mathrm{max\ image\,size\ RAW}(\mathrm{V})} = 4.3\,\mu\mathrm{m}, \tag{3.1.5}$$

- sensor resolution (H), R_{CMOS}:

$$R_{\mathrm{CMOS}} = \frac{1000 \cdot 25.4}{\mathrm{pixel\,size}\,(\mathrm{H})} \cong 6000\,\mathrm{pixels/inch}, \tag{3.1.6}$$

- system resolution:

$$R_{\mathrm{sys}} = R_{\mathrm{CMOS}} \cdot \mathrm{PMAG} \cong 330\ \mathrm{dpi}. \tag{3.1.7}$$

The numerical parameters above indicate a perfect suitability of chosen components with assembly's requirements. From optical point of view the camera equipped with the objective, provide an imaging system, whose parameters are summarized in table 3.1.3.

Table 3.1.3 Numerical parameters of the optical system

Parameter	Value
Focal length, f‘	56 mm
Autofocus	Yes, DOF = 10 mm
Working distance, WD	~500
Max. field of view, FOV	400 mm (linear), 43^{o} (angular)
Image resolution, R_{sys}	> 300 dpi

The illumination device digitLITE DI-600 [91] was chosen for its excellent photometric and colorimetric properties.

Figure 3.1.10 provides a general image of the scanning equipment named “tm-book’s”.

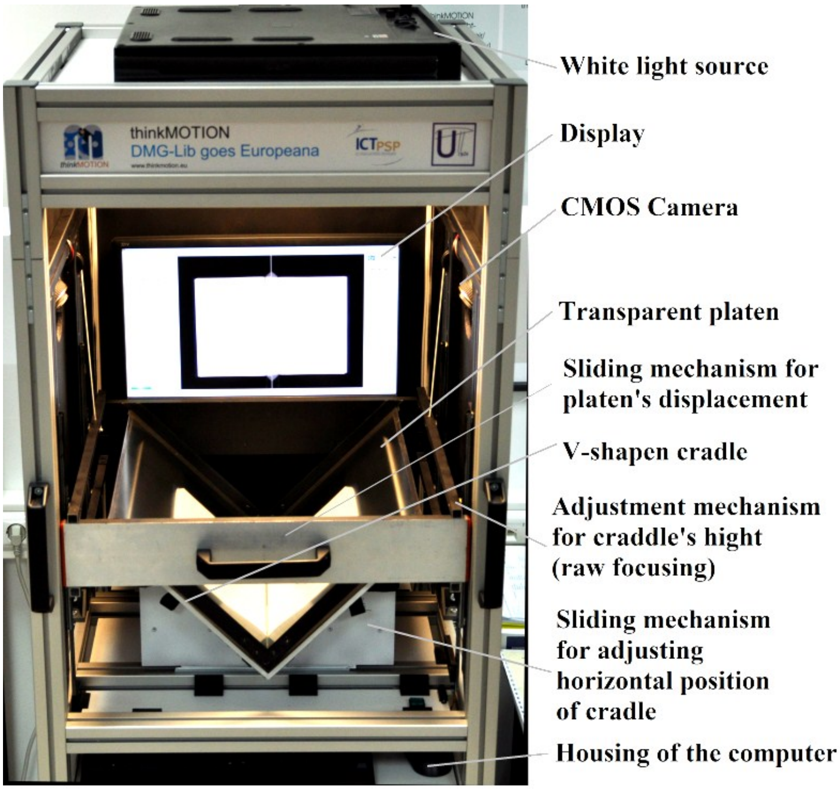

Figure 3.1.10 General view of “tm-book’s”

The mechanical design provided solutions for housing the optical components, the V-shaped cradle and three sliding adjustment mechanisms:

- mechanism for vertical sliding of the cradle in order to achieve raw focusing according to the thickness of the book
- mechanism for vertical displacement of the transparent platens, which flatten the pages to scan
- horizontal sliding mechanism, which adjusts cradle’s position so that the original document covers the central area of the field of view.

On the upper side of the housing is mounted the Lambertian lamp. In order to avoid multiple reflections of light that come from the lamp, the inner faces of the housing were painted in opaque black. In addition, to remove glare from the scanned images, the platens were manufactured from anti-glare glass.

On the upper-back wall of the housing hangs the display, on which the human operator watches previews and final scanned images. The lower half of the housing hosts the computer to which the cameras and the display are connected and some other electrical devices.

3.1.3.3 Design of software tools

The cameras are equipped with USB terminals, which provide the data fed, received and processed by means of software. The program allows the preview of the original document. Preview is necessary for single sheet documents and at least once for books, in order to adjust the vertical and horizontal position of the cradle and of the scanned document.

The program’s interface is foreseen with controls, which allow the human operator to command functions or choose options, as follows:

- to manage files and folders in order to create a hierarchical database, easy to access
- to start the image capturing
- to choose capturing left/right/both pages
- to work in preview mode
- to watch a list containing the names of raw files, which are automatically numbered accordingly to the order of their generation
- to perform common Windows functions, such as opening management programs or shutting down the computer.

Also the captured images are available on-screen, replacing the preview images once the files were downloaded from the cameras (figure 3.1.11). The color mode chosen is 256 levels gray scale (8 bit format).

The two cameras capture images when the user presses a button on the program interface or through making use of the “AutoScan” function. This tool allows using of either a button mounted on the frame of the scanner (in such a way that minimizes the hand movement of the user) or an optical distance sensor. This sensor can be configured to trigger the image capturing process when the glass platen is lowered under a certain limit (the book thickness, which can be selected for every book by hand).

Figure 3.1.11 Print-screen of the program's interface, showing a captured image

Post processing of the scanned images is done by other software tools and the final result is a searchable PDF document.

3.1.4 Conclusions and contributions

The research work developed within the present chapter can be summarized as follows:

- Digitization techniques are used on the purpose of retrieving the history of mechanism science and of creating a coherent description of its development since early ages until present days.
- Digitization of analogue documents requires special resources regarding equipment and software.
- The team from the University Politehnica Timisoara, as partner in the thinkMOTION project, developed a workstation specialized in digitization of all-type documents.
- Design and assembling of the scanning equipment as well as the capturing, stocking and managing raw image files software were developed as original contributions of the team.
- Thousands of high quality pages are now available online for a large range of users (academic staff, students, PhD. students, engineers, historians etc.).
- The scanning equipment "tm-book's" is functional for over 8 years and proves to be reliable, productive and easy to use. The scanned documents respect the project requirements and they are high quality digitized copies regardless of the physical state of preservation. Most of the documents scanned with this equipment

(Romanian old thesis, conference proceedings and patents) can be seen on the DMG-Lib's webpage, www.dmg-lib.de, provided as "text-under-image" searchable PDFs.

- The equipment itself raises only small maintenance issues and also provides some knowledge base useful in improving the design for the next versions. Considering these aspects one can conclude that the initial goal of the scanner is achieved and that a robust and cost-effective "in-house" book scanning solution was developed.

The original contributions in this chapter are:

- Planning of the workflow in the digitization process.
- Planning of steps in the process of image enhancement and selection of adequate software.
- optical design of the scanning equipment
- mechanical design of the scanning equipment
- development of software tools for the scanning equipment
- choice for optical and mechanical components and assembling of the scanning equipment.

3.2 Interactive animation production by means of advanced image processing

3.2.1 Statement of problem

The current availability of computer-type devices and the internet provides a great tool for information and knowledge spreading in all fields of human activity and in particular in the technical fields. The European project thinkMOTION is intended to offer knowledge in the field of mechanisms and machine science through a specialized site called DMG-Lib which is a digital library that provides content originating from a wide range of sources such as universities, libraries, patent offices, museums etc. [45]

One of the content categories posted on the DMG-Lib site (aside books, articles, images, biographies etc) is represented by the interactive animations. These animations have the role of bringing the users closer to the real functioning mode of the mechanisms (physical or CAD models) listed on the portal, by allowing to virtually “drive” those models with the mouse or with the touch of a finger.

3.2.2 The TU-Ilmenau digitizer

Content sources as the basis for mechanism descriptions are physical demonstration models (figure 3.2.1 left), pictures, movies and animations but also pieces of literature such as technical books, journal articles, research reports, patent specifications or mechanism catalogues.

Figure 3.2.1 Physical demonstration models from the University of Hannover (left) and descriptive texts in books (right) as examples for content sources for mechanism descriptions

A lot of these literature sources contain design solutions or structures of mechanisms in form of technical drawings, solution principles or images (figure 3.2.1 right) for creating mechanism descriptions. Interactive animations can be produced for all these content sources, and in the case of drawings or images an image sequence can be generated from some CAD software and then further processed using the AIS generator software.

For the case of physical models a digitization workstation was developed at the Ilmenau University of Technology, Germany, which works with a digital (photo) camera, a variable lighting system and a PC-controlled stepper motor (figure 3.2.2). For each series of models an individual adapter between the motor and the model input and an invisible fixing for the model must be designed. A customized lighting position for each series and sometimes for each model is necessary to get contrast and remove shadow in images.

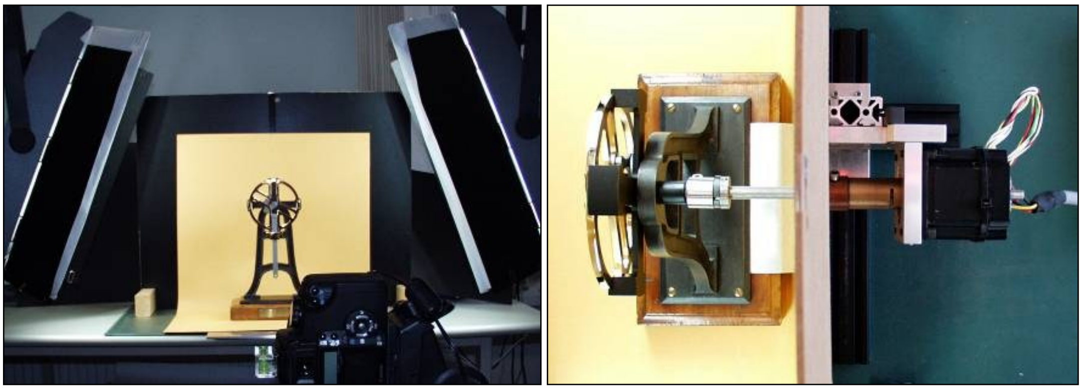

Figure 3.2.2 Workstation at the Ilmenau University of Technology for digitalization of the physical demonstration models (left: front view, right: top view)

The stepper motor drives the model step by step and the camera takes a photo after each step. The stepper motor and the camera are controlled by a PC. The controlling software (figure 3.2.3) allows different settings depending on the peculiarities of the models. In this way, from each model a sequence of usually 400 images per turn is recorded.

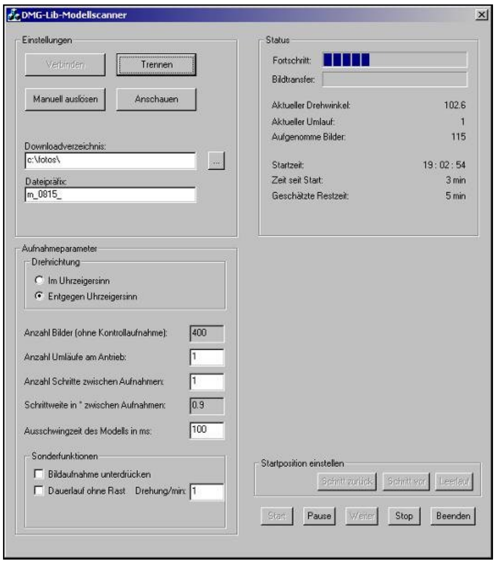

Figure 3.2.3 PC software for controlling stepper motor and camera

With the image sequence recorded, the next step consists of processing these images inside the AIS generator software.

3.2.3 The UPT digitizer

The method approached at UPT for digitizing the physical mechanisms models is to use a compact system that can be easily carried around and can be set up in a few minutes. This compact PC-less option is preferred due to the fact that it is more difficult to bring a bunch of physical models into a digitizing lab especially when they are in a large number and/or in sparse locations (multiple universities). In order to achieve this goal the system uses a programmable logic controller [104] connected to a digital servo-motor [101] and also to a digital photo camera (figure 3.2.4 left).

The chassis of the system supports the motor, the controller, the power source and also the user interface buttons. The servo-motor can be positioned on its vertical axis in order to accommodate the coupling to different mechanisms (which can have their driving element at different heights).

In order to solve the mechanical coupling to the driven mechanisms, the motor benefits from a standard chuck attached to its driving shaft via an elastic element. In this way, mechanisms having their driving axle with a diameter between 2 and 10 mm can be driven by this digitizing system.

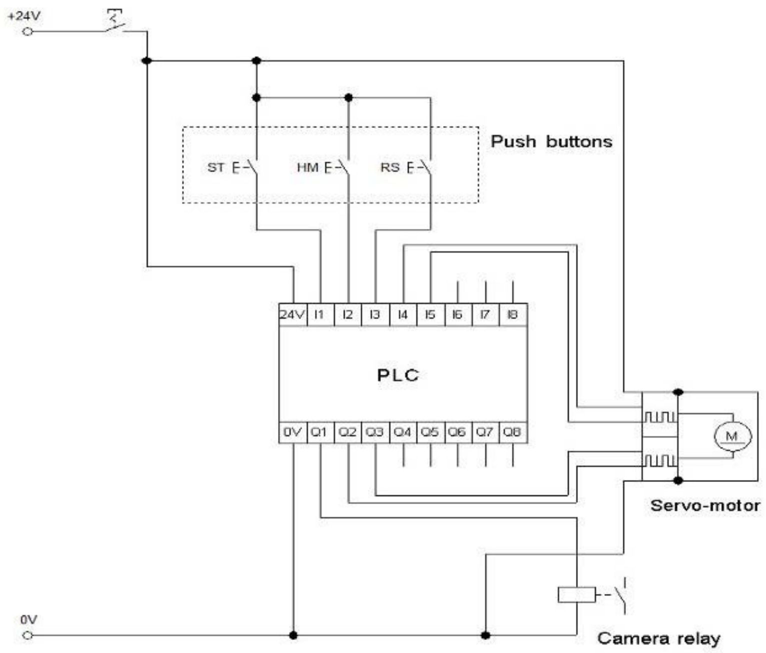

Figure 3.2.4 Electrical assembly schematic for the digitizing stand

From an electric point of view the controller is connected to the motor's electronics and is also connected to a digital camera that takes the pictures of the mechanism between each movement increment, and to the user buttons board. A schematic of the electrical assembly is represented in figure 3.3.4.

Beside the aforementioned components the digitizing system also benefits from a led lamp for illuminating the digitizing scene. The advantage of this lamp is its high light output combined with very low heat emissions, thus making it suitable for placing it very close to the photo camera or to the physical model of the mechanism.

Figure 3.2.5 right presents the model being photographed, having a cardboard sheet (with an appropriate cut-out) placed between the model and the motor's chuck in order to hide the stand behind it from being captured by the camera.

From the software point of view, the image capturing sequence can be regarded as event-driven loop. After the mechanism is securely affixed to the motor's shaft, the lights are arranged and the camera is set up, the user pushes the homing (HM) button in order to define the current position of the motor as "home" and then the start (ST) button to begin the process. The motor is then commanded to rotate to its next relative stored position (CCW, 0.9 deg.) and the controller waits for the "motion complete" signal from the motor.

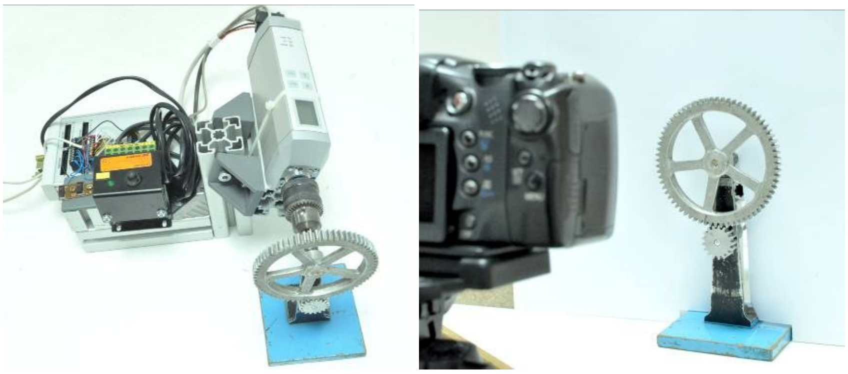

Figure 3.2.5 General view of the digitizing stand, coupled to a physical model (left) and the physical model being digitized (right)

After receiving this signal the controller sends a low voltage pulse (via a relay and a voltage divider) to the photo camera through its USB port. The camera uses a modified firmware that allows for remote shooting when its USB interface detects a rising edge pulse on the cable power lines. After the time delay reserved for taking the photograph expired, the process repeats and the controller commands another 0.9 deg. rotational increment of the motor.

In the event of a motion error or a motion watchdog catch (e.g. after commanding an increment it takes more than 1 sec. for the motor to send the "motion complete" signal) the process is paused and the user can either eliminate the cause of the malfunction and continue (press ST button) or reset (RS button) the system and start the process again from the current location.

When the mechanism inched a full rotation (400 increments / 360 deg) the controller commands the motor to return the model to its initial position and with this motion completed the process ends. The 400 pictures can now be downloaded from the SD card to a PC and then further processed using the AIS-Generator software.

3.2.4 The AIS-generator software

Producing the interactive animation requires the processing of the image sequences. For this, "thinkMOTION" uses an interactive web video technology called AIS which originated from project DMG-Lib and has been improved since. AIS stands for Augmented Image Sequence and consists of three essential parts: the generator software, the data format and the web player software.

The generator software uses videos or image sequences as input data. Some manual preparation steps are necessary before automatic processing can begin. At first, the user needs to specify a crop region to select the part of the image to be used in the interactive animation. Then a logo and its position may be selected. The software also allows adding information for linking the created animation to existing content in the DMG-Lib database (e.g. description of the mechanism featured in the animation).

The last and most important preparation step is the specification of the driving element and its parameters. The user interactively draws lines that represent the position and orientation of the driving element at the beginning and at the end of the animation. This information is necessary to map user interactions to video frames in the finished animation. Currently, the AIS generator and player support rotational and translational driving motions.

Once these manual steps are completed, the generator software processes the input data and creates the AIS animation. In addition to the actual video content and a preview image it contains an XML file that holds the interaction-related parameters to be interpreted by the AIS player software. Typically, a finished AIS animation will be uploaded to the DMG-Lib database. There it will be listed and may be loaded in to the AIS player. The player is a Java applet that can be embedded into web pages. It features play controls like a normal, non-interactive video player. Still, the most interesting mode of interaction is to directly „grab" the driving element with the mouse and move it. The video content in the player will react accordingly (figures 3.2.6 and 3.2.7).

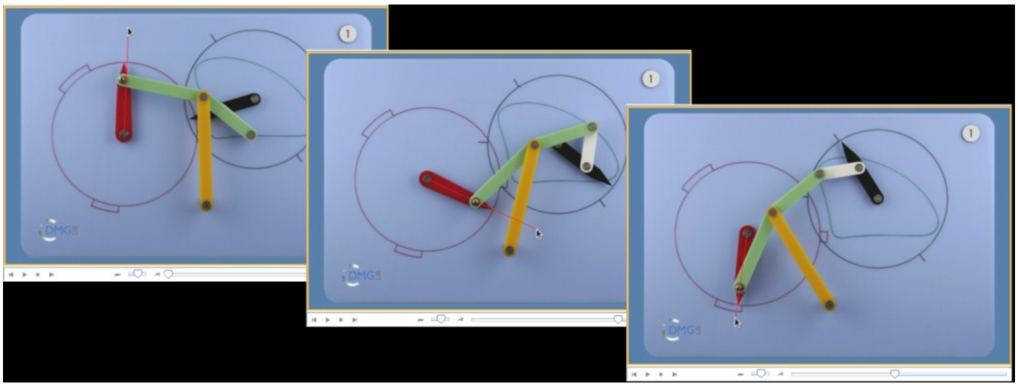

Figure 3.2.6 Digitized and processed mechanism in the AIS Player. The mouse cursor controls the motion of the mechanism in the animation

Figure 3.2.7 Interactive animation for a digitized physical model (left) and for a CAD generated model (right), on the DMG-Lib portal

This creates the illusion of actually touching and operating the mechanism. It brings the user closer to the real demonstration model that has been digitized. That way, the interactive animation facilitates to understand the mode of operation and the kinematic properties of the mechanism.

3.2.5 Conclusions and contributions

The research work developed within the present chapter can be summarized as follows:

- Physical demonstration models are the basis for creating mechanism descriptions in the DMG-Lib. The physical working models of the mechanisms are digitally recorded as a sequence of images, usually covering a full rotation of the input (driving) element.
- With further handling steps, these image sequences are composed to interactive animations, which can be started inside the DMG-Lib Internet portal with a special player or can be downloaded as video files for local use.
- By digitizing these content sources as interactive animations, the working principles and kinematic properties of these mechanisms can be observed much easier and

with a greater impact on the information quantity and quality obtained by the user of the web site.

- ❒ The mechanisms and physical models presented in this paper, and many more, can be viewed and interactively animated by accessing the DMG-Lib portal, available at www.dmg-lib.org.

The original contributions in this chapter are:

- ❒ Optical and electrical design and assembling of a digitizer at the University Politehnica Timişoara
- ❒ Taking of sequence images of a big number of physical models in the Mechanism Laboratory of UPT
- ❒ Processing of images with the software which generates the interactive animations.

4. Optical engineering in medical investigation

4.1 Modeling of human spinal column and evaluation of spinal deformities

4.1.1 Statement of problem

Modeling and simulation is widely used in all domains as resourceful tools in design, enhancement, improving or forecasting behavior of different systems. A wide range of software is available to aid solving engineering problems. However, there are systems, such as the biological ones, to which modeling and simulation is a very difficult task. The difficulty originates in two essential features:

- human body parts are very irregularly shaped
- anthropometric normal data is very scattered, regarding age, sex, race, profession, local environment traits and so on.

Therefore, biological models are not yet developed on large scale even though they would be very useful in investigating and monitoring patients suffering of wide-spread diseases. However, there is an encouraging start in modeling different parts of human body [60, 21]. The purpose of modeling is either depicting abnormal anatomical shapes or designing of devices such as prosthesis.

The present work focuses on the class of spinal deformities, which are very common in now-days. Most individuals suffer of mild or severe spinal column deformities, such as scoliosis, lordosis, kyphosis or combinations of these. Deformities cause diminution of personal comfort and of physical or intellectual capacity of effort. When severe, deformities bring on large distortions of thorax shape and alteration of respiratory process. Such spinal diseases occur frequently at school-age population, due to incorrect posture and/or to improper desk design and less frequently to adult population, due to sedentary activities (teachers, librarians, IT specialists etc.). The elder population also suffers because of irreversible bone alteration. Plenty of statistics describe the prevalence of such diseases in different places of the world, taking into account a lot of aspects such as: age, sex, profession, life standard etc. [52, 57, 87]. The studies emphasize in detail the importance of identifying early stages of spinal deformities because of cautious prognostic and very high costs of treatment [5].

Engineering sciences offer a large series of equipment to investigate the human bone system. Among the methods of investigation in use, the most common are X-ray, CT or MR imaging, Moire topography, digital ultrasonic mapping and optical scanning [9, 18, 38, 42, 43, 49, 61, 83, 48, 75]. The stating order of these methods is chronological regarding the implementation and inversely from invasive character standpoint.

Countries which develop long term healthcare programs always include spinal deformities among the main issues to investigate and monitor, especially to school children and persons involved in specific professional activities. The main problems in tracing and monitoring spinal deformities consist of:

1. Finding a quick and less invasive method of investigation
2. Establishing a set of numerical parameters to describe completely the column's shape
3. Storing of a large amount of data considering the big number of subjects in the database
4. Accessing data and evaluating the evolution of patients.

In order to model the spinal column and simulate its behavior, considering a long-term monitoring of an extended sample of population, the following workflow was conceived (fig. 4.1.1).

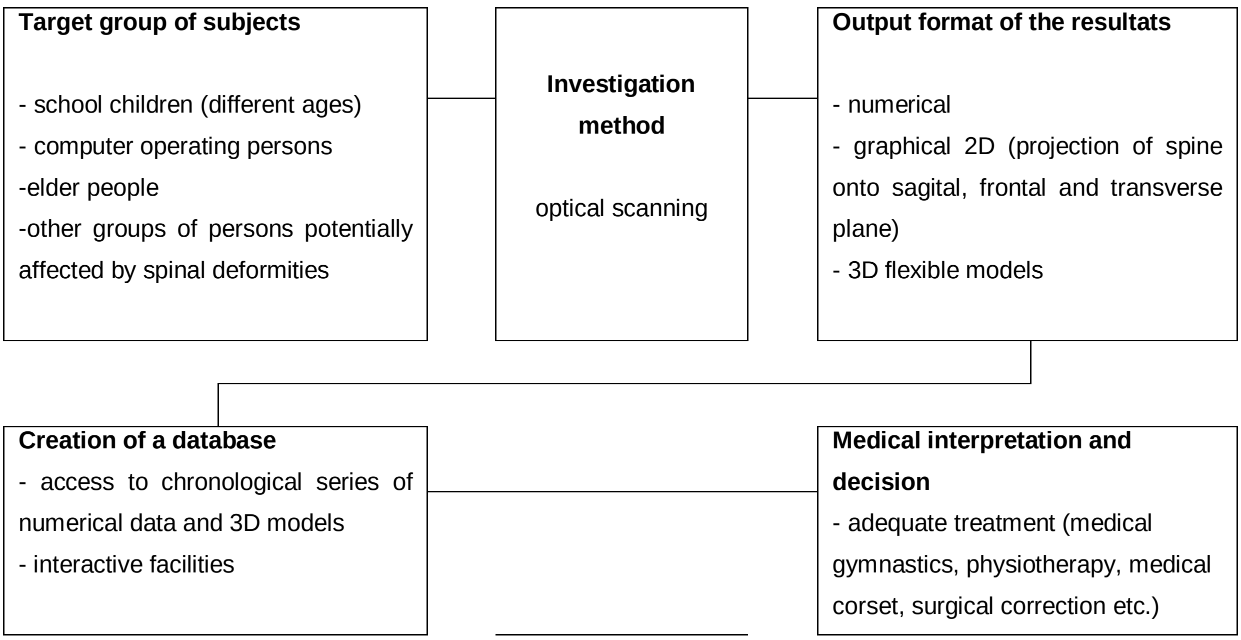

Figure 4.1.1 Workflow

The text-boxes in figure 4.1.1 indicate the logical steps to follow from establishing the target group of subjects to physician's decision regarding the results of a complete, objective and non-invasive investigation. The lower text contains the concrete goals to fulfill at each step.

4.1.2 Equipment and software to provide data for modeling

As figure 4.1.1 shows, the choice for the investigation method went to a totally non-invasive method, based on optical scanning.

Such an integrated system assumes both capture and analysis of image. Accurate results require several technical conditions, such as:

- adequate configuration of the scene where the image is captured
- imposed optical specifications of the capturing equipment (field of view, object distance, depth of field, resolution)
- general software for processing images and specific software for calculus and rendering of medical parameters.

The configuration and choice for equipment followed the logics imposed by specific conditions and goals, as listed below:

- the system must provide a diagnosis regarding the geometrical condition of the spinal column. In this regard, there are a lot of habitual incorrect postures or variously rooted deformities, such as scoliosis, kyphosis, lordosis or combinations of those. World Health Organization (WHO) classifies the spinal deformities as diseases. WHO and DIMDI (German Institute of Documentation and Information) provide a full table of diseases, up-dated to 10th revision of International Classification of Diseases (ICD-10) [90].
- the investigation method should be non-invasive, if possible. Most of the now days investigation are more or less invasive
- the equipment must acquire images over a large field of view (FOV) as the 3D reconstruction of torso's shape is intended
- the resolution of images must be high enough to allow depiction of spatial coordinates. The markers applied over patient's body emphasize the points of interest
- the processing of images must supply a set of numerical parameters and render several images with simplified projections of the spine on the reference planes (sagittal, frontal and transversal).

Considering the above requirements, a team of multidisciplinary specialists developed a diagnosis method based on the equipment supplied by the Canadian Company InSpeck [110]. The technical team chose to implement the system InSpeck 3D Halfbody, which needs three cameras (fig. 4.1.2).

The cameras must be optically aligned (their optical axes must intersect in one point, placed in the centre of the scene, where the patient stands. Figure 1 emphasizes the common FOV of the three cameras, which defines a virtual cylindrical space where the image capturing is efficient and where the patient is standing.

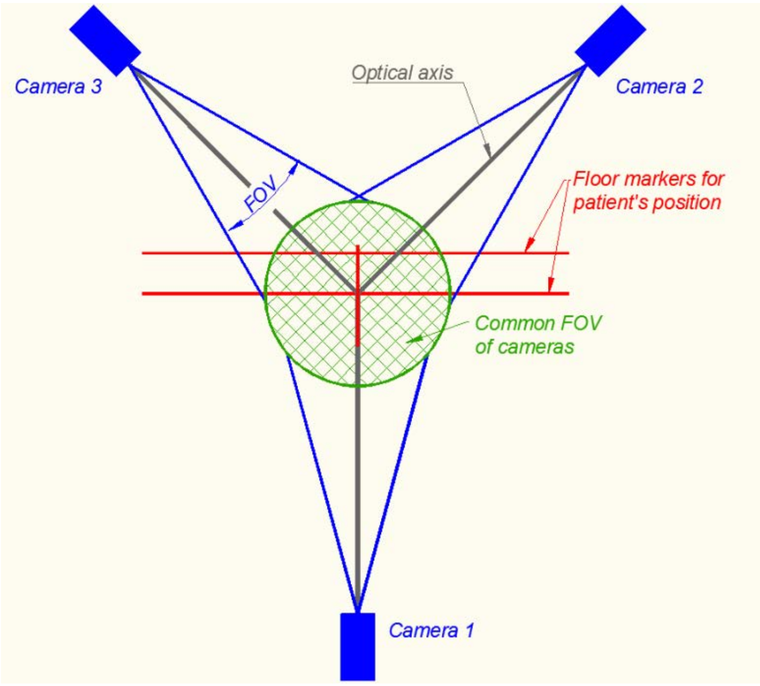

Fig. 4.1.2 Imaging in Halfbody configuration

The red lines (fig. 4.1.2) marked on the floor bound the area where the subject of investigation must step on.

The cameras Mega Capturor II are not still image capturers, but scanners, which acquire sequences of image. This is a good solution because of the very large FOV required by a human torso, at a distance of about 1.5 m.

The optical image from each camera, turned into an electrical signal, reaches a PC, where the software FAPS 5.5 (Fringe Acquisition and Processing Software) creates a 3D virtual model. The second software in the original package – EM 5.5 (Editing and Merging) – allows complex processing of data. The technique of 3D digitization finally renders a three-dimensional copy of the physical surface placed in front of the cameras.

In order to collect useful data, the specialists thought of a way to designate the points where 3D coordinates were going to be recorded. Two sets of markers were designed. One set consisted of simple rectangular shaped markers. They are stuck on the reference point of the vertebrae and provide data for calculus of postural and deformity parameters. Figure 4.1.3 renders an image created with FAPS. The central point of the red markers shows the points of interest in a projection of torso on the front plane.

For calculus of relative rotation of vertebrae, the markers are complex shaped, so that coordinates are possible to collect in more points.

Fig. 4.1.3 Front plane image to show markers' shape and position on human torso

The solution presented in figure 4.1.4 contains four significant points (denoted A, B, C and D).

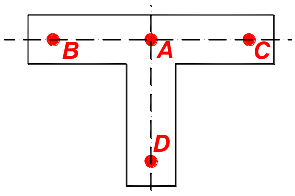

Fig. 4.1.4 "T" shaped marker, which allows measurement of coordinates in four points

The thinking in markers' design regarded subsequent mathematical processing of data, which should be as simple as possible.

The markers were manufactured of plastic behaviour materials, so that they entirely adhere to the skin around the vertebra. The Laboratory used markers made of a silicon material, which allows geometrical adhesion on the skin, is not toxic, and provides weak adhesion, for short temporary fixing. Four holes drilled in the body of the marker, correspond to points A, B, C and D.

Determination of postural parameters, spinal characteristic distances and angles and, finally, global deformities need the knowledge of vertebrae coordinates along a zone as extended as possible. The practical measurements included a long segment of the spine comprising the vertebrae from C7 to S3. For a better description of posture and deformities, six supplemental markers picked coordinates of shoulders (U1 and U2), scapulae (O1 and O2) and iliac crests (P1 and P2) – fig. 4.1.5.

As the equipment is able to pick 3D coordinates, the characteristic parameters of spine are defined within one of the three anatomic planes: xy –frontal plane, zy –sagital plane and xz – transversal plane.

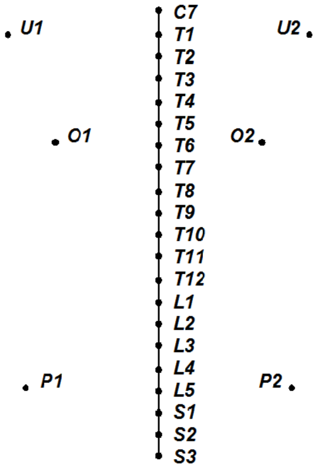

Figure 4.1.5 Position of 29 markers to indicate the points where 3D coordinates are picked

Knowing 27 triplets of coordinates (x,y,z), a large series of parameters can be defined. In tables 4.1.1, 4.1.2 and 4.1.3 are presented the significant parameters of the vertebral column, as proposed by the authors.

Table 4.1.1 Parameters in sagital plane (zy)

Parameter	Definition	Scheme
Total trunk inclination	angle between the vertebrae line (C7 – L5) and the vertical axis containing C7	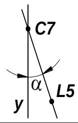
Thoracic kyphosis	angle between the vertebrae line (C7 – T1) and vertebrae line (T12 – L1)	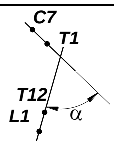
Lumbar lordosis	angle between the vertebrae line (L1 –L2) and vertebrae line (L5 – S1)	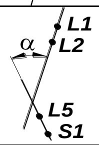
Sacral angle	angle between the vertebrae line (S1 – S3) and the vertical line containing C7	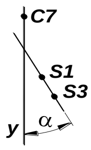

Table 4.1.2 Parameters in frontal plane (xy)

Parameter	Definition	Scheme
Pelvic obliquity	angle between pelvic line (P1 – P2) and a horizontal line	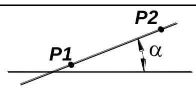
Shoulder obliquity	angle between shoulders line (U1 – U2) and a horizontal line	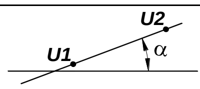
Scapula distance right	distance between the top of the right scapula and the scapulas line projected along y – axis	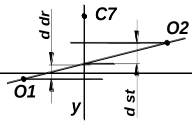

Scapula distance left	distance between the top of the left scapula and the scapulas line projected along y – axis	
Right scoliotic deformation	angle between vertebrae line (C7 – T1) and vertebrae line (T11 – T12)	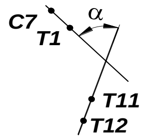
Left scoliotic deformation	angle between vertebrae line (T11 – T12) and vertebrae line (S1 – S3)	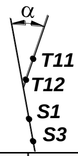
Lateral inclination	angle between vertebrae line (C7 – S1) and the vertical line containing C7	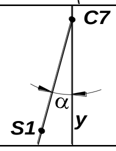
Cobb angle	angle between the perpendiculars to vertebrae line (C7 – T1), respectively line (L4 – L5)	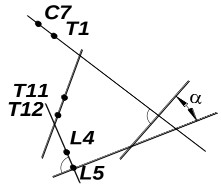

Table 4.1.3 Parameters in transversal plane (xz)

Parameter	Definition	Scheme
Pelvic rotation	angle between the pelvic line (P1 – P2) and scapulas line (O1 – O2)	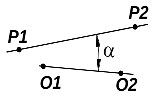

Beside the parameters of the vertebral column within the projection planes, the effective lengths in 3D measurement should be also considered: total length (from C7 to S3), thoracic length (from C7 to L1) and lumbar length (from L1 to L5).

From mathematical point of view, the angles in the tables above are computed considering the line containing the points drawn in the schemes or one point and one of the reference axes.

Generically, the slope of two straight lines, defined by points $A(x_A,y_A)$ and $B(x_B,y_B)$, $C(x_c,y_C)$ and $D(x_D,y_D)$ is:

$$\text{Line AB}: m_{AB} = \frac{y_B - y_A}{x_B - x_A}, \tag{4.1.1}$$

$$\text{Line CD}: m_{CD} = \frac{y_D - y_C}{x_D - x_C}. \tag{4.1.2}$$

The angle between the lines is given by the relationship (fig. 4.1.6):

$$\tan\alpha = \frac{m_{CD} - m_{AB}}{1 + m_{AB} \cdot m_{CD}}. \tag{4.1.3}$$

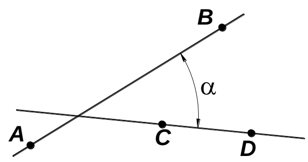

Fig. 4.1.6 The angle between two lines

The angles may result positive or negative. For some parameters, the algebraic values are significant. For other parameters, only absolute value is relevant (with or without specifications such as right/left, forward/backward).

The lengths of column segments result from summation of distances between successive vertebrae:

$$L = l_1 + l_2 + l_3 + \ldots = \sum_i l_i . \tag{4.1.4}$$

where

$$l_i = \sqrt{(x_i - x_{i+1})^2 + (y_i - y_{i+1})^2 + (z_i - z_{i+1})^2}, \tag{4.1.5}$$

with (x_i,y_i,z_i) and $(x_{i+1},y_{i+1},z_{i+1})$ – coordinates of two successive vertebrae.

4.1.3 Software development

The newly developed program, written as Visual Basic Application, was designed aiming the following requirements:

- Development of a data basis containing a minimum set of information about the patients. The information should be accessed selectively, using different filters and should allow introducing and saving new data
- Import of data (coordinates of vertebrae) from an *.xls file
- Automated processing of data in order to obtain 16 parameters of posture or deformity
- Numerical and graphical display of results
- Print of an investigation report containing complete information about the patient (personal characteristics – such as name, age, profession – numerical and graphical results of investigation and notices of the physician if necessary).

The graphical interface of the program, named INBIRE is presented in figure 4.1.7.

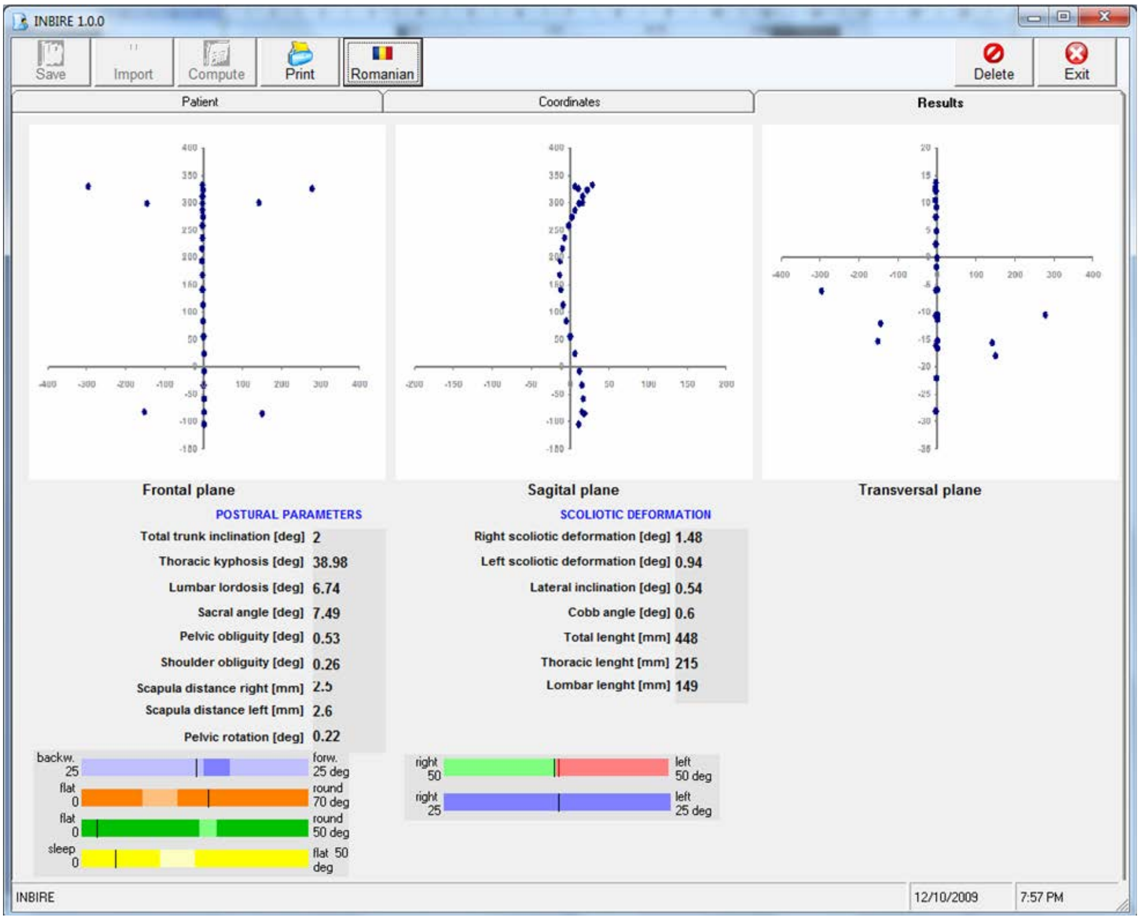

Fig. 4.1.7 Image of results' display

In order to get information on relative rotation between vertebrae, one must use the "T" shaped markers. The principle of measurement is presented in figures 4.1.8 and 4.1.9.

The marker is fixed so that point A superposes the spinous process of the investigated vertebra and point D lies on the line containing the successive spinous processes.

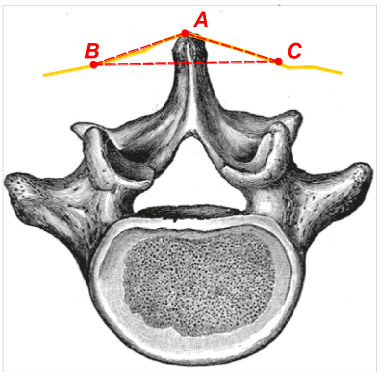

Fig. 4.1.8 Deformation of the marker applied on the skin (yellow) and generation of the triangle ABC (red)

In the beginning, the marker is flat and the points B, C and D are equidistant to the central point A. Sticking the marker on the vertebra of a patient deforms the marker, which gets a spatial shape. The points A, B and C, first aligned, displace and determine the vertexes of a triangle. Figure 4.1.8 shows a top view of a lumbar vertebra and the displaced position of the points A, B and C. The point A superposes the spinous process no matter the shape the marker gets.

Ideally, points A and D belong to a vertical line, triangle ABC is horizontal and its sides AB and AC are equal in length. This situation is very less probable, even for patients considered biologically normal. Generally, the triangle ABC belongs to a spatially random plane. Its projection both on a horizontal and vertical plane is a scalene triangle.

To compute the relative rotation angle between two successive vertebrae, indexed 1 and 2, one needs to develop the following sequences:

- ❒ gathering coordinates of points A, B and C for the vertebra 1
- ❒ drawing the normal AE ⊥ BC
- ❒ projection of the triangle ABC on a horizontal plane. It results a triangle A'B'C' and a corresponding segment A'E' (red coloured in figure 4.1.9.a). This segment is taken for reference to characterize the spatial position of the triangle
- ❒ the above items repeat for vertebra 2 (geometrical elements blue coloured in figure 4.4.1.9.a

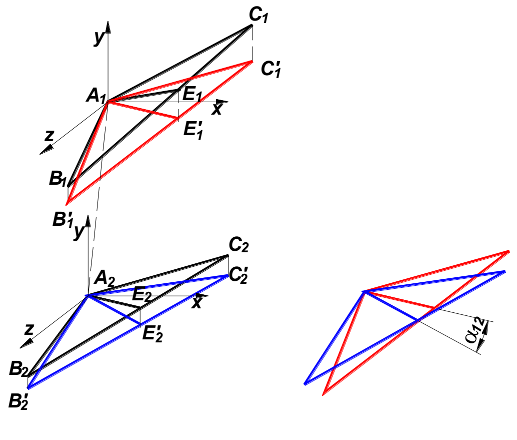

a. b.

Fig. 4.1.9 Principle of computing the relative rotation between two vertebrae

- ❒ translation of projections A'B'C' into a common horizontal plane and computation of the angle α_{12}, between the projections of the altitudes. This angle indicates the relative rotation of the two vertebrae (fig. 4.1.9 b)

- measuring the coordinates of the point D is not necessary for rotation calculation. Its existence is important for the correct positioning of the marker.

Mathematically, the algorithm to compute the angle α_{12} needs to accomplish the following steps:

- measuring of coordinates for vertebra 1 [$A_1(x_{1A}, y_{1A}, z_{1A})$, $B_1(x_{1B}, y_{1B}, z_{1B})$, $C_1(x_{1C}, y_{1C}, z_{1C})$]
- writing the equation of the line $B'_1C'_1$ in a horizontal plane containing the point A_1:

$$\frac{x - x_{1B}}{x_{1C} - x_{1B}} = \frac{z - z_{1B}}{z_{1C} - z_{1B}} \Rightarrow z = m_1 x + n_1 . \tag{4.1.6}$$

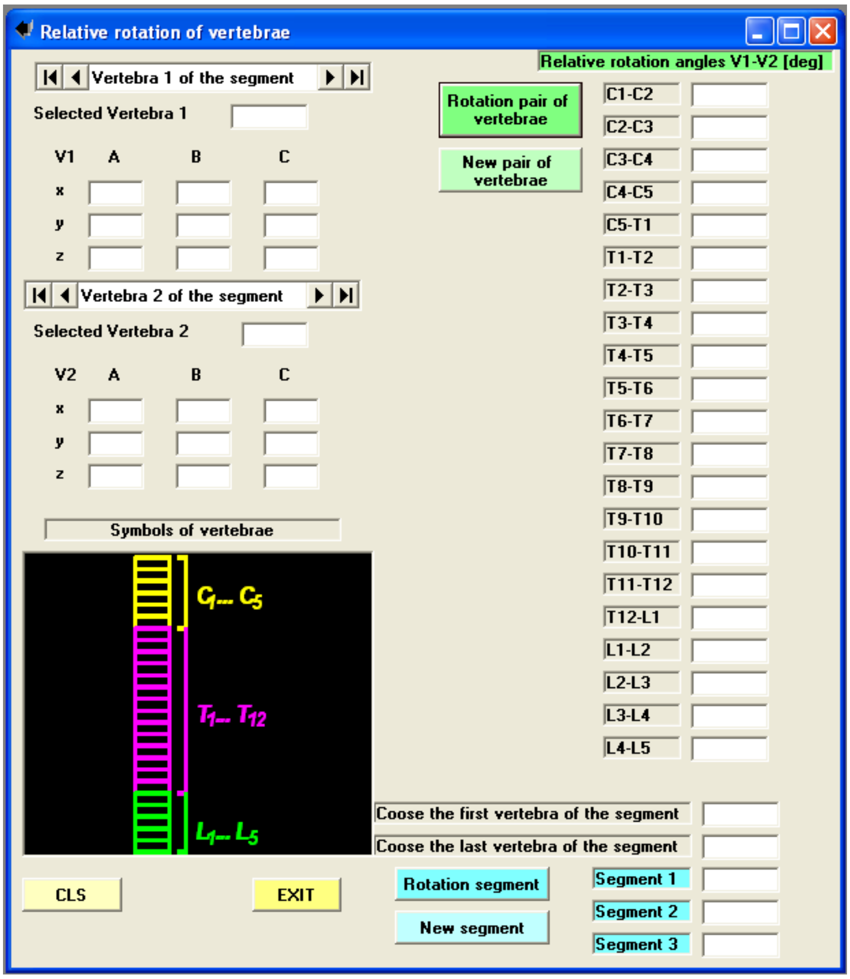

Fig. 4.1.10 Graphical interface of the VBA application

- computation of the slope of a perpendicular line to $B'_1C'_1$ (equal to the slope of the altitude from the vertex A_1):

$$m_{E1} = -\frac{1}{m_1} . \qquad (4.1.7)$$

- ❒ measuring of coordinates for vertebra 2 [$A_2(x_{2A}, y_{2A}, z_{2A})$, $B_2(x_{2B}, y_{2B}, z_{2B})$, $C_1(x_{2C}, y_{2C}, z_{2C})$], writing the equation of the line $B'_2C'_2$ in a horizontal plane containing the point A_2 and computation of the slope of a perpendicular line to $B'_2C'_2$ (equal to the slope of the altitude from the vertex A_2) – similar to the operations performed for vertebra 1
- ❒ calculus of the tangent of the angle between $A_1E'_1$ and $A_2E'_2$:

$$\tan\alpha = \frac{m_{E2} - m_{E1}}{1 + m_{E1} m_{E2}} . \qquad (4.1.8)$$

For automated processing of data, a Microsoft Visual Basic application was conceived. The graphical interface of the programme is given in figure 4.1.10.

4.1.3 Modeling of vertebrae and simulation of column deformations

Modeling of the spinal column is a difficult task so that the literature mentions only a few attempts to fulfill it [7, 3, 41]. Taking into account the specific problems occurring in modeling biological parts, it was conceived the workflow presented in figure 4.1.11.

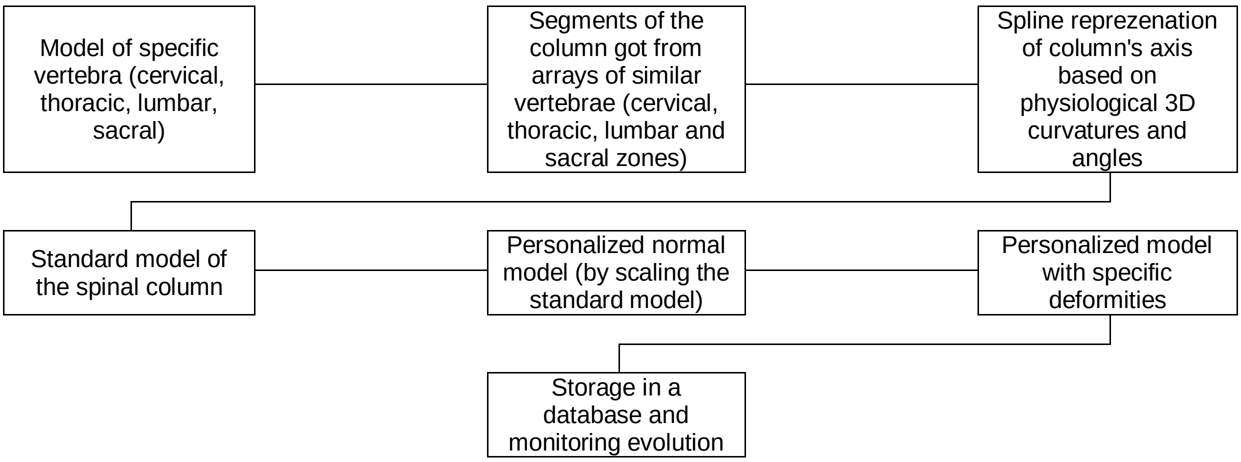

Figure 4.1.11 Workflow

The program chosen to work in was 3Dmax. The general initial data consider the following elements:

- ❒ The spinal column is a complex biological structure, containing 33 - 34 vertebrae, 344 joints and 24 intervertebral discs

- There are 5 distinct segments of the column: cervical (7 vertebrae), thoracic (12 vertebrae), lumbar (5 vertebrae), sacral (5 vertebrae stiffed together) and coccyx (4-5 rudimentary vertebrae).
- The column axis is 3D shaped curve:
  - Curvature angle of approximately 9^o, cervical zone (C1-C7)
  - Curvature angle of approximately 40^o, thoracic zone (T1-T12)
  - Curvature angle of approximately 57^o, lumbar zone (L1-L5)
- Statistical height of a vertebra is ~ 3cm.

For each zone the shape of the vertebrae is different. Each type of vertebra was created starting from a regular shape, namely a cylinder. The functions of the program, such as Cut, Chamfer, Extrude, Smooth, Scale etc., allowed modifying the primary shape until it attained a perfect match with the vertebrae described in Grey's Anatomy Atlas [85].

Figure 4.1.12 contains a print screen from the process of modeling a thoracic vertebra, whereas figure 4.1.13 renders all types of vertebrae together with their adjacent discs. To make the models more realistic, colors and textures were assigned to all elements. Specific zones of the column were obtained by cloning the appropriate type of vertebra and disc, in the required number. The function Array aligned the vertebrae along a spline, drawn using the physiological curvatures. The result is a standard model of spinal column (fig. 4.1.14 and fig. 4.1.15).

Personalized models result using the coordinates got from the program INBIRE, to trace the spinal axis. Functions PathDeform and Modifiers allow relatively easy and fast editing of the standard model.

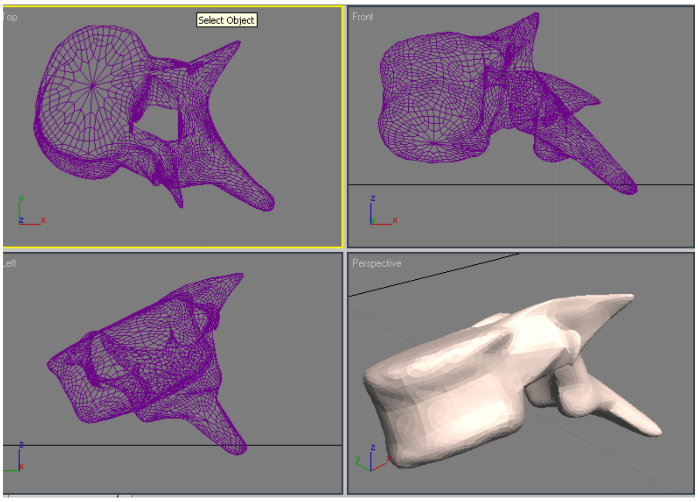

Figure 4.1.12 Model of a thoracic vertebra

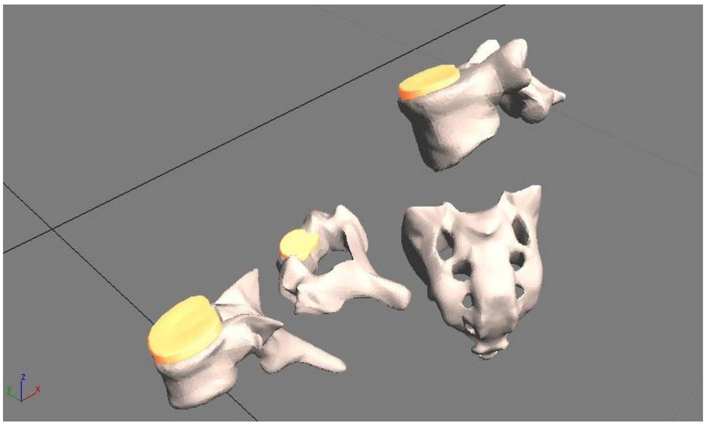

Figure 4.1.13 Models of cervical, thoracic, lumbar and sacral vertebrae with adjacent discs

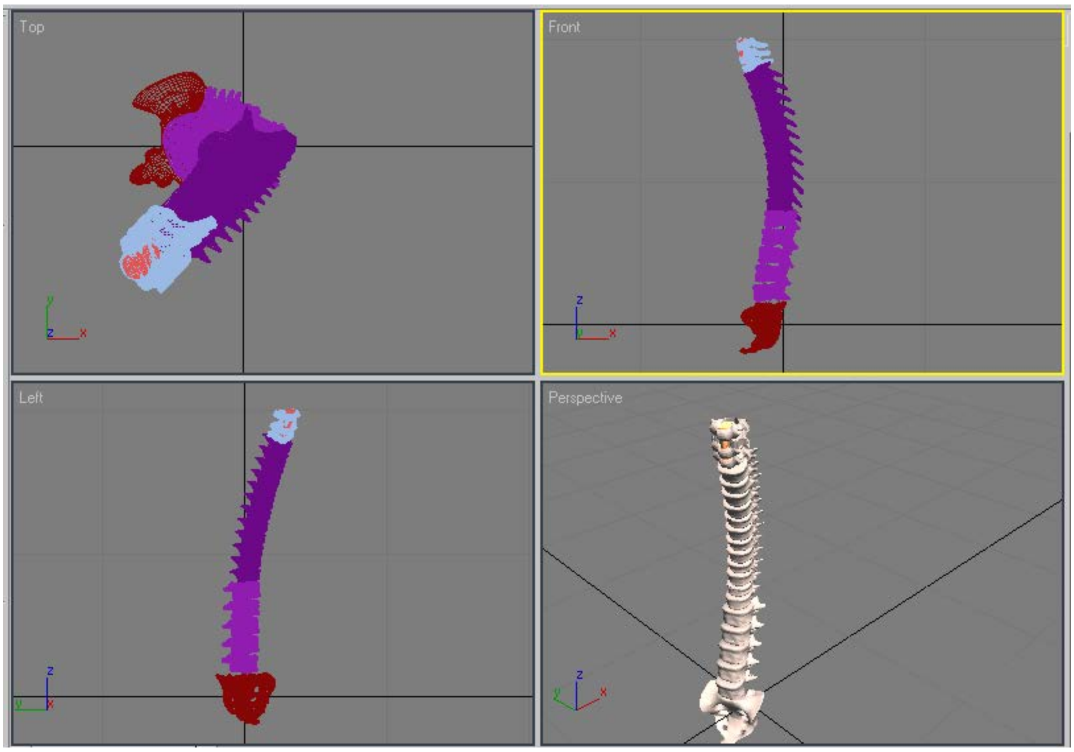

Figure 4.1.14 Standard model of the spinal column

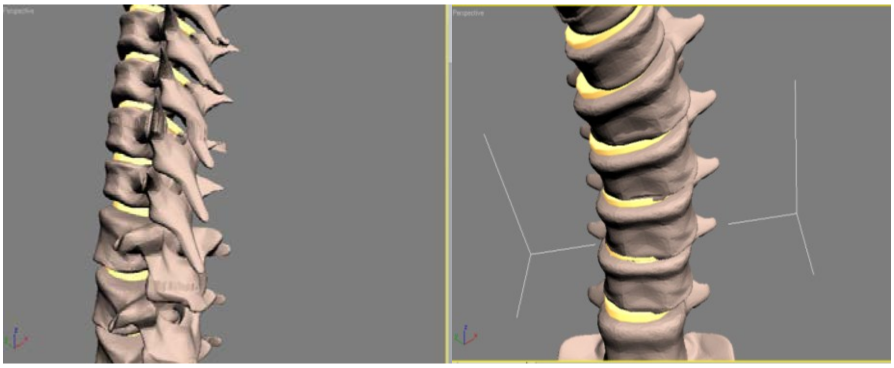

Figure 4.1.15 Details of a column

4.1.4 Conclusions and contributions

The research work developed within the present chapter can be summarized as follows:

- ❒ The subject of the research refers to the implementation of a totally non-invasive method of investigation for the spinal column, which is frequently affected by deformities.
- ❒ A large number of numerical parameters were suggested for the description of the column's shape and special software – INBIRE – was developed to work with the all-purpose imaging system InSpeck. The program provides an interactive database and the facility to export data to the modeling program 3Dmax.
- ❒ Using anthropometrical data, the individual vertebrae and finally the entire column was modeled as a standard. The coordinates provided by INBIRE allow modeling of personalized spinal columns, which can be stored and used by physicians to monitor the evolution of the deformities.
- ❒ The achievements of the research project contribute to development of local or national healthcare programs, bringing in numerical precision and efficiency in screening and monitoring spinal deformities, which are wide-spread, hard and costly to treat in advanced stages.

The original contributions in this chapter are:

- ❒ Design of an investigation method of the vertebral column by using the all-purpose imaging system InSpeck.
- ❒ Defining of 16 parameters of posture or deformity and setting algorithms to compute them using triplets of co-ordinates picked from 27 points (21 on the column from C7 to S3, two from the shoulders, two from the scapulae and two from the iliac crests).
- ❒ Developments of a VB application to render the shape of the column projected onto the frontal, sagittal and transverse plan, to display the values of the parameters and to perform common tasks such as management of files and so on.
- ❒ Development of a VB application to analyze the relative rotation of the vertebrae.
- ❒ Modeling in 3Dmax of the spinal column, containing 33 vertebrae, 344 joints and 24 intervertebral discs, with 5 distinct segments: cervical (7 vertebrae), thoracic (12 vertebrae), lumbar (5 vertebrae), sacral (5 vertebrae stiffed together) and coccyx (4 rudimentary vertebrae).

4.2 Experimental method for evaluation of spinal column deformation

4.2.1 Statement of problem

Vertebral disorders are very common in recent years among children and adults, due to lack of physical activity [34] and long-term prolonged sitting position [40]. Spinal deviations, such as scoliosis, may occur from younger ages continuing to aggravate in puberty and in adulthood, and can cause painful syndromes, low self-esteem, and even cardiopulmonary complication.

Among the deviations of the spine, scoliosis is the most common deformity in children and adolescents [1]. Scoliosis is a progressive disease characterized by one or more lateral curvatures of the spine, visible in the frontal plan and accompanied by the rotation of the vertebral bodies [33].

Over the last 40 years, numerous studies have been conducted on the incidence of scoliosis among children. In the literature, idiopathic scoliosis has a prevalence of 0.47% to 5.2% [1]. The girls are most affected and the risk of increasing the deviation is higher than for boys.

The orthopedic doctor is the one who establishes the diagnosis of scoliosis and follows the evolution in time. The follow-up protocol of scoliosis involves performing every 6 months the clinical and imaging control over the entire period of time until bone maturation is achieved. Currently, the examination can be achieved by X-ray, CT, MRI, Moiré topography, integrated shape imaging system (ISIS) and computer raster stereography. Because some of these investigations use radiations that are harmful for children [33], new approaches of investigation have been attempted in a non-invasive manner for the human body. These new devices are not widespread for use at this time: thermography, mapping the three-dimensional digital image acquisition using InSpeck system [29, 20, 43, 48] mapping with ultrasonic digital equipment such as Zebris [48], 3D scanning and 3D reconstruction using Kinect sensor [10], a wearable monitoring system based on inertial sensors [76].

As a result of the imaging examination, the orthopedic doctor establishes the diagnosis and the magnitude of the scoliotic curvature by calculating the Cobb angle. This represents the angle formed by the intersection of the tangent line to the upper plateau of the upper vertebra of the curvature and the tangent line to the lower plateau of the lower vertebra of the curvature. Depending on the value of the Cobb angle, the treatment followed by the patient will be determined by the protocol proposed by Stagnara:

- if the Cobb angle is between 0°- 30°, physical therapy is recommended

- if the Cobb angle is between 30°-50°, physiotherapy and orthopedic brace are recommended
- if the Cobb angle is over 50°, the spine surgery is indicated.

There had been done numerous studies during the last decades on the effectiveness of physical therapy treatments. The authors of [55] conducted a systematic review of the effectiveness of specific exercises used in rehabilitation of scoliosis (AIS – adolescent idiopathic scoliosis). There have been studied:

- Non-specific physical therapy exercises
- Exercises from Schroth therapy: exercises based upon fixing the pelvis, thus actively performing a trunk elongation, derotation of the ribs and flattening the ribs hump. Patients do an intensive treatment for 6-8 hours a day for 4-6 weeks and after this period, they continue at home a program of specific exercises for 90 minutes a day [39, 79]
- Side-shift therapy (original approach by Min Mehto): auto-correction exercises for the trunk (in time, these auto-correction have to be applied in activities of everyday life) [51]
- Exercises DoboMed: symmetric position to perform active movements in closed kinematic chain in order to facilitate the active correction in between the two symmetric stable girdles and to support the consolidation of the correct postural habit.
- Exercises from SEAS (Scientific Exercises Approach to Scoliosis) by ISICO (Italian Scientific Spine Institute): exercises based on auto-elongation of the former Lyon method [55]
- ISR (integrated scoliosis rehabilitation): exercises to correct the scoliotic posture by means of proprioceptive and external stimulation [80]. The patient is supervised by a team consisting of a physician, a therapist and a psychologist.

Almost all studies all over the world (Asia, USA, and Europe) have concluded that specific exercises play an important role in the evolution of scoliosis. Unfortunately, there are mentioned in the literature cases where, regardless of the method used, the Cobb angle continued to evolve. It is very difficult to calculate the percentage of progression in patients under 16 years old [54]. The progressing rate of scoliosis depends on age, magnitude of the Cobb angle, sex, the method of rehabilitation, the patient's conscious involvement. In the literature the progression values of scoliosis are based on the factors listed above, from 2.8% [80] to 11.6% [64] and even 19.5% [80].

Starting from the data presented above, this work proposes to study the effects of the specific exercises used in the scoliosis recovery programs by analyzing the change of the Cobb angle in the course of the movement and if it is possible to choose from a given number of exercises only those that are most effective for the patient. An individual recovery program, specific to each patient, according to its particularities, is to be established.

For this purpose, a set of accelerometers is attached to the patient's trunk and provides data in order to generate a dynamic mathematical model of the spine.

4.2.2 Mathematical approach and equipment

During physical exercises, the spinal column changes its shape both in frontal and lateral plans. However, for pursuing the Cobb angle, which is relevant for scoliosis, it is necessary and sufficient to acknowledge the changes in shape within the frontal plan. From mathematical point of view, the task of the researcher is to study the projection of the column onto the frontal plan. Thus, the mathematical purpose is to get a plane curve and to record its changes during an exercise prescribed by the physiotherapist, so that the variation of the Cobb angle to be monitored and assessed.

The projection of the column onto the frontal plane is traditionally got by means of radiography. The present study proposes an alternative method, which uses a set of sensors applied on the vertebrae. The sensors, type accelerometer, provide 3D coordinates of the points where they are attached. At a healthy, normal person, the shape of the column in the frontal plan varies from a straight line, in straight posture to a curve with one curvature, in any bended position. With scoliosis, the shape is also curved in straight posture, with one or two curvatures.

The bigger the number of precision points is the better approximation of the modeling curve is got. However, a big number of points imply more sophisticated mathematics. The authors decided to use a number of eight sensors, which is reasonably big to provide complex shapes.

The set of nine angles φ_I and eight lengths $l_{i,\ i+1}$ (i = 1 ... 8) - fig. 4.2.1 - is used to determine an approximation function. Further processing, meaning finding of the inflection points, allows the computation of Cobb angles.

The theory of function approximation starts from the following statement of problem: a function $y=f(x)$, $x \in X$ and $y \in Y$ is, usually not known in its analytical expression, but is available as a set of pairs (x, y) [71]. The task is to find a function $h(x) \sim y$ for all pairs (x, y).

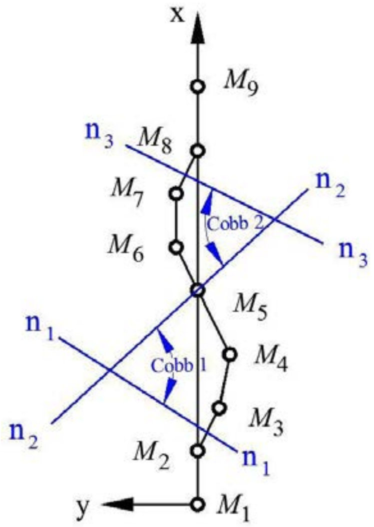

Figure 4.1.1 Nine points on the deformed spine and Cobb angles

The approximation function may be chosen among different classes of approximation functions, which are:

- polynomial
- exponential
- logarithmic
- trigonometric functions
- linear combinations of the above types.

For the given problem, the mathematical model of the spine is chosen the class of polynomials, for the following reasons:

- the “C” or “S” shape of the column can be easily represented with a high degree polynomial
- working with polynomials is relatively easy.

Other classes of approximation functions are unsuited to model the spine or unreasonably difficult to apply from calculus point of view.

A polynomial of n^{th} degree is an expression:

$$P_n(x) = a_0 + a_1x + a_2x^2 + a_3x^3 + ... + a_nx^n, \tag{4.2.1}$$

where a_i, $i = \overline{0,n}$ are constants and x is the variable. If (n+1) pairs of values (x_i, y_i), $i = \overline{0,n}$ are known, the coefficients of the polynomial result from the following system of equations:

$$\begin{cases} a_0 + a_1 x_0 + a_2 x_0^2 + \ldots + a_n x_0^n = y_0 \\ a_0 + a_1 x_1 + a_2 x_1^2 + \ldots + a_n x_1^n = y_1 \\ a_0 + a_1 x_2 + a_2 x_2^2 + \ldots + a_n x_2^n = y_2 \\ \vdots \\ a_0 + a_1 x_n + a_2 x_n^2 + \ldots + a_n x_n^n = y_n \end{cases} . \tag{4.2.2}$$

The function $h=P_n(x)$ is the searched approximation function.

For the specific given problem, the coordinates of the nine points are computed with the relationships, which consider the orthogonal reference system attached to the first lower point:

$$\begin{cases} x_{M1} = 0 \\ y_{M1} = 0 \\ x_{Mi+1} = x_{Mi} + l_i \cos\varphi_i \quad i = \overline{1,8} \\ y_{Mi+1} = y_{Mi} + l_i \sin\varphi_i \quad i = \overline{1,8} \end{cases} . \tag{4.2.3.}$$

The approximation polynomial of eight degree is given by the expression:

$$h = a_0 + a_1 x + a_2 x^2 + a_3 x^3 + a_4 x^4 + a_5 x^5 + a_6 x^6 + a_7 x^7 + a_8 x^8 , \tag{4.2.4}$$

where a_i result from the system of equations (4.2.2).

Equation (4.2.4) provides the shape of column. The graphs drawn with the mathematical model were compared with the x-Ray images and, thus, validated.

Further mathematical processing of the eighth degree polynomial is quite heavy and therefore, it was approximated with a smaller degree polynomial. In order to get three inflection points, a fifth degree polynomial would be suited, but the attempt to use it provided too large approximation errors. From mathematical handling point of view the best fit was got with a fourth degree polynomial:

$$g = b_0 + b_1 x + b_2 x^2 + b_3 x^3 + b_4 x^4 . \tag{4.2.5}$$

The roots of the second derivative of equation (4.2.5), if they result within the domain X and a third point, which was chosen the first or last value of the variable x provide the inflection points of the polynomial function. Considering the inflection points $I_1(x_1, y_1)$, $I_2(x_2, y_2)$ and $I_3(x_3, y_3)$, the gradient of the normal to the polynomial (4.2.5) is given by the relations:

$$m_1 = -\frac{1}{g'(x_1)}, \qquad m_2 = -\frac{1}{g'(x_2)}, \qquad m_3 = -\frac{1}{g'(x_3)} , \tag{4.2.6}$$

where g’ is the first derivative of the polynomial (4.2.5).

The Cobb angles (fig. 4.2.1), as angles between two normal lines, can be computed as follows:

$$Cobb1 = \arctan\left|\frac{m_1 - m_2}{1 + m_1 m_2}\right|, \qquad Cobb2 = \arctan\left|\frac{m_2 - m_3}{1 + m_2 m_3}\right|. \tag{4.2.7}$$

The angles φ are recorded as functions of time during the exercises performed by the patient under the supervision of the physiotherapist and thus, it is possible to get the variation of the Cobb angles.

The sensors applied on the vertebrae body provide data, consisting of three angles (φ_x, φ_y, φ_z) around the axes of a reference system, attached to each bone. The shape of the spine is relevant especially within the frontal plane. The mathematical model is going to be generated as a plane curve contained in the frontal plane. In addition, the relative rotation angles between the vertebrae in the transverse plane can be easily computed from the differences between the angles φ_z. The angles φ_x are recorded as functions of time and thus, it is possible to get the variation of the Cobb angles during the exercises performed by the patient under the supervision of the physiotherapist.

4.2.3 Equipment for the experimental measurement of coordinates along the spinal column

In order to collect the angles of the vertebrae, an acquisition system must be set up. This consists of an assembly of 8 MEMS IMUs [84] (inertial measurement units) connected via their I2C bus to an I2C multiplexer [89] and ultimately to a microcontroller board [88] (fig. 4.2.2 – a: scheme and b: experimental arrangement). The multiplexer is needed because the IMUs have two fixed bus addresses, these being the same for all 8 IMUs. Considering that the IMU boards are PCB carriers these have been protected against ingress of foreign material (adhesive, liquid droplets, finger touch) by encapsulating them in thermo-contractile tubes, which also provided for a stronger cable ending and also a flat surface ready to be applied to the patient's skin.

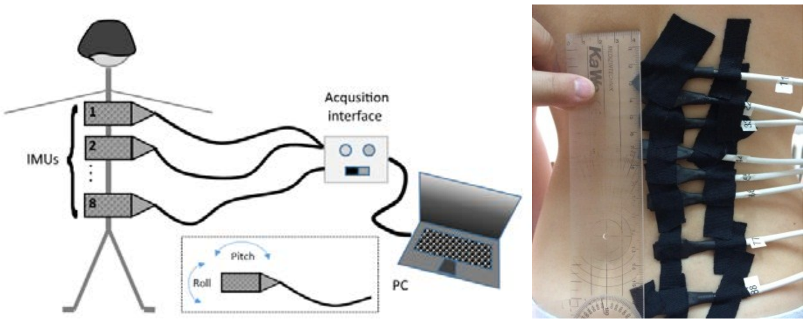

Figure 4.2.2 Angle acquisition assembly. Scheme (a) and experimental arrangement (b)

For the current experiments the Roll and Pitch angles are recorded and transmitted to a PC in the form of comma separated values, via a serial port. The angles are computed from the accelerometer values by considering the IMU's own coordinate reference system [62]:

$$\mathrm{Roll} = \arctan\left(G_y / G_z\right), \qquad \mathrm{Pitch} = \arctan\left(-G_x / \sqrt{G_y^2 + G_z^2}\right), \tag{4.2.8}$$

where: G_x, G_y, G_z are the raw gravitational acceleration values measured in the earth's reference frame, recorded by the IMU.

Since above equations give multiple solutions in the [0…2π] region, the angles must be limited and the selected convention for this application is to limit both *Roll* and *Pitch* to [0…π] in the microcontroller code and enforce the vertebrae application position to that pictured in figure 4.2.2. With this restriction respected, the base angles (IMUs vertical with cable to the right and flat PCB surface facing patient's skin) are both π/2.

The microcontroller reads all 8 IMU raw accelerometer values in a continuous loop, computes the angles and sends the values to the connected PC with a frequency of 5 Hz. Considering the nature of the therapeutic exercises that the patient must conduct (which are mostly static – assume a pose and keep it for a few seconds) the amount of angle data collected is sufficient for further analysis.

4.2.4 Example of data acquisition and processing results

A first set of data was acquired from a patient in static straight posture, which is a sequence of a prescribed exercise by the physiotherapist for the treatment of a spinal deformity. Data acquired for this position is used to test and validate different mathematical algorithms, which pursue the obtaining of an analytical shape of the spine and the computation of Cobb angles.

In order to apply the algorithm for getting the interpolation polynomial, only the angle φ_x and the distances li are necessary.

Table 4.2.1 Acquired data and computed coordinates

Sensor number	φ_x [deg]	l [mm]	y [mm]	x [mm]
	0	0	0	0
1	3.5	28	1.70	27.94
2	7.91	28.5	3.91	56.13
3	12.3	28.5	6.06	83.94
4	4.58	26.9	2.14	110.78
5	-0.77	11.5	-0.15	122.32
6	-5.76	16.9	-1.69	139.15
7	-4.3	15.4	-1.15	154.50
8	1.48	14.6	0.37	169.11

Table 4.2.1 contains the values of the acquired data and computed coordinates of the nine interpolation points in a reference system attached to the lowest vertebra, which is considered as the origin of the system. The coefficients of the eighth degree polynomial described in equation (4.2.2) are:

$$\begin{aligned} &a_0 = 1.76 \cdot 10^{-14},\ a_1 = -1.25 \cdot 10^{-11},\ a_2 = 3.57 \cdot 10^{-9},\ a_3 = -5.27 \cdot 10^{-7} \\ &a_4 = 4.25 \cdot 10^{-5},\ a_5 = -1.86 \cdot 10^{-3},\ a_6 = 4.14 \cdot 10^{-2},\ a_7 = -0.30,\ a_8 = 0. \end{aligned} \qquad (4.2.9)$$

The curve is represented in figure 4.2.3(a). The computation and graph are performed by means of an application, written in Mathcad 14.

The inflection points are found for the coordinates:

$$I_1(35.52;\ 2.20),\ I_2(110.45;\ 2.23),\ I_3(161.80;\ -0.61). \qquad (4.2.10)$$

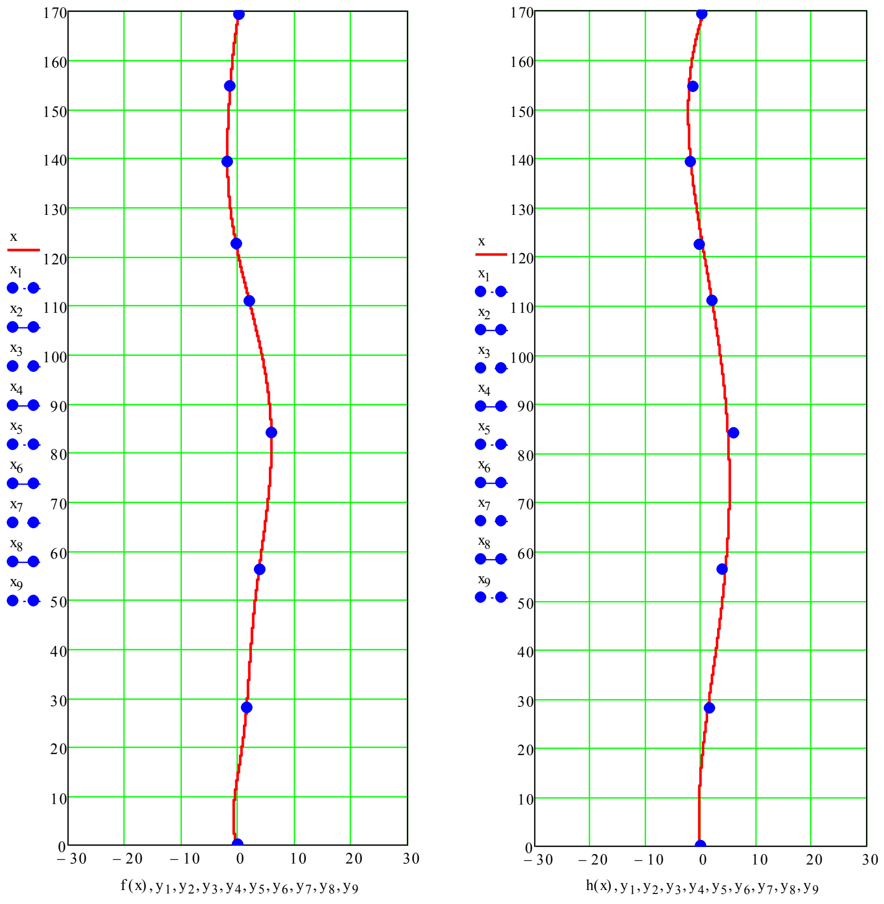

a) b)

Figure 4.2.3 Model of the spine - polynomial of 8th degree (a) and polynomial of 4th degree (b)

The last point I_3 did not result on mathematical basis, but it was selected as the midpoint of the last vertebrae distance l_8.

The computation of the normal line's slope in these points and applying the relations (4.2.4) provide the following Cobb angles:

$$Cobb1 = 15.63^\circ, \quad Cobb2 = 17.45^\circ . \tag{4.2.11}$$

The correctness of the shape is confirmed by a simpler approximation, with a fourth degree polynomial:

$$y = b_0 x^4 + b_1 x^3 + b_2 x^2 + b_3 x + b_4 , \tag{4.2.12}$$

got in a different software application, MS Excel Office 2010, by means of the function *Trendline* applied to the graph passing through the nine precision points.

The coefficients of the fourth degree approximation polynomial are:

$$\begin{aligned} & b_0 = 2.437 \cdot 10^{-7}, b_1 = -7.432 \cdot 10^{-5},\ b_2 = 5.97 \cdot 10^{-3}, \\ & b_3 = -6.178 \cdot 10^{-2},\ b_4 = 0 \end{aligned} , \tag{4.2.13}$$

The resulting graph (also drawn in Mathcad for uniformity) is given in figure 4.2.3 (b). The inflection points of the approximation polynomial are found for the coordinates:

$$I_1(34.73;2.30), I_2(117.57;1.19), I_3(161.80;-1.11) . \tag{4.2.14}$$

The computation of the normal line's slope in these points and applying the relations (4.2.4) provide the following Cobb angles:

$$Cobb1 = 15.78^\circ, \quad Cobb2 = 18.25^\circ . \tag{4.2.15}$$

The curves in figure 4.2.3 look very similar. In addition, their inflection points are very close, so that the Cobb angles are different with less than 1deg, i.e. the relative error is of approximately 4.3%.

The dynamic recording of data through the whole rehabilitations exercise allows the therapist to establish whether the exercise is appropriate in nature and intensity.

4.2.5 Performing measurements and interpreting data

Measurements were performed within a recovery clinic with the consent of patients and their parents. Initially, data acquisitions were taken from orthotic position, the same position in which the patient performed x-ray exposure. Data taken from the accelerometer sensors in the orthostatic position were compared with the results calculated by the doctors on x-ray. The subject under study has a double dorsal scoliosis with the Cobb angles calculated by the radiologist: 22° lumbar and 28° dorsal. Of the mathematical calculation using the polynomial of 8th degree, revealed the Cobb angle on the lumbar area of 20.7^{o} and the Cobb angle on the thoracic area of 25.4^{o}. The values obtained being very close to those calculated on radiography and the very similar curves could be taken into account for the desired experiment. In figure 4.2.4 it can be seen the deviation of the spine on x-ray and comparatively, the graph obtained by the mathematical method.

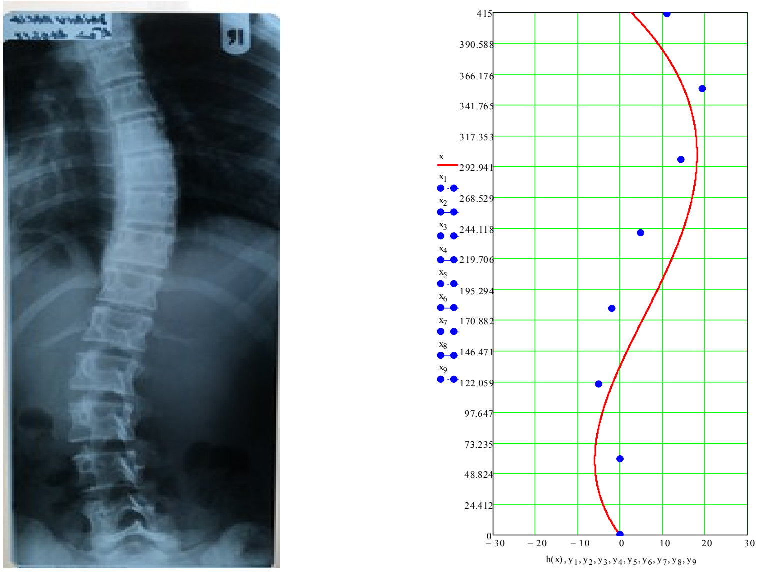

Figure 4.2.4 On the left, the x-ray of the double scoliosis and on the right, the model of the spine – the polynomial of 8th degree

The treatment for scoliosis involves only physical exercise for scoliosis with Cobb angle below 25° (light scoliosis), and for medium scoliosis, with a Cobb angle between 25 and 50°, the wearing a brace for more than 18 hours a day is recommended besides specific exercises. The exercises performed by the scoliotic patient are prescribed by a physiotherapist.

There are many approaches to perform exercise for scoliosis. Depending on the physiotherapist's training, one can choose between exercises from Schroth method (most commonly used in Germany), DoboMed method, from Cotrel method, from Klapp method, from Mézièr method, stretching and toning exercises or postural correction exercises.

In this study, three of the most commonly used exercises in scoliosis recovery are analyzed using the equipment made up of accelerometer sensors to track how the Cobb angle changes during treatment.

- ❒ The first exercise was chosen from Schroth method - "muscular cylinder standing". The patient performs the Schroth tilts.
- ❒ The second exercise was chosen from Mezier method. The patient is in a position with the lower legs apart and the arms raised parallel to the ground, he maintains lumbar lordosis activating the lumbar erector muscles, makes elongations and corrective breathing with derotation of the shoulders, rib hump and pelvis.

- The third exercise was chosen from the hanging position to the wall bars with arms apart and legs together: the patient keeps all the sagittal and frontal corrections for several seconds and performs deep breaths.

For a better understanding of the description of the exercises, these are below schematically represented in figure 4.2.5.

Figure 4.2.5 Model of the exercises

For testing, on the back of the patient were positioned the accelerometer sensors at equal distances between them. The first sensor was positioned at the level of the first sacral vertebra S1 and the last one at the level of the last cervical vertebra C7, as can be seen in figure 4.2.6.

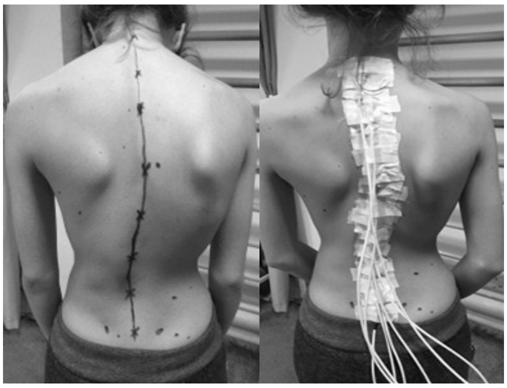

Figure 4.2.6 The position of sensors for testing

For a first test there were used the exercises described above having as a starting point, the vertical position of the column. The distances between the sensors along the column were known from the beginning and the values of the angle φ have been read by the sensors. The values of angles φ_i and the distances l_i were introduced into Mathcad 14, where the computation and graphs were further developed. Further, the curves obtained from the computation are shown in figure 4.2.7.

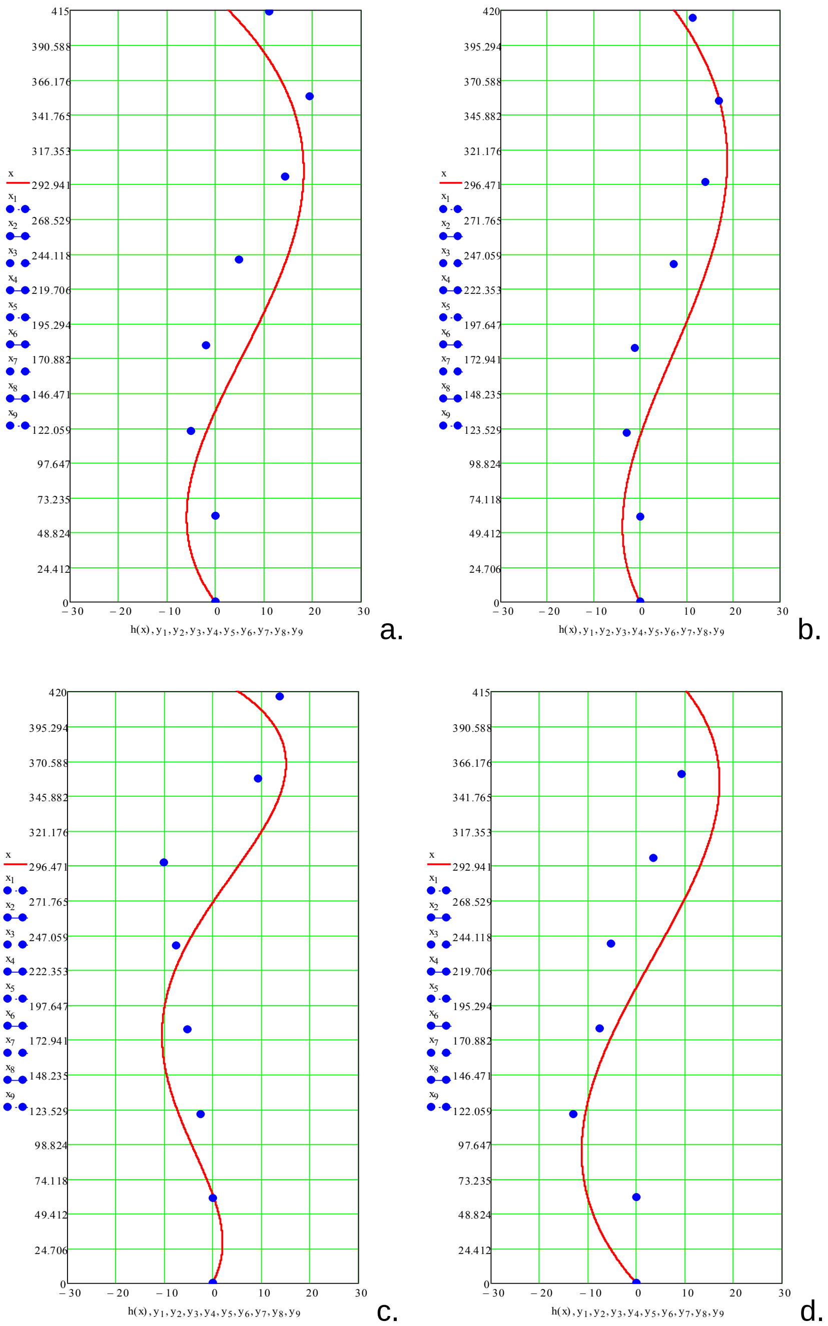

Figure 4.2.7 Model of the spine - polynomial of 8th degree – standing position (a), Schroth position (b), Mézièr position (c) and hanging position (d)

The values of the Cobb angles obtained during the test performing the exercises were compared with the value of the Cobb angle obtained on the x-ray. In all 3 exercises taking into study, the Cobb angles decreased compared to the reference value (table 4.2.2).

From the table and the graphs it can be observed that the position in which both Cobb angles decrease the most is part of the Schroth method. Also, a significant decrease of the angular values can be observed in the Mezier position, but after the curve described by the polynomial of 8th degree calculated during the exercise, an increase of the compensatory curves can be observed. In the hanging position there was only an improvement in the value of the Cobb angle in the dorsal area while in the lumbar zone the Cobb angle is increased. This last position is in the open kinetic chain and requires from the subject under test a strong control of the lower part of the body.

Table 4.2.2 The values of the Cobb angles on the x-ray and those computed from the mathematical approach

Values of Cobb angles	X-Ray	Standing position	Schroth Method	Mézièr Method	Hanhing on wall bars
Cobb 1	22°	20.747°	16.032°	16.558°	23.878°
Cobb 2	28°	24.536°	19.041°	19.041°	22.099°

The position in which both Cobb angles decrease the most is part of the Schroth method. Also, a significant decrease of the angular values can be observed also in the Mezier position, but after the curve described by the grade 8 polynomial calculated during the exercise, an increase of the compensatory curves can be observed. in the hanging position there was only an improvement in the value of the Cobb angle in the dorsal area while in the lumbar zone the Cobb angle is increased.

This last position is made in an open kinetic chain, it is instable for the lower limbs and pelvis and requires from the testing subject a strong control of the lower part of the body (perhaps this is why the Cobb angle in the lumbar region showed a worsening of the value compared to the one in the standing position). Analyzing the results we can conclude that the person tested is the most appropriate to perform the Schroth based exercise in which the Cobb angles showed a significant improvement while the exercise from Mezier method and the hanging on the wall bars will have to be executed with increased attention to compensatory curves and of the lumbar muscle control.

4.2.6 Conclusions and contributions

The research work developed within the present chapter can be summarized as follows:

- The research work proposes a new investigation method, based on data provided by a set of eight accelerometers, which are stuck on the body of the vertebrae during the whole therapy exercises.
- The goal of the study is to develop a method to record the Cobb angles variation, which should provide in the future an evaluation of the therapy exercises. Adequate equipment enables the analysis of changes in the segments of the column involved in the exercise. In this way, after the exercise, the therapist can analyze which area

of the column worked correctly and in which areas the curves worsen. Thus, the therapist can choose the most effective exercises for each subject.

- The acquired angular data is used to compute an eighth degree polynomial as a model of the spine. The high degree of the polynomial is not very convenient because the large number of inflection points and not recommendable for automated computation. The mathematical model was improved by using an approximated polynomial of lower degree, which has high correlation coefficient.
- The mathematical model is intended to be further confronted with the results of other types of investigation, such as traditional and modern imaging.
- From mathematical point of view, the polynomial approximation was validated. Further studies will involve other classes of functions of approximation.

The original contributions in this chapter are:

- Generation of a theoretical mathematical model of the vertebral column, within the frontal plan, as a plan curve, described by a polynomial expression.
- Establishment of an algorithm to compute the Cobb angle.
- Design and assembling of an original acquiring system, based on eight accelerometers attached to the patient's vertebrae.
- Performing of measurements, processing of data and interpreting of results from the point of view of the physiotherapist.

III. Academic and professional achievements

I am employed at the University Politehnica Timisoara since 1988 and I defended my PhD thesis in 1989.

My teaching activities developed within the Department of Mechatronics on the following courses:

- Descriptive geometry and engineering design
- Technical optics
- Optical apparatuses
- Photometers and spectrophotometers
- Medical optics
- Reliability in mechatronics
- Optical sensors
- Illumination ergonomics.

I offered printed or electronic books to support theoretical and practical activities of the students. Several titles are listed bellow:

1. Gruescu C. 2012 Ingineria optică Ed. Politehnica Timisoara ISBN 978-606-554-551-9
2. Gruescu C., Nicoară I., Costache M., Ionescu C. 2008 Aplicaţii ale metodei Ray Tracing în optica imaging şi non-imaging Ed. Politehnica Timisoara ISBN 978-972-625-542-7
3. Nicoară I., Gruescu C., Atiţoaiei V., Duma V. 2000 Aparate optice, vol. I Editura Orizonturi Universitare Timişoara ISBN 973-9400-95-7
4. Gruescu C., Nicoară I. 2004 Aparate optice, vol. II, Analiza şi sinteza subansamblurilor optice lenticulare Ed. Politehnica Timisoara ISBN ISBN 973-625-158-6
5. Gruescu C. 2000 Elemente de optică tehnică şi aparate optice Editura Orizonturi Universitare, Timişoara ISBN 973-8109-19-1
6. Nicoara I., Gruescu C., Sticlaru C. 2009 Fiabilitate si terotehnica Ed. Politehnica Timisoara ISBN 978-973-625-638-7
7. Gruescu C., Bodea R., Pommersheim A. 2006 Masurari optice Ed. Politehnica Timisoara ISBN 973-625-195-0

8. Gruescu C., Bodea R. 2006 Elemente de analiza si sinteza a sistemelor optice. Aplicatii Ed. Politehnica Timisoara ISBN ISBN 973-625-196-9

The research activities were developed alongside with the teaching activities within similar areas. The first research works were developed in the field of optical engineering and biomechanical engineering. The grants were approved by the National Council of Scientific Research in Higher Education CNCSIS, in the call programs ANSTI and AT. These projects were continued with grants for Excellence Centers CEEX, EU ICT-PSPFP7 and CDI program of Romanian Space Agency. The projects I was involved in, are the following:

1. Cercetări privind tehnicile pentru detecţia şi localizarea surselor de radiaţii în infraroşu, contract nr.36/98, tema 27, cod CNCSU 301 (Nicoara I., project leader)
2. Corelarea indicatorilor de calitate a imaginii cu parametrii de executie si montaj ai reperelor in constructia aparatelor optice, contract GR 6153/2000, tema B.25 (Balaban A., project leader).
3. Corelarea indicatorilor de calitate a imaginii cu parametrii de executie si montaj ai reperelor in constructia aparatelor optice, contract GR 6153/2001, tema A.17.2 (Balaban A., project leader).
4. CEEX-88, INBIRE, Dezvoltarea şi implementarea unor sisteme performante de investigare şi recuperare a deformaţiilor de coloană vertebrală la populaţia de vârstă şcolară şi categorii profesionale cu activităţi sedentare (2006-2008)(Lovasz E.-Chr., UPT project partner leader).
5. CEEX-247, NANO – PV Cercetari privind cresterea eficientei celulelor fotovoltaice nanostructurate (2006-2008) (Lovasz E.-Chr., UPT project partner leader).
6. PNII 91 – 022 ERGINDENT, Ergoingineria locului de munca. Aplicatii in medicinadentara (2007-2009) (Argesanu V., UPT project partner leader).
7. Project 250485/CIP-ICT-PSP-2009-3, Digital Mechanism and Gear Library goes Europeana ThinkMOTION (2011-2013) (Lovasz E.-Chr. UPT project partner leader).
8. Project CDI 113/19.11.2012, New Haptic Arm Exoskeletons for Robotics and Automation in Space, acronim EXORAS (Lovasz E.-Chr., UPT project partner leader).

I took part in projects with 2 industrial beneficiaries:

1. Numerical Analyses and Optimization of the Conti-Safety-Ring, contract nr. 577/2000, Continental AG Gmbh Hannover
2. Contract de cercetare nr. 686/14.06.07, Măsurări de determinare a rugozităţii, beneficiar: S.C. ESSER Romania S.R.L. Timişoara

I organized the exchange of students and teachers within 3 ERASMUS programs:

1. Bilateral Agreement for the academic year 2004/2007 SOCRATES program: higher education (ERASMUS), UPTimişoara, Facultatea de Mecanică – Institute Universitaire de Technologie Cachan Paris
2. Bilateral Agreement for the academic year 2005/2008 SOCRATES program: higher education (ERASMUS), UPTimişoara, Facultatea de Mecanică –Ecole Nationale d'Engenieurs Tarbes, France
3. Bilateral Agreement for the academic year 2006/2009 SOCRATES program: higher education (ERASMUS), UPTimişoara, Facultatea de Mecanică – Universite d'Artois, France.

During the period of report I published 7 papers in journals indexed in ISI Web of Knowledge:

1. Gruescu C., Nicoara I., Popov D., Bodea R., Hora H. 2008 Optical Glass Compatibility For the Design of Polychromatic Systems *Science of Sintering* **40** 131-140
2. Popa M. Lupea A.X. Popa S. Gruescu C. 2010 Colour of Bilberry (Vaccinium Myrtillus Fruits) Extracts *International Journal of Food Properties* **13**(4) 7771-777
3. Gruescu C., Ionescu C., Nicoara I., Lovasz A. 2012 Experimental Optimization of Process Parameters in Laser Cutting of Polycarbonate Gears *Mechanika Journal* **2** 233-238
4. E-C. Lovasz, K.-H. Modler, R. Neumann, C. M. Gruescu, D. Perju, V.Ciupe, I. Maniu 2015 Novel Design Solutions for Fishing Reel Mechanisms *Chinese Journal of Mechanical Engineering* **28**(4) 726-736
5. Gruescu C. M., Garaiman A., Lovas, E. C. 2015 Modeling of human spinal column and simulation of spinal deformities *Mechanika* **3** 214-219
6. Popa S., Padure M., Gruescu C. M., Boran S. 2015 New Salicilic Acid-Based Azo Dyes Synthesis, Characterization and Colour Properties *Revista de chimie* **66**(12) 2021-2027
7. E. C. Lovasz , D. T. Mărgineanu, V. Ciupe, I. Maniu, C.M. Gruescu, E. S. Zăbavă, S. D. Stan 2017 Design and control solutions for haptic elbow exoskeleton module used in space telerobotics *Mechanism and Machine Theory* **107** 384–398

I was invited to perform reviewing activities for important journals and conferences (Journal of Mechanisms and Robotics, 2015-2018, Measurement Journal, 2015, Optical Engineering 2013, 14th IFToMM World Congress - Taipei 2015, MTM&Robotics 2016 - Aachen, Germany, Scientific Bulletin of the Politehnica University of Timisoara, SYROM 2017 - Brasov, RO, MESROB 2018 – Cassino, Italy, MEDER 2018 – Udine, Italy and others).

I worked within the international professional association IFToMM, as observer member of the Technical Committee Linkages and Mechanical Controls (since 2014). I made part of the organizing committees for several events developed under the patronage of IFToMM (First Conference on Mechanical Transmissions and Applications, MeTrApp 2011 Timisoara; 3rd Conference MAMM 2014, Timisoara; Summer School on MMDR 2014 Timisoara, MTM&Robotics 2016 Aachen Germany). I am co-editor of the volume:

> Corves B., Lovasz E.-C., Huesing M., Maniu I., Gruescu C.2017 Joint International Conference of the 12th International Conference on Mechanisms and Mechanical Transmissions MTM 2016 and the 23rd International Conference on Robotics Robotics 2016 Springer.

During the report period I visited for scientific purposes many universities from Europe: Technische Universität Ilmenau, Germany; RHWT University Aachen, Germany; Technical University of Liberec, Cech Republic; Institut Français de Mécanique Avancée IFMA, France; University of Basque Country Bilbao, Spain; University of Cassino, Italy; Université d'Artois, France; Université Cachan Paris, France; Tallin University of Technology, Tallin, Estonia.

My managerial activity includes the position of member of the Department council at the Mechatronics Department, since 2012.

Since 2001 I collaborated with the Department for the Training of Teaching Staff. I supervised over 20 theses of teachers from the secondary education, graduates of Mechatronics and candidates to the rank of first degree teacher. I took part in numerous exam commissions for the promotion of teachers in secondary school.

IV. Career evolution and development plans

The scientific achievements in my research fields of optical engineering applied in mechatronic applications are the basis for further career development. My personal scientific achievements and topics were always oriented to development of algorithms implemented in design of machines, equipment and devices integrating optical modules.

My career evolution and development plans are guided by the following research directions:

Basic optical design

- ❒ image quality analysis of optical systems by means of waveform and Fourier indicators
- ❒ synthesis of optical components and subassemblies using original methods or adaptation of traditional algorithms
- ❒ implementation of synthesis and analysis techniques by designing original software or by using optical computing programs
- ❒ optimizing of image quality by original methods, based on mathematical modeling of optical systems and simulation of influence parameters
- ❒ fundamental research aimed directly at the synthesis of optical systems limited to diffraction
- ❒ synthesis of functional exploration devices based on image transmission through optical fibers
- ❒ design of the optical diagram and synthesis of gratings for UV-VIS-IR spectral

Integration of optical engineering in mechatronic applications

- ❒ design of lighting systems implemented in industrial and home applications, in accordance with the line guides of the EU Framework Programme for Research and Innovation HORIZON 2020, regarding energy consumption and ergonomics
- ❒ free-form optics integration in lighting systems, in order to reduce secondary optics as subassembly and material and energy, in general
- ❒ integration of optical sensors in mechatronic applications based on imaging and non-imaging schemes.

Integration of optics in medical engineering

- ❒ design, application and use of new methods of investigation based on imaging and image processing
- ❒ design of new rehabilitation devices for lower and upper limbs, based on original mechanical structure, flexible automated equipment and procedures involving quantitative evaluation of the cure progress for the leg, arm and spinal column.

Objectives

The objectives pursued in my career development will be classified in two major categories:

Short term goals

- ❒ developing a research group in the field of Mechatronics and Robotics and starting together with other PhD advisors the grounding of a new Doctoral Field of Mechatronics and Robotics inside of the Doctoral School of UPT – IOSUD
- ❒ using and extending the cooperation with the researchers and professors from both Romania and abroad for connecting the researches on the highest level
- ❒ participation in consortiums for preparing proposals for EU HORIZONT 2020 projects and national research and structural grants
- ❒ attracting students as PhD candidates among the best students graduating Mechatronics and Robotics
- ❒ attracting of commissions and developing of projects with domestic and multinational companies from Timisoara and Romania.

Long term goals

- ❒ accreditation of the new Doctoral Field of Mechatronics and Robotics inside of the Doctoral School of UPT – IOSUD
- ❒ preparing of strategic project proposals for EU projects, bilateral country projects and national research grants
- ❒ development of a network with professors and researchers from Romania and abroad to correlate and connect the research results on the highest level
- ❒ attracting of European and foreign PhD students for enriching and exchanging the research field knowledge

Planed activities

In order to achieve the previously proposed objectives several activities should be developed:

- documentation and preparing the required conditions for developing and accreditation of the new Doctoral Field of Mechatronics and Robotics inside of the Doctoral School of UPT –IOSUD
- continuous development of devices and equipment in the laboratories and own development of prototypes for the specific applications
- permanent connection and research exchanges with the researchers and professors from both Romania and abroad for discussion and preparing of new research topics
- preparing and sending of own or joint papers with the news research results to major Journals
- contribution to reviewing papers in major Journals and Conferences
- participation of PhD students at several Summer Schools to improve their knowledge
- preparing and applying in several consortiums for proposals for EU HORIZONT 2020 projects, bilateral collaborations and national research or structural grants
- developing of a multinational ERASMUS + project for exchange of the PhD students between the participant PhD advisors
- publishing of new books improved with the newest research results and improving the quality of the teaching activity.

V. References

1. Balla I., Hantiu J.B. *School screening programs of scoliosis: a meta-analysis*. The annals of the Oradea University, Facultuy of Physical Education and Sport,2015, XXV, 90-98.
2. Bass M. *Handbook of Optics. Fundamentals. Techniques. Design,* McGraw-Hill, 1995.
3. Benameur S., *Reconstruction 3d biplanaire non supervisée de la colonne vertébrale et de la cage thoracique scoliotiques par modèles statistiques*, Doctorate Thesis École de Technologie Supérieure, Montréal, 2004.
4. Bertelli F., Meza E.S., Goulart P.R., Cheung N., Rivae R., Garcia A. *Laser remelting of Al–1.5 Fe alloy surfaces: Numerical and experimental analyses.* Optics and Lasers in Engineering, 2011, 49, 490–497.
5. BirchallD., Hughes D.G., Robinson L. *Analysis of intravertebral axial rotation in adolescent idiopathic scoliosis using three-dimensional MRI,* Research into Spinal Deformities, 1999, 59, 61-64.
6. Brecht R., Henkel V. *thinkMOTION: DMG-Lib goes Europeana – Portal für Europas Ingenieurwissen.*Universitätnachrichten Ilmena,2011, 54(1), 33-35.
7. Breglia D. P. *Generation of a -3d parametric solid model of the human spine using antrophomorphic parameters*, Doctorate thesis, Faculty of Engeneering and Tehnology Ohio University, 2006.
8. Brix T., Döring U., Reeßing M. *Creating Present-Day Solutions from Historical Knowledge.*, World Congress in Mechanism and Machine Science Guanajuato, México, 2011,13.
9. ChernukhaK., DaffnerR.H., Reigel D. *Lumbar Lordosis Measurement: A New Method Versus Cobb Technique,* Spine 1998, 23, 74-79.
10. Ciobanu O., Ciobanu G., Aiello A. *An application of Kinect sensor for scoliosis and kyphosis screening,* Proceedings of the International Conference on Medical and Bio-logical Engineering (CMBEBIH), Springer, 2017, 713-717.
11. Ciupe V., Lovasz E.C., Reessing M., Henkel V., Gruescu C.M., Zabava E.S. *Interactive animation production by means of advanced image processing*, 2nd Conference on Mechanisms, Transmissions and Applications, MeTrApp 2013, Mechanisms and Machine Science, 17, 329-337.

12. Ciupe V., Lovasz E-C., Gruescu C.M. *High Quality Document Digitization Equipment,* Mechanisms, Mechanical Transmissions and Robotics, Applied Mechanics and Materials, 2012, 162 589-596.
13. Curatu E. *Calitatea sistemelor optice. Funcţia optică de transfer*, Ed. Academiei Române, Bucureşti, 1992.
14. Davila A., Huntley, J.M., Pallikarakis, C., Ruiz, P.D. *Wavelength scanning interferometry using a Ti:Sapphire laser with wide tuning range*, Optics and Lasers in Engineering, 2012, 50, 1089–1096.
15. Dobbert T. *Matchmoving. The invisible Art of Camera Tracking*. Second Edition, Wiley&Sons, Indiana, 2013.
16. Döring U., Brecht R. and Brix T. *thinkMOTION – DMG-Lib Goes European,* Mechanisms, Transmissions and Applications, Springer, 2011, 37-40.
17. Fisher R. et al. *Optical System Design,* SPIE Press, McGraw Hill, 2008.
18. Friedrichs A., Kletzin U. *Entwicklung intelligenter mobiler Systeme zur Langzeiterfassung von Körperdaten*, Proc. 47. Wissenschaftliches Kolloquium, TU Ilmenau. 2002, 11-12.
19. Fusco C., Zaina F., Atanasio S., Romano M., Negrini A., Negrini S. *Physical exercises in the treatment of idiopathic scoliosis: An updated systematic review*, Physiotherapy Theory and Practice, ISICO, 2011, 80-114.
20. Garaiman A. *Contributions to the implementation of advanced non-invasive techics for investigation of spine deformities*,Ph.D. Thesis, University Politehnica Timisoara, 2010.
21. Gąska D., Kijak E., Lipski T., Margielewicz J. *Numerical modelling of human masticatory organ kinematics*, Mechanika, 2012, 18(4), 447-452.
22. Gruescu C. et al. *Comment on Specific Features of Optomechanical Fits*, Proceedings of the 5th IASME /WSEAS International Conference on CONTINUUM MECHANICS, University of Cambridge, UK, 2010, 54-59.
23. Gruescu C. et al. *Influence of Mechanically Induced Birefringence*, Proceedings of the 6th International Conference of DAAAM Baltic, Industrial Engineering, Tallinn, 2008, 245-250.
24. Gruescu C. et al. *Optical Glass Compatibility For the Design of Polychromatic Systems*, Science of Sintering, 2008, 40:131-140.
25. Gruescu C., Balaban G. *Analyse of transverse spherical aberration of a tilted lens*, The 8.th Symposium on Mechanisms and Mechanical Transmissions with international participation, Timişoara, 2000, 143-148.

26. Gruescu C., Ionescu C., Nicoara I., Lovasz A. *Experimental Optimization of Process Parameters in Laser Cutting of Polycarbonate Gears*, Mechanika Journal, 2012, 18(2) 233-238.
27. Gruescu C., Lovasz E.-C., Ciupe V. *Optics Optimization in Laser Spot Radius Minimization,* International Conference on Production Research – Regional Conference Africa, Europe and the Middle East, 3rd International Conference on Quality and Innovation in Engineering and Management, 2014, 231-234.
28. Gruescu C.M. *Motion laws of a varifocal objective working with a 1/2" CCD camera*, MeTrApp 2011, Mechanisms and Machine Science 3, 133-140
29. Gruescu C.M., Garaiman A., Lovasz E.-C. *Modeling of human spinal column and simulation of spinal deformities*, Mechanika Journal, 2015, 3, 214-219.
30. Gruescu C., Ionescu C., Nicoara I., Breaban F. *Increase of Precision and Efficiency of Laser Cutting by Means of Optical System Optimization*, Proceedings of the 6th International Conference of DAAAM Baltic, Industrial Engineering, Tallinn, 2008, 245-250.
31. Hawes M.C. *The use of exercises in the treatment of scoliosis: An evidence-based critical review of the literature*, Pediatric Rehabilitation, 2003, 171-182.
32. Hecht E. *Optics*. 3rd ed., Eddison Wesley Longmann, 1998.
33. Jianu M. *Pediatric scoliosis.* Bucuresti, Publishing House and Typography Pro, 2010.
34. Juskelene V. Magnus P., Bakketeig L.S., Dailidiene, N. *Prevalence and risk factors for asymmetric posture in preschool children aged 6-7 years,* International Journal of Epidemiology, 1996,5, 1053-1059.
35. Kerle H., Mauersberger, K., Ceccarelli, M. *Some Historical Remarks on Past Model Collections of Machines and Mechanisms in Europe.* World Congress in Mechanism and Machine Science Guanajuato, México, 2011,13.
36. Kingslake R. *Lens design fundamentals.* N.Y. Academic Press, 1978.
37. Kletzin F.A. *Entwicklung intelligenter mobiler Systeme zur Langzeiterfassung von Körperdaten.* U. Ilmenau, Wissenschaftliches Kolloquium, 2002, 47, 11-12.
38. Lam G. et al. *Vertebral rotation measurement: a summary and comparison of common radiographic and CT methods*, Scoliosis,2008, 3, 16.
39. Lehnert-Schroth C. *Three-dimentional treatment for scoliosis. A physiotherapeutic method for deformities of the spine,* The Martindale Press, Palo Alto, California , 2007.
40. Linton S.J. Hellsing A.L., Halme T. and Akerstedt, K. *The effects of ergonom-ically designed school furniture on pupils' attitudes, symptoms and behavior,*Applied Ergonomics, 1994, 5, 299-304.

41. Liu J. *A two-dimensional human spine simulation and threedimensional spine model construction*, PhD Thesis, University of Florida, 2001.
42. Lovasz E.-C., Mateas M. Fernengel V. *Geometric Determination of the Human Spine in 3D,* Inter-Ing. Conference Tg.-Mures, 2003, 131-137.
43. Lovasz E.-C., Mateaş M., Micea M. *Determination of the Human Spine Geometry with CCD-cameras,* Proc. of the Scientific Reunion of the Special Program of the Alexander von Humboldt Timişoara, 2005, 2, 292-295.
44. Lovasz E-C., Gruescu C. M., Garaiman A., Carabas I., Bodea R. *Scanning System Integrated within Biometric Measurements*, New Trends in Medical and Service Robots. Theory and Integrated Applications. MeSRob 2013, Mechanisms and Machine, Science 16 131-144.
45. Lovasz E-Ch., Gruescu C.M., Ciupe V., Carabas I., Margineanu D., Maniu I., Dehelean N. *Advanced Digitization Techniques in Retrieval of Mechanism and Machine Science*, Proc. of the XIth TMM Liberec 2012, Mechanisms and Machine Science, 8, 35-42.
46. Luther A., Inglis A. *Video Engineering*, 3rd ed., McGraw Hill, USA, 1999.
47. Maruyama T., Kitagawa T., Takeshita K., Makizuki K., Nakamura K. *Conservative treatment of adolescent idiopathic scoliosis: Can it reduce the incidence of surgical treatment?,* Pediatric Rehabilitation, 2003, 215-219.
48. Mateaş M. et al. *About a new method for the 3D determination of the human spine geometry*, Proc. of the XII-th IFToMM internaţional Congress Besancon, 2007,1, 300-305.
49. Mayer G., Tencer F., Kristoferson S. *Use of Noninvasive Techniques for Quantification of Spinal Range-of-Motion in Normal Subjects and Chronic Low-Back Dysfunction Patients.* Spine, 1984, 9, 588-595.
50. McCluney R. *Introduction to Radiometry and Photometry*. Artech House Inc., Norwood, MA, 1994.
51. Mehta M.H. *Active Corection by side-shift: an alternative treatment for early idiopathic scoliosis,* Warner JO New-York 1985, 126-140.
52. Milenkovic S., Kocijancic R., Belojevic G., *Left Handedness and Spine Deformities in Early Adolescence*, European Journal of Epidemiology, Springer Verlag, 19 (10), 2004, 969-972.
53. Naumann A., SchroderG. *Bauelemente der Optik. Taschenbuch der technischen Optik.* München, Carl Hanser Verlag, 1992.

54. Negrini S., Antonini G., Carabalona R. and Minozzi S. *Physical exercises as a treatment for adolescent idiopathic scoliosis. A systematic review,* Pediatric Rehabilitation, 2003,6, 227-235.
55. Negrini S. Fusco C., Minozzi S., Atanasio S., Zaina F., Romano M. *Exercises reduce the progression rate of adolescent idiopathic scoliosis: results of a comprehensive systematic re-view of the literature.* Disability and rehabiliation, 2008, 772-785.
56. O'Shea D. *Elements of Modern Optical Design,*: John Wiley&Son, 1985.
57. OxborrowN.J. *Assessing the Child with Scoliosis: the Role of Surface Topography,* Arch. Disease in Childhood, 2000, 83, 453-455.
58. Otman S., Kose N., Yakut Y. *The efficacy of Schroth 3-dimentional exercise therapy in the treatment of adolescent idiopathic scoliosis in Turky*, Saudi Medical Journal, 2005, 1429-1435.
59. Pană I., Vlădăreanu M., Rovența N., Mihăiță I. *Radiology I- Spinal column*, Didactic and Pedagogical Publishing House, Bucureşti, 2000.
60. Pauk J., Griškevičius J. *Ground reaction force and support moment in typical and flat-feet children*. Mechanika, 2011, 17(1) 93-96.
61. Pearsall D.J., HeddenD.M. *Comparison of three noninvasive methods for measuring scoliosis,*Physical Therapy, 1992, 72, 648-657.
62. Pedley M. *Tilt Sensing Using a Three-Axis Accelerometer – Freescale Semiconductor Ap-plication note*. [Online] https://cache.freescale.com/files/sensors/doc/app_note/AN3461.pdf.
63. Pugna A. et. al. *Optimizing the Hydrothermal Growth Process Parameters of the α-quartz Monocrystals Using Taguchi's Robust Design.* New Trends in Collaborative Design, Publishing House of Poznan University of Technology, 2006, 327-336.
64. Rigo M. et al. *Scoliosis intensive out-patient rehabilitation based on Schroth method,*Stud Health Technol Inform, 2008, 208-227.
65. Romano F., Minozzi S., Bettany-Saltikov J.A., Zaina F., Chockalingam N., Kotwicki T., Maier-Hennes A., Negrini S. *Exercises for adolescent idiopathic scoliosis*, Cochrane Database Systematic Reviews, 8. Art. No. CD 007837
66. Romoli L., Tantussi, G., Dini, G. *Experimental approach to the laser machining of PMMA substrates for the fabrication of microfluidic devices.* Optics and Lasers in Engineering, 2011, 49, 419–427.
67. Ryer A. *Light Measurement Handbook*, International Light Inc., Newbury Port, MA, 1998.
68. Saleh B.E.A., Teich, M.C. *Fundamentals of Photonics*, 2nd ed., Wiley & Sons, New Jersey, 2007.

69. Schröder G. *Technische Optik. Grundlagen und Anwendungen*. Vogel Buchverlag Würzburg. 1990.
70. Smith W.J. *Modern Optical Engineering.* N.Y. McGraw-Hill., 2000.
71. Stalph P. *Analysis and Design of Machine Learning Techniques*, Springer Fachmedien Wiesbaden, 2014.
72. Taguchi G. et. al. *Robust Engineering.* New York. McGraw-Hill, 2000.
73. Taguchi G.et al. *Quality Engineering in Production Systems*. New York. McGraw-Hill, 1989.
74. Terheyden J.H., Wetterkamp M., Gosheger G., Lange T., Schulze Bövingloh A., Schulte T.L. *Rasterstereography versus radiography for assessing shoulder balance in idiopathic scoliosis: A validation study relative to patients' self-image,* Journal of Back and Musculoskeletal Rehabilitation, 2018, 1-9.
75. Văcărescu V. et al. *The method for the evaluation of spinal column posture,* Proc. of the 19-th International DAAAM Symposium Intelligent Manufacturing & Automation, 2008, 1435-1436.
76. Voinea G.-D., Butnariu S., Mogan G. *Measurement and Geometric Modelling of Human Spine Posture for Medical Rehabilitation Purposes Using a Wearable Monitoring System Based on Inertial Sensors.* Sensor, 2017,17.
77. Vutan A.M., Ciupe V., Gruescu C.M., Lovasz E.-C. *Experimental Method for Dynamic Evaluation of Spinal Column Deformation Exercises*, Proc. of The 12th IFToMM International Symposium on Science of Mechanisms and Machines (SYROM 2017), MMS, 2018, 47, 137-146.
78. Vutan A.-M., Gruescu C.M., Ciupe V., Margineanu D., Lovasz E.-C. *Effectiveness of Physical Exercises in the Treatment of Scoliosis - Mathematical Approach,* MESROB 2018 MMS 65 25-34.
79. Weiss H.R. *Influence of an in-patient exercise program on scoliotic curve,* Italian Journal of Orthopeadics and Traumatology, 1992, 395-406.
80. Weiss H.R., Klein R. *Improving excellence in scoliosis rehabilitation: a controlled study of matched pairs,* Pediatric Rehabilitation, 2006, 190-200.
81. Weiss H.R., Weiss G., Petermann F. *Incidence of curvature progression in idiopathic scoliosis patients treated with scoliosis in-patient rehabilitation (SIR): An age- and sex-matched controlled study*, Pediatric Rehabilitation, 2003, 23-30.
82. Zheng R., Hill D., Hedden D., Moreau M., Southon S., Lou E. *Assessment of curve progression on children with idiopathic scoliosis using ultrasound imaging method*, Eur Spine J., 2018,1-6.

83. Zsidai A., Kocsis L. *Ultrasound-based spinal column examination systems*,Facta Universitatis Budapest. Series Physical Education and Sport,2001, 1(8), 1-12.
84. *** MinIMU-9 v5 Gyro, Accelerometer, and Compass https://www.pololu.com/product/2738.
85. ***. *Grey's Anatomy, 39th edition.* NY : Elsevier , 2005.
86. ***. *Schott Catalogue.* 2000.
87. *** *The Burden of Musculoskeletal Diseases in United States*. http://www.boneandjointburden.org.
88. *** A-Star 32U4 Micro .https://www.pololu. com/product/3101.
89. *** TCA9548A 1-to-8 I2C Multiplexer Breakout. https://learn.adafruit.com/adafruit-tca9548a-1-to-8-i2c-multiplexer-breakout?view=all.
90. http://apps.who.int/classifications/apps/icd/icd10online/
91. http://ekasilp.com/digitlite.html.
92. http://scantailor.sourceforge.net.
93. http://usa.canon.com/cusa/consumer/products/scanners.
94. http://welcome.hp.com/country/us/en/prodserv/scanners-copiers-fax.html.
95. http://www.abbyy.ro.
96. http://www.canon-europe.com.
97. http://www.datacomit.com.au/products/large_format_scanning_products.php.
98. http://www.dmg-lib.org/dmglib/main/portal.jsp.
99. http://www.edmundoptics.com
100. http://www.epson.com/.
101. http://www.europeana.eu/portal/.
102. http://www.hoya-opticalworld.com/english/datadownload/index.html
103. http://www.festo.com/cat/ro_ro/products_MTR_DCI.
104. http://www.festo.com/net/SupportPortal/Files/142497/FEC-Standard_0609_EN.pdf.
105. http://www.fujitsu.com/us/services/computing/peripherals/scanners/.
106. http://www.giz4geeks.com/2008/09/08/auto-book-scanner.
107. http://www.i2s-bookscanner.com/.
108. http://www.iiviinfrared.com.
109. http://www.indususa.com/bookscanner.php.
110. http://www.inspeck.com
111. http://www.ophiropt.com.
112. http://www.thinkmotion.eu.
113. http://www.tokinalens.com.
114. http://www.worldmicrographics.com/CopyMaster.html.

Anexa. 10 lucrări relevante

1. Gruescu C., Nicoara I., Popov D., Bodea R., Hora H. 2008 Optical Glass Compatibility For the Design of Apochromatic Systems *Science of Sintering* **40** 131-140.

Science of Sintering, **40** (2008) 131-140

doi: 10.2298/SOS0802131G

UDK 666.3-128:621.315.612

Optical Glass Compatibility For the Design of Apochromatic Systems

C. Gruescu[1], I. Nicoara[1], D. Popov [2*)], R. Bodea[3], H. Hora[3]
[1] University "Politehnica" Timisoara, Mechatronics Department, RO-300002, Victoriei 2, Timisoara, Romania
[2] University "Politehnica" Timisoara, Department of Technical Physics, RO-300223, B-dul Vasile Parvan No. 2, Timisoara, Romania
[3] University of Oradea, Precision Mechanics Department, RO-410087, Universitatii 1, Oradea, Romania

Abstract:
The design of apochromatic systems is difficult because of two problems: the glass sorts compatibility and the c_I/c_a arbitrary input ratio. The optical glass manufacturers offer a wide range of sorts, so that the choice of triplet compatible glasses becomes itself an important separate problem. The paper provides a solution of mathematical modeling for the glass compatibility and, practically, analyses the sorts presented by Schott GmbH. The original software provided 22 compatible glass triplets. The authors explored the possibilities of enlarging the c_I/c_a ratio from the value 0.6 indicated in the literature to a range of [0.5…0.8]. Therefore, they designed and analyzed a set of 88 triplets. A correct glass choice can insure twice-larger apertures than the traditional ones for best quality apochromats (diffraction-limited).
Keywords: Optical glass compatibility, Triplet design, Image quality, Large aperture, Aspherical surface

1. Introduction

Apochromatic optical systems need a specific combination of optical glass sorts, whose dispersive properties insure correction of the longitudinal chromatic aberration and secondary spectrum. An apochromatic system accomplishes the superposition of image abscissas for three wavelengths, so that the secondary spectrum is much lower than for any other optical entity. The traditional optical system, which satisfies these conditions, is the cemented apochromatic triplet (fig.1). The design algorithm supposes that the operator has already chosen the glass sorts. Existing literature offers only general recommendations or a minimum number of compatible glasses [1, 2]. Efficient use of a large number of glass sorts needs a mathematical approach.

The database to investigate contains the glass sorts offered by the Schott Catalogue. The parameters taken into account are the refractive indexes of the spectral lines g, F', e, C', s, the Abbe number ν_e and the relative partial dispersion P_{ge}. The Schott Catalogue contains

*) Corresponding author: dusan_popov@yahoo.co.uk

2. Gruescu C., Lovasz E.-C., Ciupe V. 2014 Optics Optimization in Laser Spot Radius Minimization, *International Conference on Production Research – Regional Conference Africa, Europe and the Middle East, 3rd International Conference on Quality and Innovation in Engineering and Management* 231-234.

2014 International Conference on Production Research – Regional Conference Africa, Europe and the Middle East
3rd International Conference on Quality and Innovation in Engineering and Management

OPTICS OPTIMIZATION IN LASER SPOT RADIUS MINIMIZATION

C. M. Gruescu[1], E.-C. Lovasz[2], V. Ciupe[3]
[1, 2, 3] University Politehnica Timisoara, Mechatronics Department, Mihai Viteazu 1,
RO-300222, Timisoara, Romania

Abstract
The paper presents a short discussion on the spot size importance and the influence factors on it in laser machining applications. As optical system quality in terms of wavefront parameters is essential for the spot size and shape, the optical synthesis of lenses is considered fundamental. For a given application, which implies CO2 laser machining, the preliminary calculus of the expander and focusing objective is presented. The components are designed as best shape lenses. The system is analyzed on different focus shift collecting data on spot size and its relation to Airy disk radius from single spot diagrams. Two solutions are provided, one with spherical objective and one with aspheric objective. Spot sizes with a tolerance factor of 10 % establish large depth of focus. Both solutions are considered very well as the wavefront analysis shows parameters in the class of diffraction limited systems.

Keywords:
optical design, laser machining, spot size minimization.

1 INTRODUCTION

Laser technology is not only a common one. It is a technology in fast progress, whose development aims to increase precision and efficiency, to reduce material and time waste. Non-conventional technologies replace conventional ones and, in addition, perform operation impossible to apply with older technologies.

Rapid spread and improvement of laser technologies implies better or new optical systems.

Laser optics comprise of two basic components, namely the expender and the focusing objective. The expander is a reversed Galileo telescope and the objective is a positive lens.

Usually, the expanders ensure a magnification within the range of [1.5…10] X, depending on the aperture of the laser beam source and the power density admitted by the lens material.

The objectives are designed for effective focal lengths within the range of [40…200] mm, depending on the working distance needed in an application. Objectives may consist of a singlet, a doublet or a system of more lenses, especially in the schemes of scanning laser systems.

Optical design is often referred to as general scheme in books [1] … [4] or papers [5]. Optical parameters such as working distance and defocusing are called in relation with the spot size [6], [7]. The spot size and shape establish the actual energy distribution and finally, the precision and efficiency of the process.

The spot size depends on the quality of the optical system. Nowadays, the quality is expressed in wavefront parameters, sometimes related directly to Airy disk.

Most industrial power lasers work within the infrared range. The optical design is more difficult than for the visible range because of the small number of materials available for lens manufacturing.

The basic principles in laser optics design, recommended by manufacturers [9], [10] and discussed in [8] are as follows:

- The optical assemblies of the expander are singlet. This major simplifying is possible because of monochromatic radiation and theoretically zero slope of the beam. The residual spherical aberration remains the most important problem. As it influences directly the size of the spot, the design of lenses must apply algorithms based on spherical aberration minimization.
- The objective, large-sized in aperture, is also exposed mainly to spherical aberration.
- The most important parameters refer to focus abscissa, shape and size of the spot and depth of focus.
- Ideally, the spot should be circular for a uniform energy distribution. Its size can be optically controlled.

Practically, the spot size assumes two additive components, one due to diffraction and second due to residual spherical aberration:

$$d_{spot\ total} = d_{spot\ diffractional} + d_{spot\ aberrational} \tag{1}$$

where:

$$d_{spot\ diffractional} = \frac{4\lambda M^2 f}{\pi D}, \tag{2}$$

$$d_{spot\ aberrational} = \frac{kD^3}{f^2}. \tag{3}$$

In relations (2) and (3) λ represents the wavelength [μm], M – modal parameter of the beam [-], f – effective focal length of the objective [mm], D – aperture of the objective [mm], k – non-dimensional coefficient depending on the refractive index [-].

The spot size is strongly dependent on the f-number of the objective:

$$f/\# = \frac{f}{D}. \tag{4}$$

Practically, the design input data asks for the focal length as well as for the aperture. The literature recommends estimation relations for one of them in case the other one is given. If the focal length is fixed, the optimum aperture is:

$$D = \sqrt[4]{\frac{4\lambda M^2 f^3}{3\pi k}}. \tag{5}$$

If the aperture is imposed, the recommendation for the focal length is:

$$f = \sqrt[3]{\frac{\pi k D^4}{2\lambda M^2}}. \tag{6}$$

3. Gruescu C., Ionescu C., Nicoara I., Lovasz A. 2012 Experimental Optimization of Process Parameters in Laser Cutting of Polycarbonate Gears *Mechanika Journal* **18**(2) 233-238.

233

ISSN 1392 - 1207. MECHANIKA. 2012 Volume 18(2): 233-238

Experimental optimization of process parameters in laser cutting of polycarbonate gears

C.M. Gruescu*, C.L. Ionescu, I. Nicoara***, A. Lovasz******

**University Politehnica Timisoara, 2 Pta.Victoriei, 300222 Timisoara, Romania, E-mail:corina.gruescu@mec.upt.ro*

***University Politehnica Timisoara, 2 Pta.Victoriei, 300222 Timisoara, Romania, E-mail: cosminionescu@yahoo.com*

****University Politehnica Timisoara, 2 Pta.Victoriei, 300222 Timisoara, Romania, E-mail: ioan.nicoara@mec.upt.ro*

*****University Politehnica Timisoara, 2 Pta.Victoriei, 300222 Timisoara, Romania,*

E-mail: agneta.lovasz@library.upt.ro

crossref http://dx.doi.org/10.5755/j01.mech.18.2.1561

1. Introduction

Polycarbonate is widely used due to its mechanical, optical, thermal and chemical properties. Tensile strength (55 - 75 MPa), Young's modulus (2 - 2.4 GPa) and hardness (~70HRC) recommend the material also for manufacturing of gears, which work with low power or special conditions transmissions. Moulding and extrusion, commonly used to machine polycarbonate pieces, are not appropriate to obtain complex shape and preciseness as gears require. Also, the usual cutting technology of gears is long-lasting and inefficient if some faster machining process can be found. Generally speaking, specially designed technologies must be designed and implemented for machining particular materials or parts [1 - 2]. In the present case a nonconventional technology, for instance laser cutting suites much better.

Still, laser cutting is not very simple to apply. Targets regarding piece's characteristics (precision in shape and dimension, roughness, thermal side-effects etc.), time of machining and energetic supply needed, are hard to attain without a process optimization. The large number of parameters involved, exclude the choice by random of their values. There are optical, electrical and mechanical factors, which influence the laser cutting process. Different combinations of their possible values might satisfy requirements to attain different target criteria (diverse in nature and value). From optical standpoint, laser cutting is a nonimaging application. The quality of the optical system included in the structure of a laser cutting machine, influences directly the general traits of the process. Flexibility and preciseness are required in order to ensure easy transforming of radiant beam's properties (spot size, defocus facilities, and variable energetic density).

Control of electrical parameters, such as power supply, ensures appropriate energetic properties of the cutting beam (for pulse lasers, also pulse duration and pause duration are very important).

Mechanical design of the nozzle, precision and speed of cutting head's displacement are involved in accuracy and efficiency of machining. Establishing the most suited combination of values for all these parameters needs a mathematical approach. There are several optimization process methods, among which, the Taguchi method proved to be one of the best.

The subject of machining is a set of four gears making part of a two – step transmission. Geometrical complexity, precision of tooth pitch, roughness of flanks, variety of modulus and number of teeth recommend a flexible technology such as laser cutting.

2. Experimental equipment

Effective machining of sample pieces was achieved using an existing laser cutting machine, whose optical system was improved [3 - 6]. The computer aided equipment uses a CO_2 pulse laser source, 2 kW power. The machine belongs to C.A.L.F.A. laboratories at I.U.T. Bethune, Universite d'Artois, France. A general image and the scheme of the machine are presented in Fig. 1.

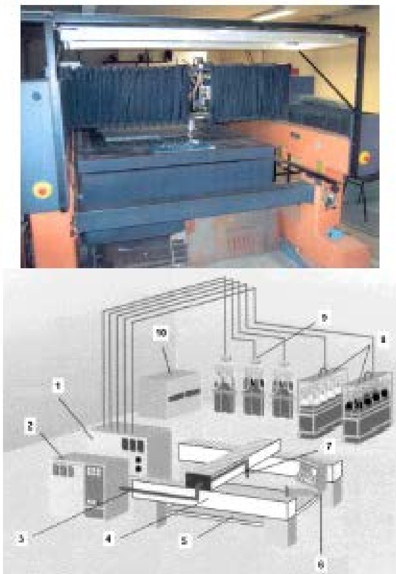

Fig. 1 Image and scheme of the laser cutting machine: *1* - power supply block, *2* - CO_2 laser source, *3* - optical beam path, *4* - mechanical structure, *5* - material to machine, *6* - numerical command block, *7* - cutting head, *8* - assemblies to provide and control auxiliary gas (He, Ar, N_2, O_2), *9* - assembly for CO_2 supply, *10* - cooling block

The general features of the laser cutting machine are wavelength, μm; beam divergence, deg; emitted power, W; cutting speed, mm/s; vertical position of the spot, duration of pulse and pause, ms; chemical nature, pressure and

4. Lovasz E-Ch., Gruescu C.M., Ciupe V., Carabas I., Margineanu D., Maniu I. and Dehelean N. 2012 Advanced Digitization Techniques in Retrieval of Mechanism and Machine Science *Proc. of the XIth TMM Liberec 2012 Mechanisms and Machine Science* **8** 35-42.

Advanced Digitization Techniques in Retrieval of Mechanism and Machine Science Resources

E-Ch. Lovasz, C. M. Gruescu, V. Ciupe, I. Carabas, D. Margineanu, I. Maniu and N. Dehelean

Abstract The European project thinkMOTION works on the purpose of retrieving all-times content regarding mechanisms and machine science by means of creating a digital library, accessible to a broad public through the portal Europeana. DMG-Lib is intended to display the development in the field, from its very beginning up to now days. There is a large range of significant objects available, physically very heterogeneous and needing all to be digitized. The paper presents the workflow, the equipments and specific techniques used in digitization of documents featuring very different characteristics (size, texture, color, degree of preservation, resolution and so on). Once the workflow established on very detailed steps, the development of the workstation is treated. Special equipments designed and assembled at Universitatea "Politehnica" Timisoara are presented. A large series of software applications, including original programs, work for digitization itself, processing of images,

E-Ch.Lovasz (✉) · C. M. Gruescu · V. Ciupe · I. Carabas · D. Margineanu
I. Maniu · N. Dehelean
Universitatea "Politehnica" din Timisoara, Timisoara, Romania
e-mail: erwin.lovasz@mec.upt.ro

C. M. Gruescu
e-mail: corina.gruescu@mec.upt.ro

V. Ciupe
e-mail: valentin.ciupe@mec.upt.ro

I. Carabas
e-mail: ioșif.carabas@mec.upt.ro

D. Margineanu
e-mail: dan.margineanu@mec.upt.ro

I. Maniu
e-mail: inocentiu.maniu@mec.upt.ro

N. Dehelean
e-mail: nicolae.dehelean@mec.upt.ro

J. Beran et al. (eds.), *Advances in Mechanisms Design*, 35
Mechanisms and Machine Science 8, DOI: 10.1007/978-94-007-5125-5_5,

5. Ciupe V., Lovasz E-C., Gruescu C.M. 2012 High Quality Document Digitization Equipment *Mechanisms, Mechanical Transmissions and Robotics, Applied Mechanics and Materials* 162 589-596.

Applied Mechanics and Materials Vol. 162 (2012) pp 589-596
© (2012) Trans Tech Publications, Switzerland
doi:10.4028/www.scientific.net/AMM.162.589

High Quality Document Digitization Equipment

Valentin Ciupe[1,a], Erwin-Christian Lovasz[1,b] and Corina-Mihaela Gruescu[1,c]

[1]Universitatea "Politehnica" din Timisoara, Mechatronics Department, 1 Mihai Viteazu, RO-300222, Romania

[a]valentin.ciupe@mec.upt.ro, [b]erwin.lovasz@mec.upt.ro,

[c]corina.gruescu@mec.upt.ro (corresponding author)

Keywords: digital image, high speed digitization, optical and mechanical design, scanning software.

Abstract. The paper describes an equipment specialized in digitization of single documents, journal-type documents and books. The equipment is designed and assembled at "Politehnica" University of Timisoara and works in a station developed within the European project thinkMOTION. The optical calculus aimed optimal illumination of two symmetrical areas and high quality of captured images. The object of scanning is printed matter, which exists exclusively in paper form and originates from different periods of scientific evolution. The mechanical design was based on criteria such as: flatness of active surfaces, quick placement and removal of the original document, mechanical raw focusing facilities, adjustment regarding the thickness of the original document and finding constructive solutions so that no damage is inflicted upon the original document, which may be one of a kind and, hence, historically very valuable. An original software was created in order to control the scanning process, to organize files and folders, which stock captured images in different stages of processing. The effective efficiency of the equipment is 10 – 12 pages/minute.

Introduction

Digital copies of analogue documents are very common in nowdays. Digitization is performed on purpose of creating multiple copies or original digital documents. The market offers a wide range of standard scanners, featuring very different technical parameters and designated to single document or thin printed matter processing [1], [2], [3], [4]. A particular class of scanners is specially designed for book scanning [5], [6], [7], [8], [9].

The requirements imposed by the activities of thinkMOTION project led to conceiving and building of an original scanning equipment.

These requirements refer to:

- possibility of scanning any type of document (single sheet, journal and book) without damaging in any way the original paper (bending, folding, scratching, tearing, heating etc.). This totally non-destructive feature is very important especially for old documents, with fragile pages, which exist in a small number of copies or even may be one of a kind
- maximum document size ~ 400 x 260 mm. Maximum page size taken into account was A4 (297x210 mm). A safety range of 50 mm was considered reasonable along three edges (top, bottom, left/right) for large non-standard old documents and also for efficiency of work on any size of page. The operator should not waste time because of a restricted positioning area
- high degree of resemblance of the copy in respect with the original. The problem of distortion toward outer sides and corners is present for most all-purpose scanners on the market, in case the original document is a thick book. Furthermore, the thicker the book is, the bending and folding are stronger
- high quality of the digitized copy. The optical resolution was imposed at 300 dpi, at least
- flexible color mode (color and grayscale)

6. Ciupe V., Lovasz E.C., Reessing M., Henkel V., Gruescu C.M., Zabava E.S. 2014 Interactive animation production by means of advanced image processing *SYROM 2013, Mechanisms and Machine Science* **17** 329-337.

Interactive Animation Production by Means of Advanced Image Processing

V. Ciupe, E.-Ch. Lovasz, M. Reessing, V. Henkel, C. M. Gruescu and E. S. Zabava

Abstract The paper describes an application developed within the European project thinkMOTION. The project aims to post online, within a digital library, heterogeneous content regarding mechanisms science and related fields. Special systems were developed in Ilmenau, Germany and in Timisoara, Romania, in order to actuate and take photographs of the physical models of the mechanisms to be digitized. The systems consist of a motor mechanically connected to the mechanism by means of a coupling device and electrically connected to a PC or a PLC. A digital still camera is connected to the same computer/controller. The logic of this system is to take a photograph after each rotational increment of 0.9°, thus obtaining a complete 400 images set that can be further processed via software in order to obtain an interactive animation which can be uploaded on the project's dedicated web portal and used in this way as an educational or informational content tool.

Keywords Interactive animation · Mechanisms · Physical models · Stepper motor · Servo motor · Java applet

V. Ciupe (✉) · E.-Ch. Lovasz · C. M. Gruescu · E. S. Zabava
Politehnica University of Timisoara, Timisoara, Romania
e-mail: valentin.ciupe@mec.upt.ro

E.-Ch. Lovasz
e-mail: erwin.lovasz@mec.upt.ro

C. M. Gruescu
e-mail: corina.gruescu@mec.upt.ro

E. S. Zabava
e-mail: eugen.zabava@mec.upt.ro

M. Reessing · V. Henkel
Technische Universität Ilmenau, Ilmenau, Germany
e-mail: michael.reessing@tu-ilmenau.de

V. Henkel
e-mail: veit.henkel@tu-ilmenau.de

I. Visa (ed.), *The 11th IFToMM International Symposium on Science of Mechanisms and Machines*, Mechanisms and Machine Science 18, 329
DOI: 10.1007/978-3-319-01845-4_33,

7. Gruescu C.M., Garaiman A., Lovasz E.-C. 2015 Modeling of human spinal column and simulation of spinal deformities *Mechanika Journal* **3** 214-219.

214

ISSN 1392–1207. MECHANIKA. 2015 Volume 21(3): 214–219

Modeling of human spinal column and simulation of spinal deformities

C. M. Gruescu*, A. Garaiman, E. C. Lovasz*****
**University Politehnica Timisoara, Mihai Viteazu 1, 300222, Timisoara, Romania, E-mail: corina.gruescu@upt.ro*
***University Politehnica Timisoara, Mihai Viteazu 1, 300222,Timisoara, Romania, E-mail: alice_garaiman@yahoo.com*
****University Politehnica Timisoara, Mihai Viteazu 1, 300222, Timisoara, Romania, E-mail: erwin.lovasz@upt.ro*

crossref http://dx.doi.org/10.5755/j01.mech.21.3.8505

1. Introduction

Modeling and simulation is widely used in all domains as resourceful tools in design, enhancement, improving or forecasting behavior of different systems. A wide range of software is available to aid solving engineering problems. However, there are systems, such as the biological ones, to which modeling and simulation is a very difficult task. The difficulty originates in two essential features:

- human body parts are very irregularly shaped;
- anthropometrical normal data is very scattered, regarding age, sex, race, profession, local environment traits and so on.

Therefore, biological models are not yet developed on large scale even though they would be very useful in investigating and monitoring patients suffering of widespread diseases. However, there is an encouraging start in modeling different parts of human body, such as feet [1], arms [2], mobile bones of the head [3] etc. The purpose of modeling is either depicting abnormal anatomical shapes or designing of devices such as prosthesis.

The present work focuses on the class of spinal deformities, which are very common in now-days. Most individuals suffer of mild or severe spinal column deformities, such as scoliosis, lordosis, kyphosis or combinations of these. Deformities cause diminution of personal comfort and of physical or intellectual capacity of effort. When severe, deformities bring on large distortions of thorax shape and alteration of respiratory process. Such spinal diseases occur frequently at school-age population, due to incorrect posture and/or to improper desk design and less frequently to adult population, due to sedentary activities (teachers, librarians, IT specialists etc.). The elder population also suffers because of irreversible bone alteration. Plenty of statistics describe the prelevance of such diseases in different places of the world, taking into account a lot of aspects such as: age, sex, profession, life standard etc. [4-6].The studies emphasize very detailed the importance of identifying early stages of spinal deformities because of cautious prognostic and very high costs of treatment [7].

Engineering sciences offer a large series of equipments to investigate the human bone system. Among the methods of investigation in use, the most common are X-ray, CT or MR imaging, Moire topography, digital ultrasonic mapping and optical scanning [8-17]. The stating order of these methods is chronological regarding the implementation and inversely from invasive character standpoint.

Countries which develop long term healthcare programs always include spinal deformities among the main issues to investigate and monitor, especially to school children and persons involved in specific professional activities. The main problems in tracing and monitoring spinal deformities consist of:

- finding a quick and less invasive method of investigation;
- establishing a set of numerical parameters to describe completely the column's shape;
- storing of a large amount of data considering the big number of subjects in the database;
- accessing data and evaluating the evolution of patients.

In order to model the spinal column and simulate its behavior, considering a long-term monitoring of an extended sample of population, the following workflow was conceived (Fig. 1).

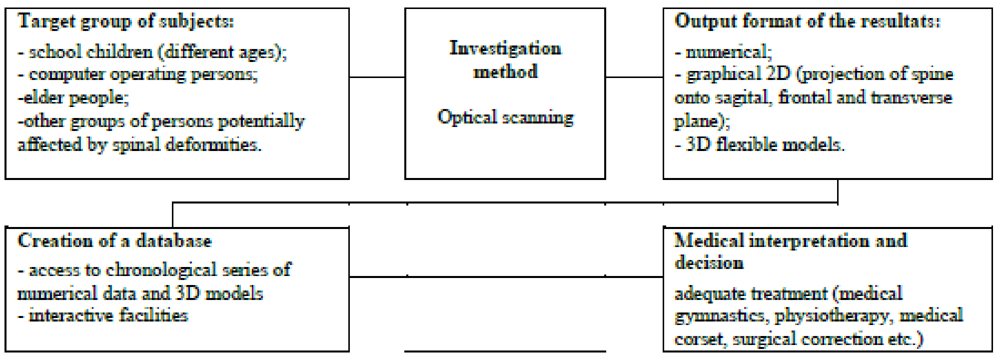

Fig. 1 Workflow of the biometric investigation and monitoring

8. Lovasz E-C., Gruescu C. M., Garaiman A., Carabas I., Bodea R. 2013 Scanning System Integrated within Biometric Measurements *New Trends in Medical and Service Robots. Theory and Integrated Applications. MeSRob 2013 Mechanisms and Machine Science* **16** 131-144.

Scanning System Integrated Within Biometric Measurements

E.-C. Lovasz, C. M. Gruescu, A. Garaiman, I. Carabas and R. Bodea

Abstract The chapter presents the implementation of a non-invasive method of investigation for the spinal column. The scanning equipment, in a proper configuration, provides 3D images of human torso. Specific software developed writes information into an interactive database and computes 16 numerical parameters, describing the column's shape, respectively the human posture. A sequence of the program computes the relative angle of rotation between successive vertebrae or segments of the column. The database also allows modelling of different types of vertebrae and, finally of personalized spinal columns.

Keywords Scanning · Spinal column · Modelling · Simulating · Spinal deformities

1 Introduction

During the last two decades, imaging became an every-day method of investigation all over the medical field. However, objective medical imaging,

E.-C. Lovasz (✉) · C. M. Gruescu · A. Garaiman · I. Carabas
University "Politehnica" of Timişoara, Timişoara, Romania
e-mail: erwin.lovasz@mec.upt.ro

C. M. Gruescu
e-mail: corina.gruescu@mec.upt.ro

A. Garaiman
e-mail: alice_garaiman@yahoo.com

I. Carabas
e-mail: iosif.carabas@mec.upt.ro

R. Bodea
University of Oradea, Oradea, Romania
e-mail: rbodea@uoradea.ro

D. Pisla et al. (eds.), *New Trends in Medical and Service Robots*, 131
Mechanisms and Machine Science 16, DOI: 10.1007/978-3-319-01592-7_10,

9. Vutan A.M., Ciupe V., Gruescu C.M., Lovasz E.-C. 2018 Experimental Method for Dynamic Evaluation of Spinal Column Deformation Exercises *Proc. of The 12th IFToMM International Symposium on Science of Mechanisms and Machines (SYROM 2017) MMS* **47** 137-146.

Experimental Method for Dynamic Evaluation of Spinal Column Deformation Exercises

A.-M. Vutan, V. Ciupe, C. M. Gruescu and E.-C. Lovasz

Abstract Spinal deformities appear very frequently in child or adult population. Researches in this field are widely spread and continuously developing now-days, as the current schemes of treatment are long-lasting, costly and not very effective. The authors propose an investigation method based on a set of sensors, which are accelerometers and provide data in order to generate a mathematical model of the spine, namely a high degree polynomial. Basic parameters, such as the Cobb angle are computed within the mathematical algorithm. The angles acquired by the sensors are recorded as functions of time, so that the change in shape of the spine during the exercises prescribed by the kinetotherapist is subject of study and a criterion for optimizing the nature and intensity of the exercises.

Keywords Spinal deformation · Accelerometer · Mathematical model of the spine

1 Introduction

Vertebral disorders are very common in recent years among children and adults, due to lack of physical activity [1] and long-term prolonged sitting position [2]. Spinal deviations, such as scoliosis, may occur from younger ages continuing to

A.-M. Vutan · V. Ciupe · C. M. Gruescu (✉) · E.-C. Lovasz
Politehnica University of Timisoara, Timişoara, Romania
e-mail: corina.gruescu@upt.ro

A.-M. Vutan
e-mail: anamariavutan@yahoo.com

V. Ciupe
e-mail: valentin.ciupe@upt.ro

E.-C. Lovasz
e-mail: erwin.lovasz@upt.ro

 137
I. Doroftei et al. (eds.), *New Advances in Mechanism and Machine Science*, Mechanisms and Machine Science 57,
https://doi.org/10.1007/978-3-319-79111-1_13

10. Vutan A.-M., Gruescu C.M., Ciupe V., Margineanu D.and Lovasz E.-C.2018 Effectiveness of Physical Exercises in the Treatment of Scoliosis - Mathematical Approach *MESROB 2018 MMS* **65** 25-34.

Effectiveness of Physical Exercises in the Treatment of Scoliosis - Mathematical Approach

A.-M. Vutan, C. M. Gruescu(✉), V. Ciupe, D. Margineanu, and E.-C. Lovasz

Politehnica University of Timisoara, Timişoara, Romania
anamariavutan@yahoo.com, {corina.gruescu, valentin.ciupe, dan.margineanu, erwin.lovasz}@upt.ro

Abstract. The treatment of scoliosis is based on physical exercises with light and medium severity of deformation. The effectiveness of the exercises is assessed by means of Cobb angle variation. In order to compute the values of the Cobb angle, a mathematical model of the spine is generated. A set of eight sensors, type accelerometer, is attached to the vertebrae in significant points of the column. Its shape is approximated with a high degree polynomial, which allows the determination of the inflection points and Cobb angles. The study consists in assessment of three exercises frequently used in treatment protocols.

Keywords: Spinal deformation · Mathematical model of the spine Cobb angle · Physical exercises

1 Introduction

Idiopathic scoliosis is a deviation in frontal plane with unknown cause. It mainly affects children over eight years old until bone maturation is achieved. The lateral inclination of the column is accompanied by the vertebral rotation vertebrae to the convexity of the curve [1]. Generally, there is a primary curve showing the highest rotation and one or more secondary (compensatory) curves [2]. When vertebral rotation is located at the thoracic region, the rotation of the vertebral body determines the movement and deformation of the entire rib cage, causing the rib hump [1]. The child with idiopathic scoliosis is evaluated periodically by the orthopedic doctor. The protocol requires clinical and radiologic evaluation every 6 months, from the moment of diagnosis until the end of bone maturation. Thus, the Cobb angle is calculated on the X-ray, representing the intersection of the perpendiculars to the tangent line of the upper plateau of the superior vertebra of the curvature and the tangent line to the inferior plateau of the lower vertebra of the curve [2]. Depending on the degree of inclination and rotation of the spine, the orthopedist determines the treatment to follow. The protocol for a scoliosis (Stagnara protocol) requires: scoliosis specific exercises (if the Cobb angle is below 25°) or specific exercises and orthopedic treatment wearing a brace (if Cobb angle is between 25° and 50°) or surgery (if Cobb angle is above 50°) [1]. Specific exercises programs for scoliosis will be part of the patient's life immediately after

G. Carbone et al. (Eds.): *New Trends in Medical and Service Robotics*, MMS 65, pp. 25–34, 2019.
https://doi.org/10.1007/978-3-030-00329-6_4